Software Development Methodology

To meet these needs, ATSC chose to use an object-oriented approach to all new software developed. Some of the MLRO software was derived from existing FORTRAN applications and routines that have existed for many years. These "legacy applications" were debugged, improved for functional expandability, but not transformed into C++ objects.

The nature of an object-oriented approach (especially one where C++ class libraries are constructed) is that development is done in a highly non-linear fashion. For the first year most of the development time was spent creating building-blocks that would be used to assemble the various daemons and processes that compose the MLRO Real-Time software subsystem. In addition to these developments we found it necessary to create several drivers, which were not available for the chosen operating system. These included a frame-grabber driver, a GPIB (IEEE-488) driver, and several low-level routines to operate instruments using parallel digital I/O and analog I/O.

The benefits of an object-oriented approach include:

- Maintainability: An increase in the maintainability and upgradability of the software since the applications are built from a common set of class-library objects. If a common unit is changed in one place, the change is automatically propagated throughout the software system.
- Talent Sharing: Since the application developers use common building blocks, the application developers are able to share the talent of the highest-level system programmer. They need not know system-level functions, or even object-oriented programming.
- New projects: Since the class libraries contain generic (very simple) functions which have already been shown to work and to be integrated, new applications can be developed rapidly. The application developer can assemble special (custom) applications or systems in a matter of a few days, rather than months or years.

Summary

The MLRO software system has been designed and developed to be a highly flexible object-oriented software and computing environment. The development philosophy and objectives have been for a long-term benefit to both the customer and to AlliedSignal. For FORTRAN-based applications, existing software has been improved to be more modular and modified to make extensive use of Oracle database software. The system uses an X-Windows interface and an advanced communications subsystem to allow for an easy upgrade to remote operation or full automation.

Crimean Laser Observatory of the Lebedev Physics Institute.

Yu.V. Ignatenko, Yu.L.Kokurin, V.V. Kurbasov, V.F. Lobanov, A.N. Sukhanovski, V.N. Triapitsin.

Upgrading the SLR station Katziveli

Summary

The current state of the SLR station Katziveli is described, as well as plans for upgrade of this station. The upgrade includes a use of a new laser transmitter (30 mJ/40ps/10Hz) and better timing, angle measurement, and receiver components. It is expected, that after finishing the modernization, planned for the year 1997, the ranging accuracy will be 1 - 2 cm RMS, approximately 3 times better than before.

SLR station Katziveli became operational in August 1984 with the observations of LAGEOS During subsequent few years we attempted to bring the parameters of the station to the level necessary for laser ranging of the Moon. Due to technical and financial difficulties this work was interrupted in 1990.

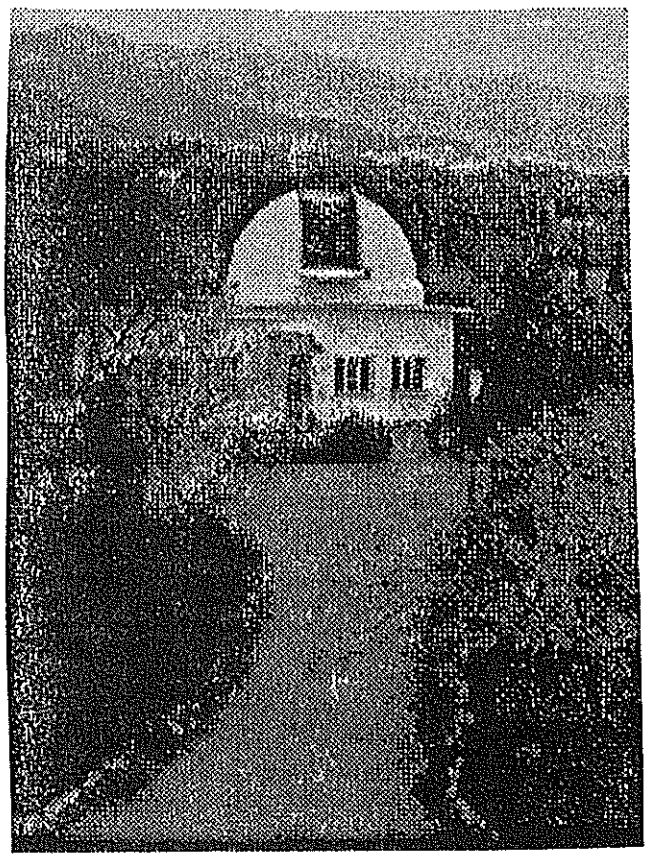

Routine observations of the geodynamical satellites were started in 1988 and continued up to present. By 1990 the station has reached the 3rd generation level. Since then, the RMS of the individual measurements has been about 5 cm for the satellites with orbits from 700 km to 40,000 km.

During the period of 1990 to 1995 due to insufficiency of funding no upgrade to the station has been made, and the station was used with extreme economy of its resources. Namely, the number of observations was reduced to approximately 500 per year. Also, the energy and repetition rate of the laser were lowered. Now, average numbers of the individual measurements per pass for different satellites are:

- For LAGEOS 2,2 - about 400
- For ETALON 1,2 - about 160
- For low - orbit satellites - about 150

With full use of the station resourses (as up to 1990) we could easily do 2000 - 3000 sessions per year with a few thousand points per pass. In order to increase the number of observations and their accuracy, as well as to provide observations at to day time, it was necessary to fundamentally upgrade the station. this became possible only in 1995 when INTAS has granted us a special funding. In 1995 - 1997 it is intended to purchase the following equipment:

- Intel Pentium TM-based computers with necessary peripherals, which will replace outdated AT-286's;
- SVee-6 GPS-receiver by Trimble;
- RI2V rotary encoders for both axes of the telescope, by Zeiss, Jena;
- Hamamatsu H5023 photo multipliers;

- SR-620 event timer.

The computers, GPS-receiver and rotary encoders have already been purchased and installed at the station. Besides, we aim to build a new laser transmitter using basic parts of the existing "Pulsar - 2M" laser. This work will be done under the contract with "Dynamic" company (Kiev, Ukraine). The new laser should have the following parameters:

- Pulse length: 40ps;
- Pulse energy: 30 mJ;
- Repetition rate: 10 Hz.

We are planning to finish upgrading the station in 1997. The expected improvement of the accuracy should bring the RMS to 1-2 cm level. Also, with the new encoders, we hope to get a real potential for day time observations.

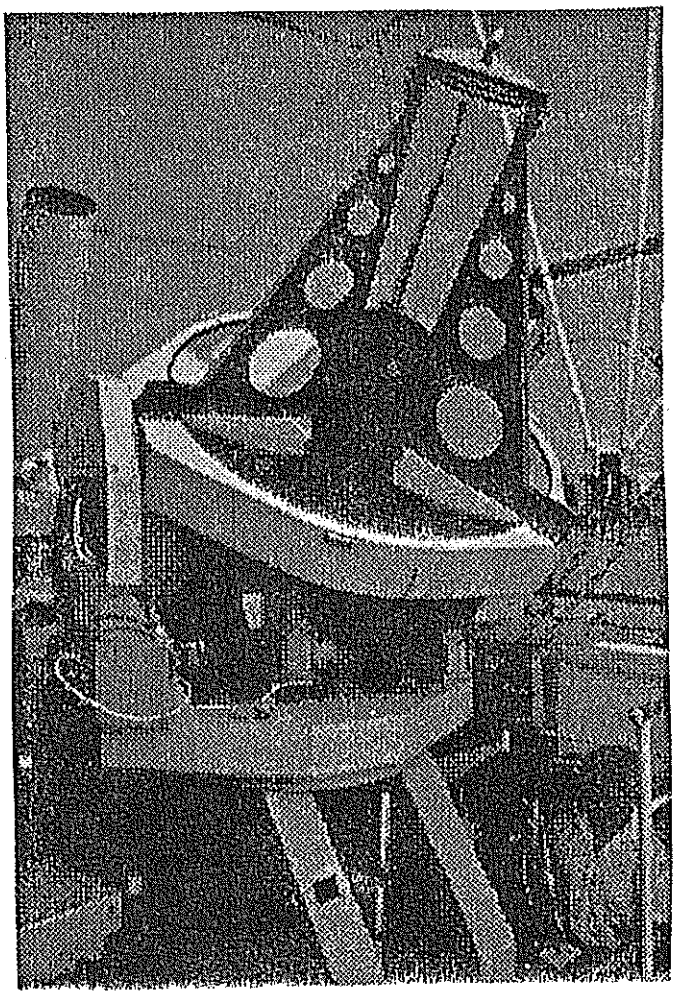

STATUS REPORT ON BOROWIEC SLR 1994-1996

S.SCHILLAK, J.BARTOSZAK, E.BUTKIEWICZ
D.SCHILLAK, S.ZAPAŚNIK

SPACE RESEARCH CENTRE
OF POLISH ACADEMY OF SCIENCES
BOROWIEC ASTROGEODYNAMICAL OBSERVATORY
62-035 KÓRNIK, POLAND
tel: +48-61-170-187
fax: +48-61-170-219
e-mail: sch@cbk.poznan.pl

ABSTRACT. The report mentions the improvements and modernisation which have been introduced at the Borowiec SLR since the last workshop. In the end of 1994, a new main computer PC-486 with real time software was installed. The first return signals from a satellite with this computer were recorded in December 1994. A new tracking system has been introduced and the pointung accuracy of the telescope is now a few times better. The subsequent aim is automation of the system and reduction of the staff on duty to a single person crew. Thanks to improvements of the system, it can trace more satellite passes and record more return signals per a single pass. At present installation of a telescope emitting a narrower laser beam is under way. It will permit tracking of GPS, GLONASS and ETALON satellites. In the nearest future due to the installation of a new detector, time interval counter, and shortening of the laser pulse width, the single shot precision will be probably about 1 to 2 cm.

The main improvements at the Borowiec SLR within the last two years were replacement of a minicomputer MERA-400 by a PC-486, exchange of interfaces and the telescope control system. This changes opened further possibilities of upgrading and automation of the system. Consequently, a significant improvement of the quality and quantity of results was noted in 1996. The nearest future the efforts will concentrate on improvement of the accuracy of the system.

1. A new control system.

The works related to exchange of computers were undertaken in 1994 (Schillak et al., 1996a). Care was taken to introduce the new computer and the control system in such a way so that observations could be continued. A new real time program was written which controls the system (STR) - its schematic presentation is included in "Automation of the Borowiec SLR" in these Proceedings. The first test observations were carried out in December 1994, when return signals from a few satellites were recorded. Regular observations were started from February 21, 1995. After a one month break in May 1995 when it was necessary to go back to MERA-400, since June 13, 1995 all observations have been made with the new system. The main problem which hindered obtaining good results was the continuous tracking system of the telescope. Having tested from June to the end of August many variants of the system work, it was eventually abandoned and a new step by step system was chosen as it proved the most accurate tracking for the heavy mount in Borowiec. A scheme of the currently used system is

shown in Fig. 1. A PC-386 is used as an interface of the system and it is connected via a high speed line with the main PC-486 unit.

2. The tracking accuracy.

The return to the step by step tracking system meant coming back the unsolved problem of the mount delay depending on the satellite velocity. The accuracy of tracking fast satellites was limited even to 5 arcmin, which significantly obstructed tracking of invisible satellites. From October 1995 the works on mathematical model of these delays have begun. The control program has been modified to facilitate introduction of a satellite into the centre of the field of view and enable read out of the azimuth and altitude corrections with reference to the emphemeris data. Realisation of this task was delayed because of the invisibility of satellites in winter. With the coming of spring the model was gradually improved and the accuracy of the telescope tracking was a few times increased. It is reflected by the increased number of return signals per a satellite pass, see Fig. 2. After completion of the works on the model, in July 1996 this value reached on the average over 1000 returns per pass.

Table 1. Results of Borowiec SLR - 1995

SATELLITE	PASSES	RETURNS	RETURNS/ PASS	SP RMS cm	NP RMS cm
LAGEOS-1	49	9850	201	5.5	2.6
LAGEOS-2	37	6766	183	5.3	2.3
ERS-1	49	10126	207	3.3	1.8
ERS-2	45	8746	194	3.4	1.9
TOPEX	98	95105	970	4.3	1.6
STELLA	25	5335	213	3.3	1.8
STARLETTE	19	2327	122	3.3	1.8
METEOR-3	45	8901	198	3.6	2.2
AJISAI	59	60882	1032	4.0	1.4
TOTAL	426	208038	488	4.1	1.9

Table 2. Results of Borowiec SLR - 1996

SATELLITE	PASSES	RETURNS	RETURNS/ PASS	SP RMS cm	NP RMS cm
LAGEOS-1	91	36274	399	5.7	2.0
LAGEOS-2	50	23616	472	5.7	2.0
ERS-1	39	25288	648	3.2	1.1
ERS-2	62	28520	460	3.4	1.3
TOPEX	98	207100	2113	4.1	1.0
STELLA	34	10866	320	3.2	1.5
STARLETTE	27	11386	422	3.6	1.6
AJISAI	59	133325	1932	3.8	0.9
RESURS	5	928	186	3.6	2.1
FIZEAU	20	2687	134	3.8	2.0
GFZ-1	16	3333	208	3.7	2.0
TiPS	5	471	94	6.3	3.0
TOTAL	516	483794	938	4.3	1.5

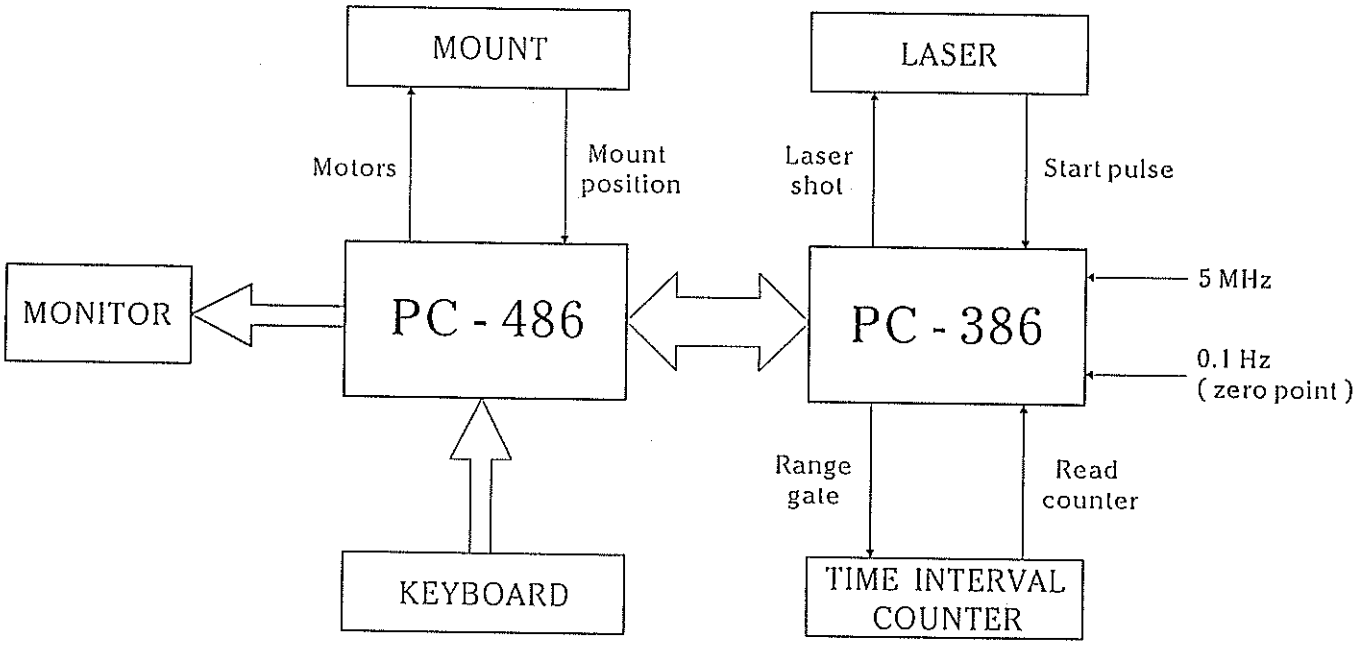
MOUNT
LASER
Motors
Mount position
Laser shot
Start pulse
MONITOR
PC - 486
PC - 386
5 MHz
0.1 Hz
(zero point)
Range gate
Read counter
KEYBOARD
TIME INTERVAL COUNTER

Fig. 1

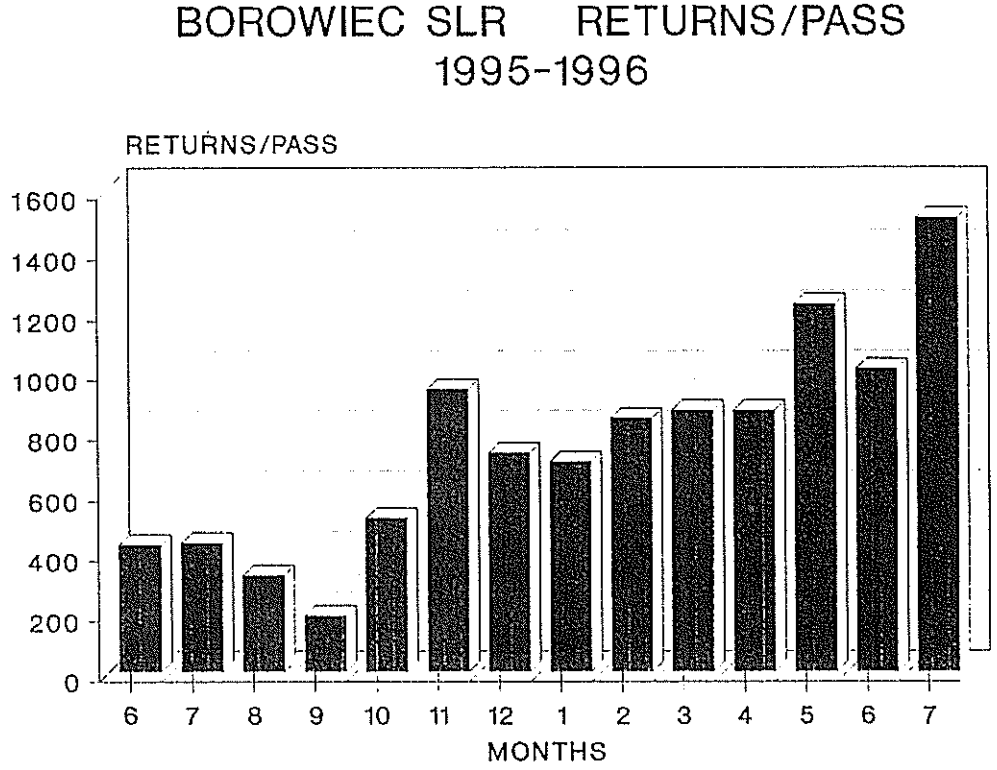
BOROWIEC SLR RETURNS/PASS
1995-1996
RETURNS/PASS
1600
1400
1200
1000
800
600
400
200
0
6 7 8 9 10 11 12 1 2 3 4 5 6 7
MONTHS

Fig. 2

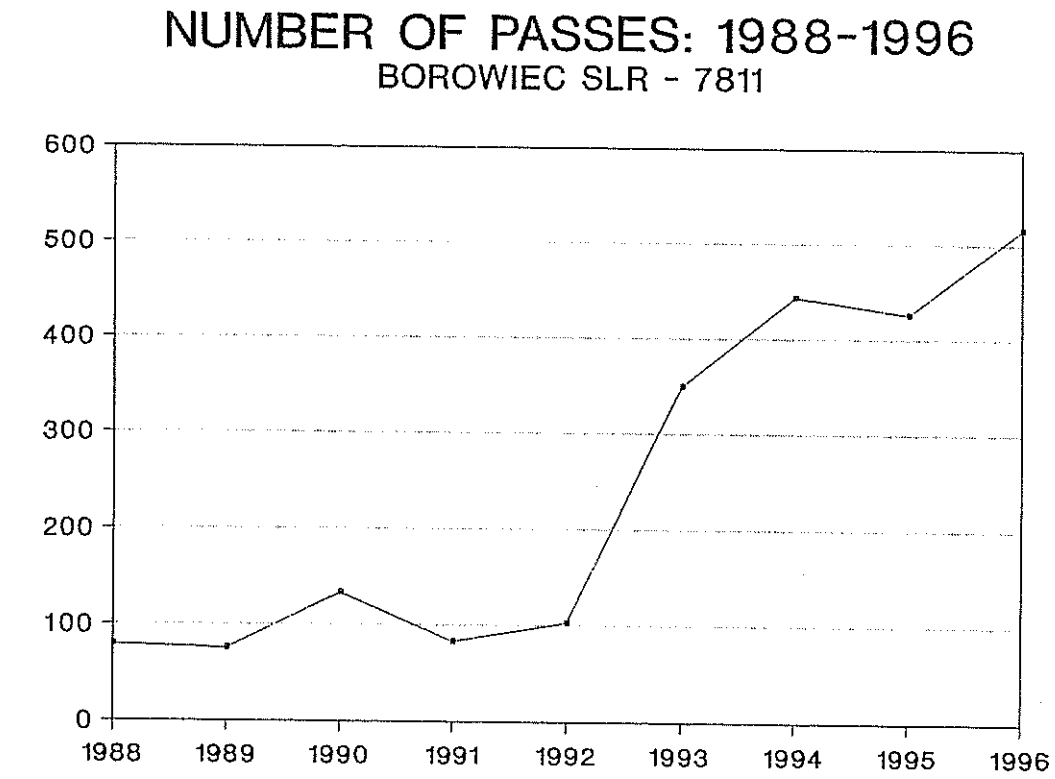

Fig. 3

3. Results of observations.

Introduction of a new computer and tracking system has led to substantial improvement of the quality and quantity of results. The increase of the number of observations from 1988 till the end of 1996 is shown in Fig. 3. Results of the observations carried out in 1995 and 1996 are collected in Tables 1 and 2, from which a significant increase in the number of return signals and improvement of the normal point precision for each satellite is visible. Introduction of a new computer and improvement of the tracking accuracy did not affect the single shot precision (Figs. 4 and 5) whose enhancement is expected as a result of the works began in the end of 1996.

4. Automation of the system.

An important task under realisation for the last two years is automation of the system. The project is discussed in detail in "Automation of the Borowiec SLR" within the same Proceedings. Connection of the main control computer to the Internet in November 1995 proved much beneficial for the process of the system automation.

5. Plans for the future.

In the nearest 3 years the introduction of the following improvements at Borowiec SLR is planned:

- increase of a single shot precision to 1-2 cm is expected after installation of a HAMAMATSU H5023 photomultiplier, time interval counter STANFORD SR-620, and shortening of the laser pulse to 35 ps,
- reduction of the range bias as a result of installation of the second target or inner calibration, enhancement of the accuracy of pressure read out, measurement of the return signal amplitude,
- increase of the number of observations through automation of the system and reduction of the staff on duty to a single operator, performance of daily observations, extension of observation

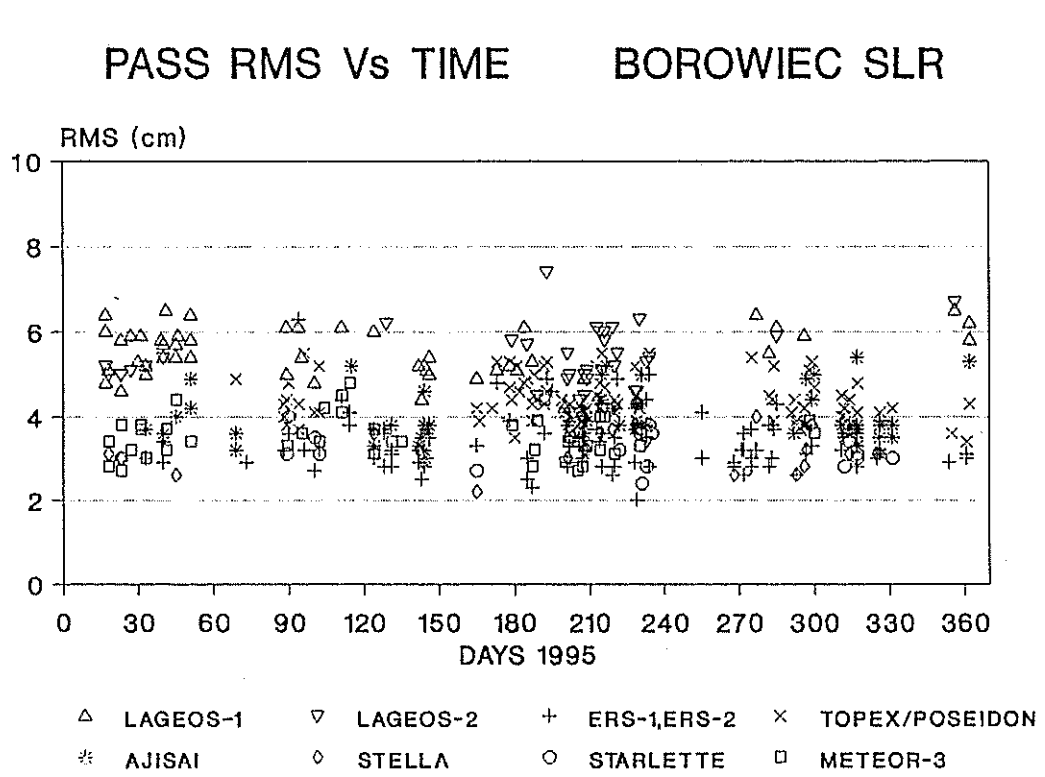
PASS RMS Vs TIME BOROWIEC SLR
RMS (cm)
10
8
6
4
2
0
0 30 60 90 120 150 180 210 240 270 300 330 360
DAYS 1995
LAGEOS-1
LAGEOS-2
ERS-1,ERS-2
TOPEX/POSEIDON
AJISAI
STELLA
STARLETTE
METEOR-3

Fig. 4

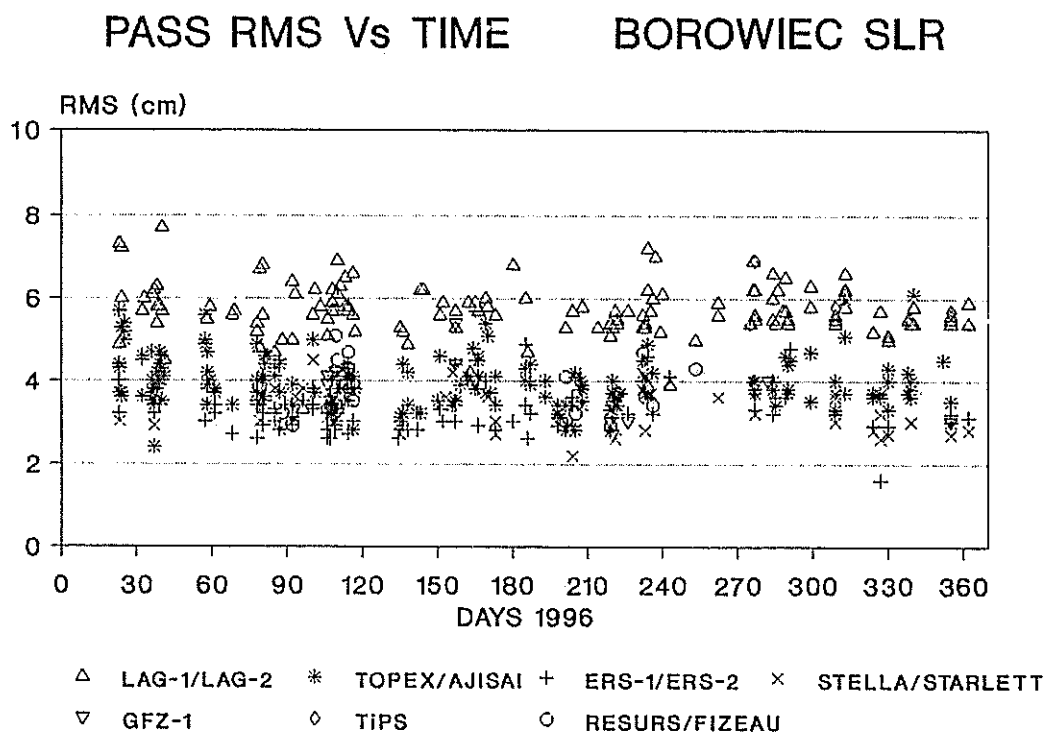
PASS RMS Vs TIME BOROWIEC SLR
RMS (cm)
10
8
6
4
2
0
0 30 60 90 120 150 180 210 240 270 300 330 360
DAYS 1996
LAG-1/LAG-2
TOPEX/AJISAI
ERS-1/ERS-2
STELLA/STARLETT
GFZ-1
TiPS
RESURS/FIZEAU

Fig. 5

time for 7 days a week and starting the observations of high orbiting satellites such as GPS, GLONASS, ETALON.

6. Borowiec -2 SLR.

For the last two years efforts have been made to install a system Borowiec-2 in Tunisia. From April to the end of June 1995, test observations were performed with this system in Borowiec, obtaining results for 25 passes (Schillak, 1996 b). Results of these observations confirmed that the system is ready for installation. The necessary changes (laser) and complementations will be made after the final decision as to the system installation in Tunisia. The Tunisian side bought the grounds on which the Geodynamical Station will be built and made architectural design of the Station building.

Acknowledgements.
This work was supported within the grant Z/137/t12/96/07 of the Committee for Scientific Research.

References 1995-1996.

Schillak S., 1995, Borowiec Laser Station-Operational Report 1994, *Publ. of Space Research Centre of the Polish Academy of Sciences,* Borowiec, January 1995, Poland, pp. 1-38.

Rutkowska M., Romay Merino M.M., Schillak S., Dow J.H. ,1995, Improvement of the SLR Borowiec station position in the global network ITRF91, *Adv. in Space Res.*, Vol. 16, No 12, pp. 97-100.

Schillak S., Butkiewicz E., Bartoszak J., Schillak D., Zapaśnik S., 1995, The satellite laser ranging performed at Borowiec with accuracy to a few centimeters, *Artificial Satellites, Planetary Geodesy-No 25,* Vol. 30, No 2-3, Warsaw, Poland, pp. 103-113.

Schillak S., 1995, The accuracy and precision of the Satellite Laser Ranging Systems, *Artificial Satellites, Planetary Geodesy-No 25,* Vol. 30, No 2-3, Warsaw, Poland, pp. 115-121,

Schillak S., Łatka J.K., Bartoszak J., Butkiewicz E., Schillak D., Zapaśnik S., 1996a, Status Report on the Borowiec Laser Ranging Systems, *Proc. of the 9 th International Workshop on Laser Ranging Instrumentation,* Canberra (Australia), 1994.11.07-11, Vol. 1, Australian Goverment Publishing Service, Canberra, Australia, pp. 264-272.

Schillak S., Butkiewicz E., Łatka J.K., Dybczyński P., Baranowski R., Frączyk P., Sczaniecki L., 1996, Software of the Borowiec-2 SLR System, *Artificial Satellites, Planetary Geodesy No 26,* Vol. 31, No 1, Warsaw, Poland, pp. 71-80.

Schillak S., 1996b, Borowiec Laser Station-Operational Report 1995, *Publ. of Space Research Centre of the Polish Academy of Sciences,* Borowiec, January 1996, Poland, pp. 1-40.

Schillak S., 1996, Satellite Laser Ranging in Poland 1976-1996, *Artificial Satellites, Planetary Geodesy No 28,* Vol. 31, No 3, Warsaw, Poland, pp. 163-177.

The Laser Ranging System of Yunnan Observatory(YLRS) and its Status

Yunnan Observatory China

Jiang Chongguo Xiong Yaoheng
Wang Wu Feng Hesheng

October 1996

I. Introduction

Yunnan Observatory is situated in the middle of Yun-Gui Plateau, southwest China. It has the latitude 25° N, the longitude 102° E and the altitude 2030m. Initially the project of the YLRS was proposed in 1985. The project was not carried into effect because of financial problem. The group rebuilt the 1.2m telescope and worked on other project, but still did not give up the goal of SLR and LLR. In April 1996, the Chinese Academy of Sciences examined the proposal of YLRS and offered partial funds to set up SLR station. Up to now we have already had:

1. Telescope
2. Imaging system for pointing calibration
3. Laser
4. Transmit/Receive optics
5. Receiver(PMT)
6. Software of satellite prediction and data pre-processing

The electronic hardwawe for transmit control, transmit/receive switch, range gate, time control, interface, and the software for observation and system control are being modificated and will soon be finished. We lack still the time system and the counter. It is estimated that the system can be completed in a few months.

II. . YLRS Overview

The YLRS is shown as F1 and F2.

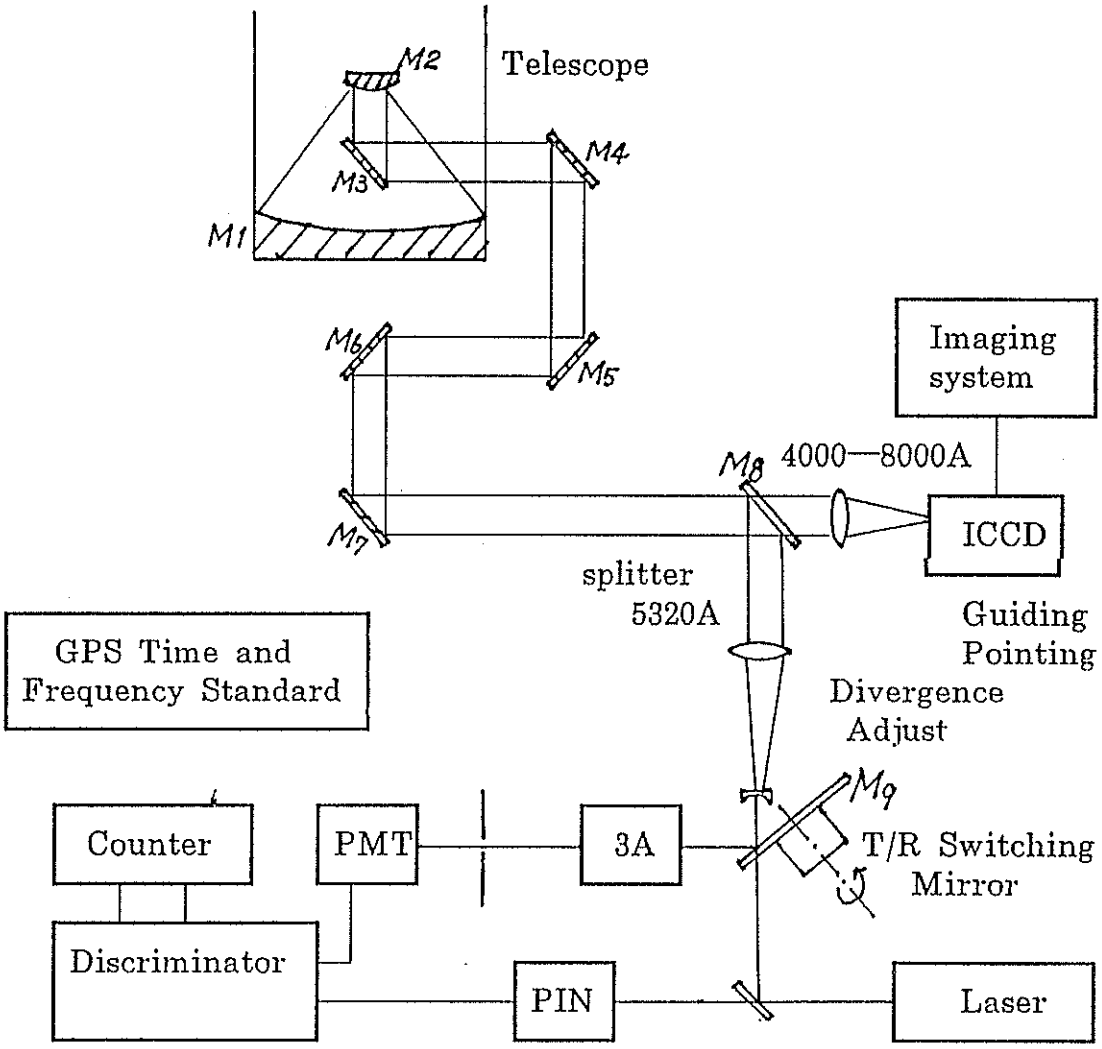

F1. YLRS Diagram

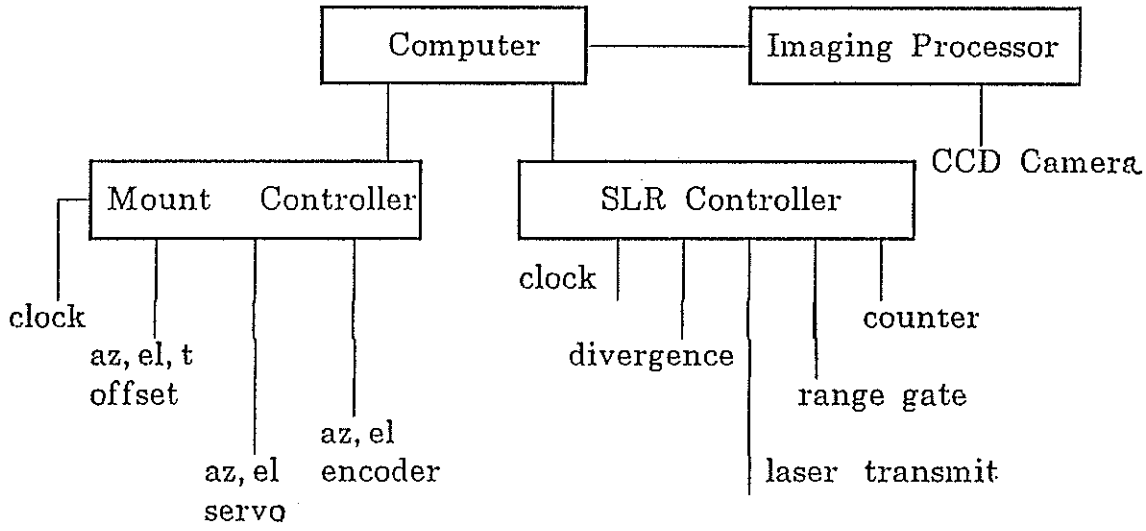

F2. YLRS Control Diagram

The YLRS Specifications is as follows:

1. Ranging Ability: 800~>20000 km
2. Accuracy: 3~4 cm
3. Repetition Rate: 4 Hz
4. Divergence: 0.01~0.4 mrad
5. Operating Time: Day and Night

III. Telescope

The telescope has the Az-Alt configuration. In resent years it was successfully used for the experiment of "real time correction of the atmospherical turbulence for stars " (adaptive optics).
It indicated that the telescope has especially good pointing accuracy. As a result of good pointing and tracking performance, relative larger apeture, and more stable Coude optics, it is expected that the YLRS is especially suitable to day and night ranging of the long distance satellites, such as Lageos, Etalon, GPS35, 36...

The characteristics of the telescope are as follows:

1. effective apeture: 1060 mm
   (It can use both in transmit and receive)
2. configuration: Az—Alt
3. transmission mode: friction transmission directly drived by torque motors
4. resolution of the encoder: 0.″ 36
5. pointing accuracy: ±1″ (R.M.S)
6. tracking accuracy: ±1—3″ (for lageos, etalon...)

IV. Laser

This is the active and passive mode-locked Nd: YAG laser, manufactured in Beijing. The laser consist of an oscillator and three stage amplifier.

The characteristics of the laser are as follows:

1. wavelength: 0.532 nm
2. energy per pulse: 150 mj (max. 200mj)
3. pulse duration: 200 ps
4. repetition frequency: 4 Hz
5. divergence: 0.8±0.2 mrad
6. output beam diameter: 10 mm
7. output laser mode: TEMoo

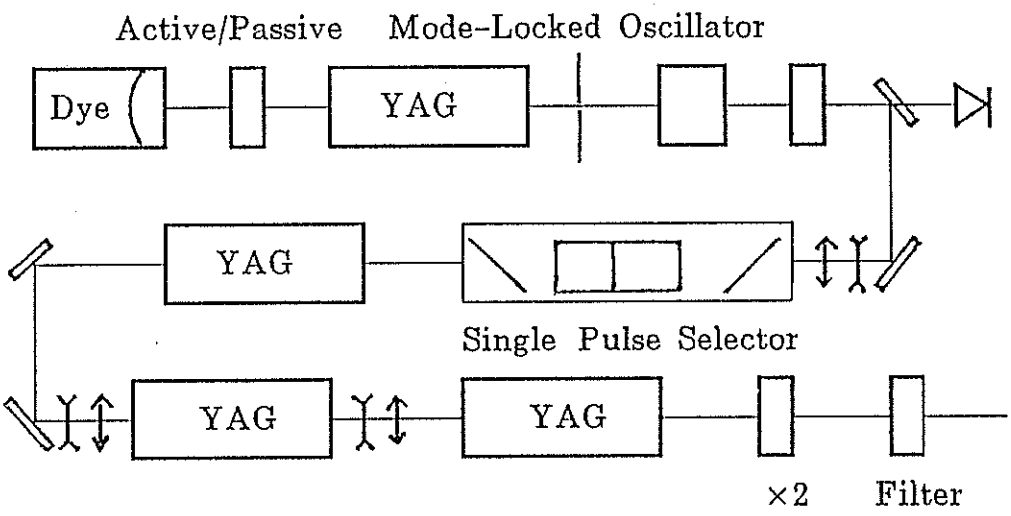

F3. Nd:YAG laser diagram

V. Time and Time Interval Measurement

The time system of Yunnan Observatory is based on the rubidium time and frequency standard calibrated by Loran-C receiver. These old devices have worked for over 20 years and will stop the routine service by end of this year. We plan to use much more reliable GPS timing sysem.

For flying time interval measurement, time interval counter model SR620 is selected. It has a resolution of 20ps and an accuracy of better than 100ps. F4 is the diagram of flying time interval measurement. The range gate has a resolution of 0.1 μs, gate width of 0.1us~6 ms and minimum range of 0~3 s.

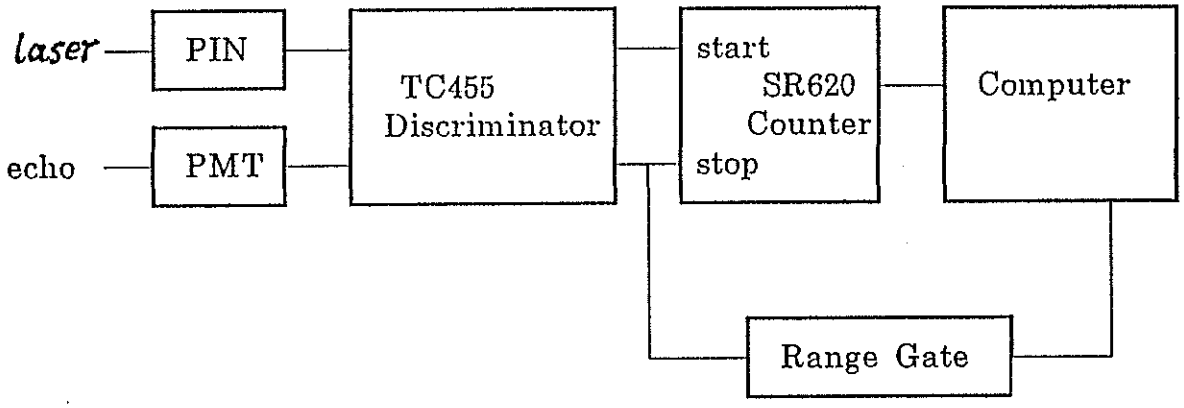

F4. Flying Time Interval Measurement

Ⅵ. T/R Switch and Receiver

The YLRS has the same optic path for both transmit and receive. These are mirrors M1~M8 of 1.2 m telescope (see F1) and two matching mirrors. The rotating mirror M9, drived by a stepping motor, switchs between transmit and receive.

To the receiver of the YLRS, PMT (RCA 8850) is used at first. The avalanche diode with transistor cooler will be developed later to improve the performance of the system.

Ⅶ. Imaging and Guiding System

M8 in F1 is the dichroic beam splitter. While the laser beam is almost totally reflected, the beam of other wavelength will transmit the splitter. The CCD camera and imaging device are installed for sky mapping to correct the pointing errors of the telescope. After imaging processing, precise positions of stars (about 0.1 arc sec.) can be measured. It is convenient to use an ICCD camera here for guiding of satellites.

THE SIMEIZ (N 1873) SLR STATION.

L.S. Stirberg (Crimean Astrophysical Observatory)
S.K. Tatevian (Institute of Astronomy, Moscow)

The Simeis satellite laser station (N 1873) is equipped with a laser ranger system, based on the 1-m telescope of the CRIMEA type. The installation of the station was made in 1989 jointly by the Institute of Astronomy and the Lebedev's Physical Institute. The initial single-shot precision of the system was 20-25 cm. In 1991-1993, to satisfy the IERS requirements, a modification of the laser system was undertaken by the Institute of Astronomy (INASAN) and the Simeis laser group. The laser transmitter and the time counter were replaced, and a new control PC (an IBM provided by the GFZ/Potsdam) was added. Specially developed software was also installed.

Simeiz SLR system Description.

Mount configuration	Azimuth-Elevation, Coude system for transmitted and received beams.
Movement drive	2 axis stepping motors and 2 driving motors of constant currents are used.
Tracking speeds	Azimuth - max 3.4 deg/sec Elevation - max 3.4 deg/sec

The Elevation-Azimuth telescope movement is provided by the two step-motors and two small constant current motors, installed in parallel, to increase the tracking velocity limit. Axes of the step and constant current motors are connected by a special belt gear. There is no need for an additional power supply for constant current motors, since they receive power through the dividing capacitors and diodes of the step motor resistances. When the frequency of the step motor pulses is increased, the capacitors let current pass to the diodes, and the constant current motors start working. The higher the frequency, the larger the current to the motors. This makes it possible to increase the velocity of the telescope movement to 4 deg/sec.

1.2 Laser Transmitter

Type of laser	Nd: YAG, Q - switched
Laser wavelength	532 nm
Pulse width	250 -350 ps
Output energy	100 - 120 mj (satellite)
Repetition rate	1 Hz
Output beam divergence	6 - 50 arcsec (adjustable)

1.3 Receiving System

Optics	Spherical mirror, diameter 1 m effective area 0.72 sq. m
Optical filter	4 nm, 60% transmission
Photomultiplier	FEU-79, rise time 0.5 ns, (since June, 1996 - C31034A PMT)
Mode	Single PE detection

The receiving-transmitting systems are controlled by the same PC/386.

1.4 Ranging Electronics

Time interval counter	PC-500
Discretion	25 ps
Resolution	100 ps
Calibration	Short external path (fiber optics)

1.5 Time and Frequency System

Frequency standard	Rubidium 3 e-12
Synchronization	TV
Resolution interval	0.1 ns counter

The new software includes a real-time tracking program, IRV and ORBMESSE predictions, graphic images of tracking passes at the screen, analysis programs and polynomial filtering.

In the receiving system there is a device for automatic recording of the energy of photomultipliers pulses for every range measurement.This makes it possible to correct measurements in real-time for amplitude variations due to the effects of multi-photons pulses. The dynamic range of the signal energy control system is 35 db. To avoid nonlinearity in the response of the PC-500 counter, it is necessary to record the time of a start pulse relative to the 5 MHz base frequency. The time registration precision of the counter is 1 ns. As a result of the SLR system upgrading (changes of the laser transmitter and time interval counter, measurements of return pulse energy, new software and data filtering), the ranging precision has been improved to 5-9 cm. The new laser transmitter will support considerably better ranging precision, but the FEU-79 photomultiplier, which we are presently using, gives a significant jitter(0.2-0.4 ns) and the PC-500 counter has limitations in resolution.Data is filtered using a polynomial fit with a rejection of no more than 15 % of measurements. The data are sent to the European Data Center (Munich) within 10 hours. The Simeiz station observes 150-300 passes per year. The data yield is limited by the instrument performance and weather conditions. The satellites observed include: ERS-1 and 2, LAGEOS 1 and 2, TOPEX-Poseidon, Ajisai, Starlette, Stella, Etalon 1 and 2, and GFZ-1.

Perspective: We plan to upgrade the SLR system and replace the time counter, photomultiplier and some other units with the help of a Grant received jointly with SAO from the Civilian Research and Development Foundation (CRDF), USA, in 1996.

STATUS OF THE SIMEIZ SLR STATION.

1. The Simeiz SLR(1873) station was established in 1989 with the ranging system based on the CRIMEA type 1-m telescope. Since then almost all of the components of the laser system, except of the telescope mount, have been replaced. Since 1993 the station may be considered as a second generation semiautomatic system with visual guiding (night tracking only) and a single shot precision of 6-8 cm.

Upgrading of the Simeiz (N 1873) SLR station. (Oct. 1996)

	1989	1996
Laser transmitter:		
pulse length	2.5 - 3.0 ns	0.25 - 0.3 ns
output energy	0.03 - 0.05 J	0.07 - 0.12 J
Time interval counter:		
resolution	1.0 ns	0.025 ns
precision	0.7 ns	0.015 ns
Control computer	" Chekan" and MERA-400 computers.	PC(ibm) 386, new S/W for system control.
Recording of measurements	magnetic and perforated-tape	Floppy-disks
Software		Software modification for the automatic guiding and data control.
Measurements of the received pulses energy	No	since 1991
Precision	14-22 cm	6-8 cm

2. a) The energy of the received calibration pulses is measured and used to correct satellite range data.

b) Polynomial filtering, 15 % of the outliers are admitted.

>> c) Results of the data orbital control, which are available by E-Mail from the SLR analyses centers, take about a week to reach the station, which makes it impossible to make effective use of this information for daily data corrections.<<

3. " Special" effect.

A nonlinearity in the PS-500 time interval counter was discovered. It was shown that if a transmitting pulse is rigidly tied to the base frequency of 5 MHz, the mean square error of the range measurements is 0.03 ns. If an impulse is emitted randomly in time, the RMS will increase by an order of magnitude. This effect was found when calibration of the PS time counter with a 100 m cable was made. To avoid this interpolator problem, a special method is used: the position of the START pulse is measured relatively to the 5 MHz frequency with 1 ns accuracy; then these data are used for data correction.

New Mobile Systems

Report on Saudi Arabian Laser Ranging Observatory (SALRO)

Attieh A. AL- Ghamdi
Research Institute of Astronomy and Geophysics (RIAG)
King Abdulaziz City for Science and Technology (KACST)
P. O Box 6086, Riyadh 11442, Saudi Arabia
e-mail: ALGHAMDI@KACST.edu.SA

ABSTRACT

Saudi Arabian Laser Ranging Observatory (SALRO) "state-of-the-art" laser ranging system is described. The system meets the SLR system performance specification. SALRO is now on mission support and every available satellite is tracked when weather and serviceability allow. The SALRO normal point analysis results for August and September 1996 is discussed and shown to be 3.6 mm (RMS) for LAGEOS satellite.

1. INTRODUCTION

Satellite Geodesy is a powerful tool for the study of the earth's kinetic and dynamics [1,2]. The rapid progress in laser technology and its applications to satellite ranging has considerably improved the accuracies to the subcentimeter level.

In the last 30 years many Satellite Laser Ranging systems have been installed on most of the global plates. Saudi Arabian Laser Ranging Observatory (SALRO) is the first SLR system to be installed on the Arabian plate. The purpose of the SALRO project is to open an access to the study of the Arabian Plate tectonic motion, which is extremely important because the availability of SALRO data to the SLR community will compliment the existing contemporary relative plate tectonic motions of the Arabian to Eurasian, Australian, South American, North American, Pacific, Nazca, and Caribbean plates.

The SALRO system was designed and developed in Australia by Electro Optic Systems Pty limited (EOS)and has completed testing at NASA, GSFC, USA. The SALRO has been installed in the Solar Village approximately 40 km north-west of Riyadh and operated by Research Institute of Astronomy and Geophysics (RIAG) of King Abdulaziz City for Science and Technology (KACST).

The SALRO uses a 0.75 meter telescope to transmit and receive optical signals from satellites equipped with corner cube retroreflectors. The SALRO laser operates at a wavelength of 532 nm with energy of 100 mJ and generates a pulse-width of 100 ps at a rate of 10 Hz. The SALRO system is easily managed by a single operator, excluding the aircraft observer. The software utilisies both VDU and graphics from the telescope flexure analysis, real-time ranging, and post-ranging data analysis functions, aiding and accelerating the operator and analysts comprehension of the systems performance.

The multi-stop epoch timing is used to measure range time-of-flight with picosecond accuracy. Open ended coupling of its

"state of the art" technologies positions SALRO to meet the emerging developments in fully automated, multicolour, high repetition rate, subcentimeter Satellite Laser Ranging.

The following description of the SALRO system (see **appendix A**) also includes some results of satellites observations from August and September 1996, respectively.

2. Collocation, Site, and Survey

The system underwent comprehensive collocation tests with the NASA network standard, MOBLAS7, prior to its arrival in Riyadh. Extensive analysis of field data at Riyadh, Saudi Arabia (see the map in **figure (1)**)conducted by three NASA-sponsored groups (*Allied Signal Technical Services Corporation, Hughes STX Corporation, and the University of Texas Center for Space Research*) have demonstrated that the LAGEOS (prime source of geodetic reference) data taken at Riyadh is comparable in quality to that of other high quality SLR systems. The SALRO system ranks among the best SLR stations in terms of data quality.

The SALRO is sited in rocky landscape i.e. no sand, with minimal airborne dust, and the elevation is approximately 790 m above the sea level with latitude 24^{0} 54'.638 and longitude 46^{0} 24'.025 (**see figure (2)**) . The first-order survey data is shown in **table (1)**. The SALRO system (**figure (3)**) was installed on a specially-prepared, and very stable concrete PAD. Retroreflectors mounted to three permanent calibration piers are being used to monitor the stability of the system before and after each satellite pass. SALRO is operating and maintaining by the KACST staff. A special building at the site is used to house the staff and support the SALRO operations where a local Area Network (LAN) was installed in the building.

One error source is an apparent large (~ 2.5 cm) discrepancy between the surveyed distance to the south monument pier and the distance determined by the SALRO data. The site survey must be repeated to resolve the calibration range ambiguities among the piers. The tests at the site conducted with the three calibration targets (West, East, South) suggested a system delay which varied with azimuth. The West target, at a distance of 200 m from the station is normally used for routine system delay calibration. The East and South targets are located 400 m and 800 m respectively from the station. The system delay computed from the South and East targets showed biases of 25 mm and 50 mm respectively relative to the West target. To resolve the issue, a special test was conducted using the retroreflector on the telescope spider array which demonstrated that azimuth biases introduced by the system were less then ± 2 mm [3].

COORDINATES			ELEV.
POINT	NORTHING	EASTING	
T-1	2755938.111	641328.533	790.241
T-2	2755786.457	641341.140	790.033
T-3	2755633.808	641378.178	798.336
T-4	2755310.543	641314.045	789.336
T-5	2755199.949	641334.847	791.142

T-6	2755428.911	641659.929	787.884
T-7	2755612.044	641565.593	789.085
0	2755813.540	641422.980	793.196
P-1	2755013.565	641422.916	792.491
P-2	2756013.609	641769.452	790.049
P-3	2755908.545	641258.467	793.763

Table (1). Coordinates and Elevations of the SALRO site.

3. SYSTEM DESCRIPTION

Figure (4) illustrate the interior layout of the SALRO trailer. The SALRO trailer consists of four sections:

- 5 Meter Dome, with 30° Contraves Telescope.
- Coude' Room, contain laser system, Transmitter, and Receiver.
- Control Room, work station for operation contain computers, Handpaddle, Printers ..etc.
- Facilities Room, contain MPACS Rack, Computer Rack, Control Rack, Electrical Distribution, ACU#1 CTRL, ACU#2 CTRL ..etc.

3.1 Dome and Telescope

The 5.1 meter diameter Dome was manufactured by observa-Dome Laboratories of Jackson, Mississippi. The Dome has single slit opening, composed of laterally moving half doors for fast performance. The rotation is unrestricted at about 5 degrees per second, with slip rings for power allowing control of the slit at any azimuth. The Dome is totally automated during ranging and star tracking operations i.e. initializing, slit opening, tracking, parking and slit closure.

The SALRO Telescope design embraces the needs of a traditional Astronomical observing platform to the specific requirement of an SLR system. The SALRO telescope is a CONTRAVES Inc. manufactured item, and is based on the standard MOMS mount. The coude path allows the full telescope aperture to be utilised for both transmit and receive. There is an adjustable secondary mirror for precise focus setting under software control (a computer readable thermistor returns tube temperature to account for thermal expansion in the telescope tube).The SALRO telescope, also provided by an indexed rotating tertiary mirror, allows the Nasmyth 2 port to be used for astronomical observations. To enhance tracking and imaging (photographic) of multiple stellar objects the telescope's also enhanced by a computer controlled derotating stage on the Nasmyth 2 port. By this way it keeps their angular relationship intact. One more enhancement is that the telescope optics are coated with enhanced aluminum with a silicon oxide over-coat for protection and to prolong the time between re-aluminising.

The control electronics reside in the facilities room. The system is the Model 30H MPACS (Modular Precision Angular Control System) and its features include position and rate driving modes and chassis display of encoder position readouts with 0.0001

degree granularity. Off-mode-stops the telescope with out requiring commands for unique positions.
It is also provided with an external computer and local keypad command/data input facilities. Another feature is the fast slew rate in both axes, reducing the traditional ranging zenith keyhole. The last feature is the high bandwidth for precise computer control at very high rates [4].

3.2 CUODE' ROOM

3.2.1 Laser and Receive/Transmit Systems

The block diagram of the SLR laser system at SALRO is shown in figure (4). The laser source consists of a Nd: YAG laser Quantal YAG 501C series modified by EOS for SLR operations. The laser has an active/active mode-locked oscillator with 80 ps minimum (80-250 ps, normally 110 ps) pulse-width and 1064 nm wavelength. Two amplifiers combine to produce in excess of 110 mJ per pulse at a repetition rate in excess of 10 Hz when needed. The frequency slicer is a Quantal solid-state slicer model SPSH-11 with H.V avalanche board and double pockle cell. It is vastly superior to the old Krytron slicer and needs no maintenance at all. The SALRO slicer is further enhanced by the EOS option of external trigger. This trigger is locked to the Active-Active oscillator trigger ensuring that the same pulse is taken every time (i.e no pulse jumping, which happens frequently with the optical feedback system).
The result is a highly stablized output. Doubled output of 532 nm beam light is generated from the second Harmonic Generator (SHG) using KD*P nonlinear crystal. The output laser light has an approximate divergence of 80 arcseconds (~ 400 micro radians). The system gives oscillator stability of 4%, output power stabilities of 5% and also provides a permanently stable pulse slicing trigger via the A/A circuit.

When the MCP detector is in use and the discriminator module has its walk characteristics optimized over a large input range, signal strengths for terrestrial (eyesafe) versus satellite ranging are matched to maintain calibration. When the SPAD is in use, by virtue of its single photon detection ability, and optical "splash" any prior signal to the internal calibration event will stop the detector, thus leading to unreliable results, real time calibrations have therefore been replaced by the standard NASA pre and post calibrations method of SYSTEM DELAY determination.

Table (2) shows the output power measured with the laser set after oscillator, 1st Amp., 2nd Amp., and SHG, for 100 ps and 250 ps. The short term RMS fluctuation in the power at the laser beam after oscillator, 1st Amp., 2nd Amp., and SHG over 1 minute period give values of 1%, 1.4%, 2.1%, and 1.2% RMS respectively. Signal strength matching is achieved by utilizing ND filters in the transmit path to maintain single photon return rates for all targets. Single photon ranging is defined by the SPAD manufacturer's as being approximately 25-30% return rate. In practice attenuation of the laser transmission for terrestrial ranging is set between ND 4.0 TO ND 5.0, depending on current atmospheric conditions.

	OUTPUT POWER (mw) for 100 ps	OUTPUT POWER (mw) for 250 ps
OSCILLATOR	65	73
FIRST AMPLIFIER	135	160
SECOND AMPLIFIER	2500	2900
SH GENERATION	1100	1500

Table (2). shows the output power measured with the laser set after oscillator, 1st Amp., 2nd Amp., and SHG, for 100 ps and 250 ps.

During operations utilizing the MCP detector, the real time calibration target can be a retro reflecting cube either on the receiver table, or mounted on the telescope secondary spider. The receiver table source is more stable because the full outgoing laser beam is sampled, whereas when the spider source is in place only a very small percentage of the outgoing diameter is sampled. Two problems can rise when utilizing the spider calibration retro:
a) The vagaries of the laser fringe patterns effect the percentage of signal arriving at the spider retro due to the high/trough pattern.
b) Even though totally internally reflective cubes are used, there is a polarizing component that reduces the returning signal, at some positions of rotation.
There are two racks in the Coude' Room; the Laser Rack and Receiver Rack. Each rack has independent cooling, controlled via thermostat sampling the return air temperature. Temperature stability is not as critical in the coude' room as in the facilities room since the electronics and optics are more stable than, say, the timing vernier in the CAMAC crate and the MPACS electronics.

The laser temperature is controlled via a twin chiller set located beneath the laser table. This set-up maintains the temperature of water used in the standard continuum heat exchange unit and is controlled via (adjustable) Evaporator Pressure Regulator valve on each chiller, thus the temperature is always above local dew point. This essential feature prevents condensation from forming on any sensitive optical surface [4].

3.3 Control Room

3.3.1 Software

The HP A900 has been installed with the standard vendor maintained operating system. The software operating on this computer includes:

1- Timing system calibrations
2- Pass alert and prediction packages (programs ALERT AND PDICT) which take as input UTX IRNs, ATSC TIVs, orbital elements and MIT lunar ephemera's. PDICT can also apply time bias corrections to its predicated pointing and ranges.

3- Star tracking and mount calibration analysis package, with graphical output.
4- Real-time range data acquisition software system for terrestrial, satellite (>500 km one-way) and lunar ranging real time operator feedback.
5- Graphics based engineering range editing/processing package that include:
   a) Standard sample quick-look data files
   b) Normal point generation according to the community accepted algorithm
   c) MERIT II full rate data files
   d) Feedback time bias data for the prediction package
   e) Graphical output to a variety of devices e.g. laser printer etc.
6- A variety of utilities for fixing corrupt range files, extracting diagnostic data etc.

The IBM compatible Vectra PC is used for the following:

1- HP graphics TERMINAL (EMULATED)
2- Data communications and file transfer
3- Word processing, spread sheet and database applications on commercial packages [4].

4. Facilities Room

The MPACS interface provides a means for diagnostic, utility and operational software to communicate with the telescope control system providing absolute positioning and tracking of satellite, lunar and stellar objects in real time. Additional features include 10 Mhz time base clock, derotator control with active error feedback loop, and self test of data addresses and data lines.

The Master Range Control System (MRCS)is the central component of the ranging system; features include:

a- Time of day Clock with synchronizing and off setting facilities.
- Issuing range gating and laser fire signals.
c- Control of the optical transmit/receive switch and receive path via solenoids.
d- Control of gating and signals for the timing verniers in the CAMAC Crate.
e- Provision of precise frequency measurements via programmable interrupts and internal gating.
f- Provision of extensive self testing and simulation facilities.
- Epoch timing to 20 ns granularity.

CAMAC Interface is the gateway to the timing verniers, meteorological sensors and charge digitisar sub 20 nanosecond timing from the range verniers is transferred via this device to the HP A900 [4].

5. COMMUNICATIONS

One significant limitation to station throughput, not foreseen when the various development contracts were put in place, is communications between the HP mainframe and the outside world. This one point was more and more of a headache as the SALRO has progressed through its scrutiny by the advisory panel, and progressed from an engineering system into a production system. The packages provided in the EOS system work well, though the engineering processing package was unacceptably labor intensive for a production site. NASA offered KACST their standard packages, and in some respects these packages have shown themselves superior, but they operate only on a high-speed PC. PCs were connected to the HP via 192K band serial link, and therefore transfer of prediction files to the HP, and transfer of formatted range data from the HP, added a significant operational overhead. In addition, Data processing was automated and routine, but took over 20 minutes to process a LAGEOS pass. To reduce this unproductive time, several sources have recommended that KACST invest in a LAN for the HP/PC network at the Solar Village. For high productivity and to reduce the data transfer bottleneck KACST has implemented a Local Area Network (LAN), where the HP A900 was connected with 3-PCs inside the main staff building, so that analysis data can be transferred and processed much more quicker.

A satellite laser ranging station requires telecommunications media that can really support the timely receipt and transmission of vital data needed for its functions. Daily access to satellite orbital position prediction and time bias information is needed for telescope pointing. The efficiency of the station depends on the format of this information and the manner by which it is transmitted. Similarly, an SLR station needs modes for the timely transmission of the acquired data to Data Centers. Most stations in the global laser network use the internet to perform these functions. SALRO also needs this capability. During SALRO test operations, there were limitations that significantly hampered station productivity and time lines of data distribution. Recently KACST has implemented a direct Internet link at the SALRO offices in Riyadh which has been connected to the SALRO site by PC Modem. An internet access was arranged, so that we may send from KACST offices.

6. Results

The system is now on mission support and every available satellite is tracked when weather and serviceability allow. The number of passes obtained in this period is very good and further successes are assured as the staff of the SALRO become more familiar and competent with the system. Establishment of INTERNET at SALRO offices facilitate the two way transfer of satellite orbit predications and data.

Tables (3) and (4) show the SALRO observations for August and September 1996, respectively. We have received the normal point results from *ATSC*. The analysis starts on the 5_{th} August through 30_{th} September 1996, but because of intermittent communications problems there are 2 days of data missing. There

are 83 passes in the 23 days period in August. Basically the results are quite encouraging, with a new system, new crew and especially when all these pass results are obtained by SPAD.

SATELLITE	TOTAL HITS	PASSES	AVERAGES	RMS
LAGEOS1	102665	27	3802	1.59
LAGEOS2	111190	32	3473	1.62
AJISAI	35317	25	1412	1.73
TOPEX	35177	29	1313	1.47
ERS2	1936	7	276	1.20
STARLETTE	13474	22	612	1.22
STELLA	122	1	122	1.43
GLONASS67	17850	7	2550	6.51
ETALON1	2667	1	2667	3.19
GPS35	1943	2	972	1.35

Table (3). SALRO observations for August 1996.

SATELLITE	TOTAL HITS	PASSES	AVERAGES	RMS
LAGEOS1	60051	28	2144	1.66
LAGEOS2	151520	42	3607	1.64
AJISAI	58340	35	1667	1.95
TOPEX	15709	16	982	1.8
EUROS2	1159	4	290	1.12
STARLETTE	14448	19	760	1.31
STELLA	1233	3	411	1.22
GLONASS63	6259	2	2086	----
GLONASS67	16584	6	2764	4.37
ETALON1	127	1	127	2.34
FIZEAU	280	1	280	----

Table (4). SALRO observations for September 1996.

Figure 6.a and **6.b** show the first data returns obtained in the Arabian Peninsula for LAGEOS-1 and AJISAI satellites respectively. Both these passes were obtained using the Czech Republic 100 micrometer SPAD.

7. Conclusion:

The SALRO meets the satellite Laser Ranging (SLR) system performance specifications and configured for fully automated, high repetition rate, subcentimeter Laser Ranging. The performance of the system, as evidenced by LAGEOS normal point precision (RMS) of 3.6 mm and a near zero range bias, placing it highly in the global SLR network.

8. Acknowledgments

The financial support of KACST is gratefully acknowledged. Many people deserve individual thanks, and I would like to acknowledge

my dept to the KACST people who contributed to SALRO (past and present); thank you Dr. A. Alqadhi, Dr. M. Alsuwyeel, Dr. F. Noor, Dr. A. Neiazi, Dr. M. Al-dail, S. Alsa'ab, A. Al-khashlan, F. Alsa'eid, F. Alhusain, Z. Almustafa. I also wish to thank the staff of EOS led by Dr. B. Greene, special thanks to John Guilfoyle for his extraordinary effort to bring SALRO to the current status.

9. References

1 Smith, D.E., R. Kolenkiewicz, P. Dunn, J. W. Robbins, M. H. Torrence, S. M. Klosko, R. G. Williamson, E. C. Pavlis, N. B. Douglas, and S. K. Fricke, "Tectonic Motion and Deformation from Satellite Laser Ranging to LAGEOS". *J. Geophys. Res.*, 95, 22, 013-22, 041, 1990.

2 Harrison, C. G. A., and N. B. Douglas, "Satellite Laser Ranging and geological constraints on plate motion". *Tectonics*, *9*, 935-952, 1990.

3 "SALRO FAT Review Board Report", SALRO, Riyadh, 20-23 July 1996.

4 a) "PRELIMINARY ACCEPTANCE BOARD REVIEW AND BRIEFING DOCUMENT", SALRO, Riyadh, 12 SEPTEMBER 1994.
b) "SALRO ACCEPTANCE TEST PLAN", by EOS PTY Limited, 22 February, 1995.

5 Greene, B., personal communication, EOS pyt Limited, Australia.

Appendix (A)

SALRO PERFORMANCE SPECIFICATIONS

TELESCOPE

Aperture	:	75 cm, both transmit and receive
Configuration	:	Alt/Azimuth
Optics	:	Coude configured for transmit and receive
Drive	:	DC Torque Motors
Pointing Accuracy	:	1 arc second RMS
Position Readout	:	to 0.5 arc seconds, both axes
Slew Rate	:	20 degrees/second (azimuth)
		5 degrees/second (elevation)
Acceleration	:	5 degrees/sec/sec (azimuth)
	:	3 degrees/sec/sec (elevation)
Sky Access	:	to 95% elevation, all azimuths
Working Foci	:	Coude (Nasmyth 1)
	:	Derotator (Nasmyth 2)

LASER

Type	:	Nd:YAG, Continuum (Quantal) YAG501C
Oscillator	:	Active/Active ML (80 ps minimum pulsewidth
Wavelength	:	532 nm
Pulse width	:	80-250 ps, nominal 110 ps
Repetition Rate	:	1 to 15 Hz
Pulse Energy	:	85 mJ/80 ps
		110 mJ/100 ps
		125 mJ/250 ps

START DETECTOR

Photo diode	:	Fast Optical Switch Detector, Czech Technical University

RECEIVER

PMTs	:	MCP (ITT 4129F)
	:	Single Photon Avalanche Diode (SPAD) Czech Technical University
Filters	:	10 Angstrom and 1.5 Angstrom

STATION TIMING

Primary Standard	:	HP5061B Cesium Beam
Secondary Standard	:	FTS 1050A Quartz Oscillator
Time Transfer	:	FTS 8400 GPS Satellite Receiver

RANGING TIMING

Resolution	:	5 picoseconds
Random Error	:	10 picoseconds RMS (single event)
Systematic Error	:	1 picosecond RMS

CALIBRATION

Modes available	:	Terrestrial Target (for Pre/Post pass)
	:	Real-Time (feedback)

COMPUTERS

	:	HP-A900 System
	:	HP Vectra 386

WEATHER SENSOR

	:	Temperature (5)
		Humidity (1)

Pressure (1)
Wind speed (1)
Wind direction (1)
Lighting conductor (1), for connection to ground mat where available

FACILITY : 13mx3m (approximately) relocatable observatory with astronomical dome. The prime mover for relocating the observatory is not included

PERFORMANCE : SLR: 5mm normal point in 2 minutes
SLL: 1 cm normal point in 20 minutes

: SALRO shall be meet or exceed the following overall system performance requirements for ranging to the Laser Geodynamics Satellites (LAGEOS1&2):

1. Single-Shot Ranging Precision shall be one centimeter (RMS) or better when:
   a. Magnitude 3 stars are visible at the site to the unaided eye, and
   b. seeing is better than 6 arc seconds.
2. Minimum Precision for two minutes normal points shall be 0.5 centimeter or better,
3. Systematic errors shall be less than one centimeter for 95% of the two minutes normal points,
4. The data yield shall, at a minimum, be 50 returns per normal point for 67% of the time the satellite is above the ranging horizon, and
5. The SALRO shall be capable of ranging during both the day and the night.

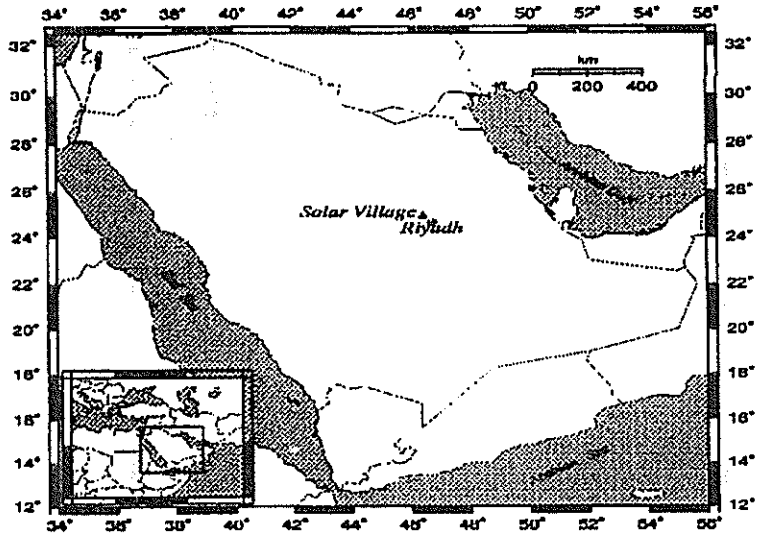

Figure (1). SALRO sited in the Solar Village 45 km northwest of Riyadh in the Arabian plate.

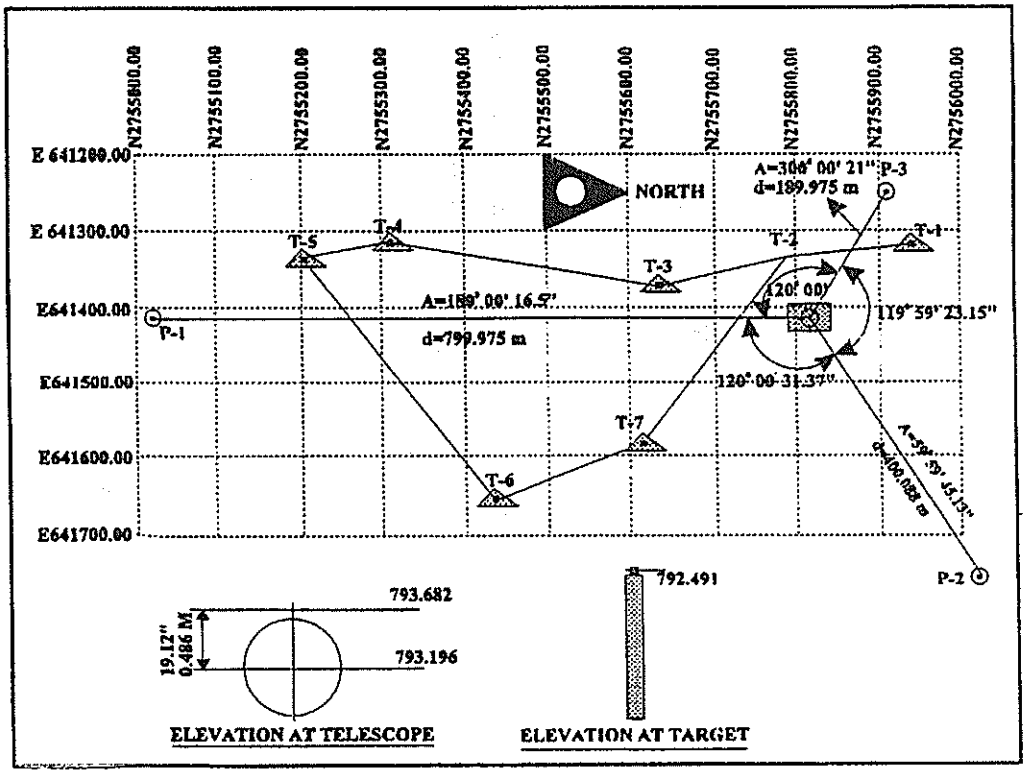

Figure (2). The site network- first order survey.

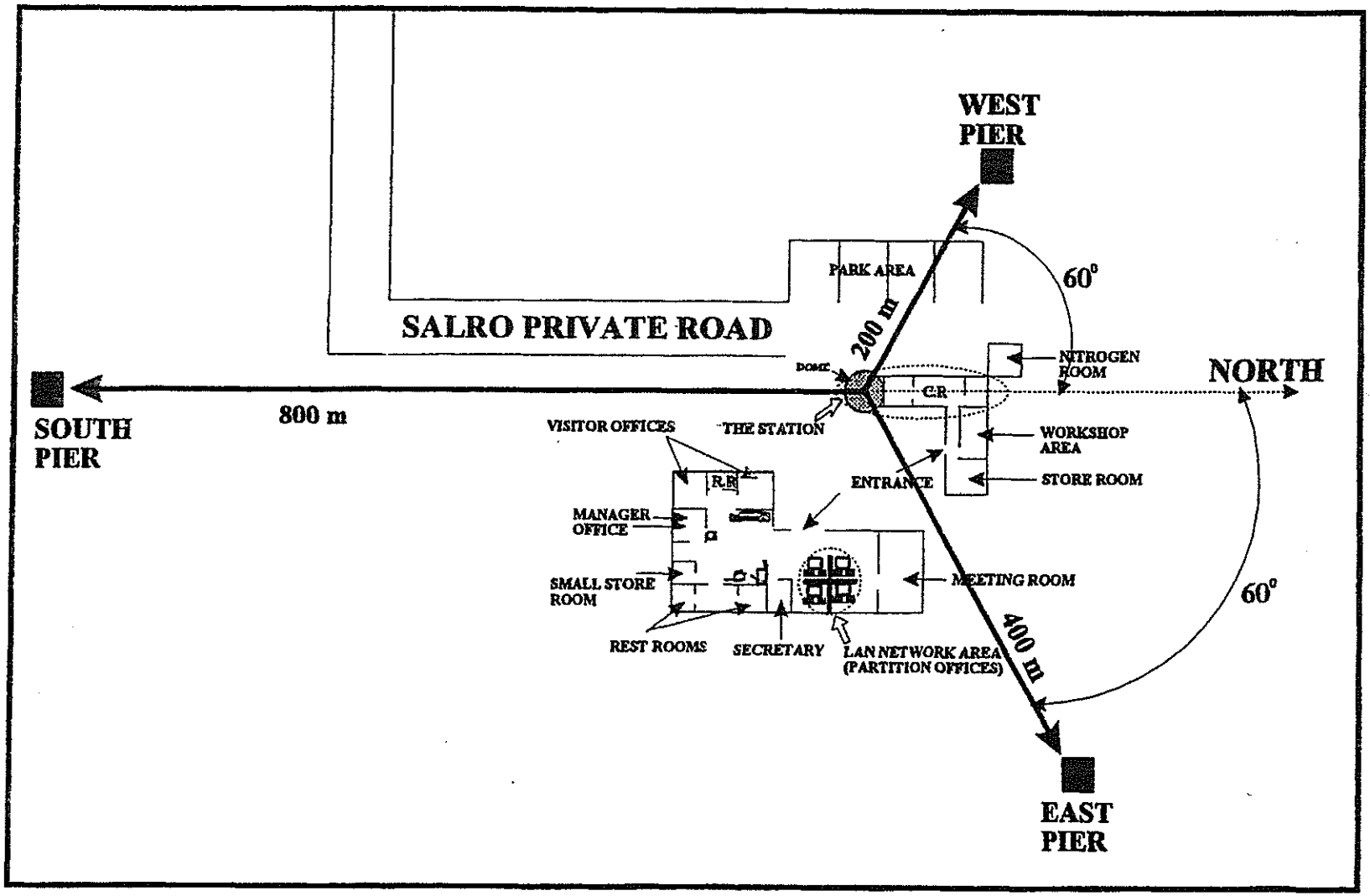

Figure (3) Salro Site Constraction

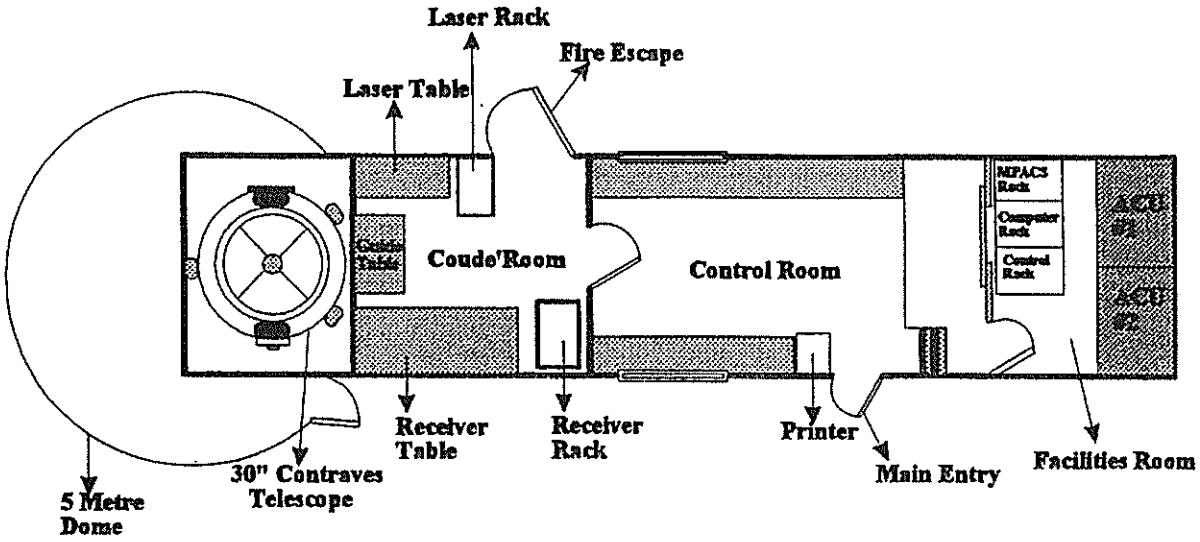

Figure (4) Schematic diagram of the SALRO system-an overall view.

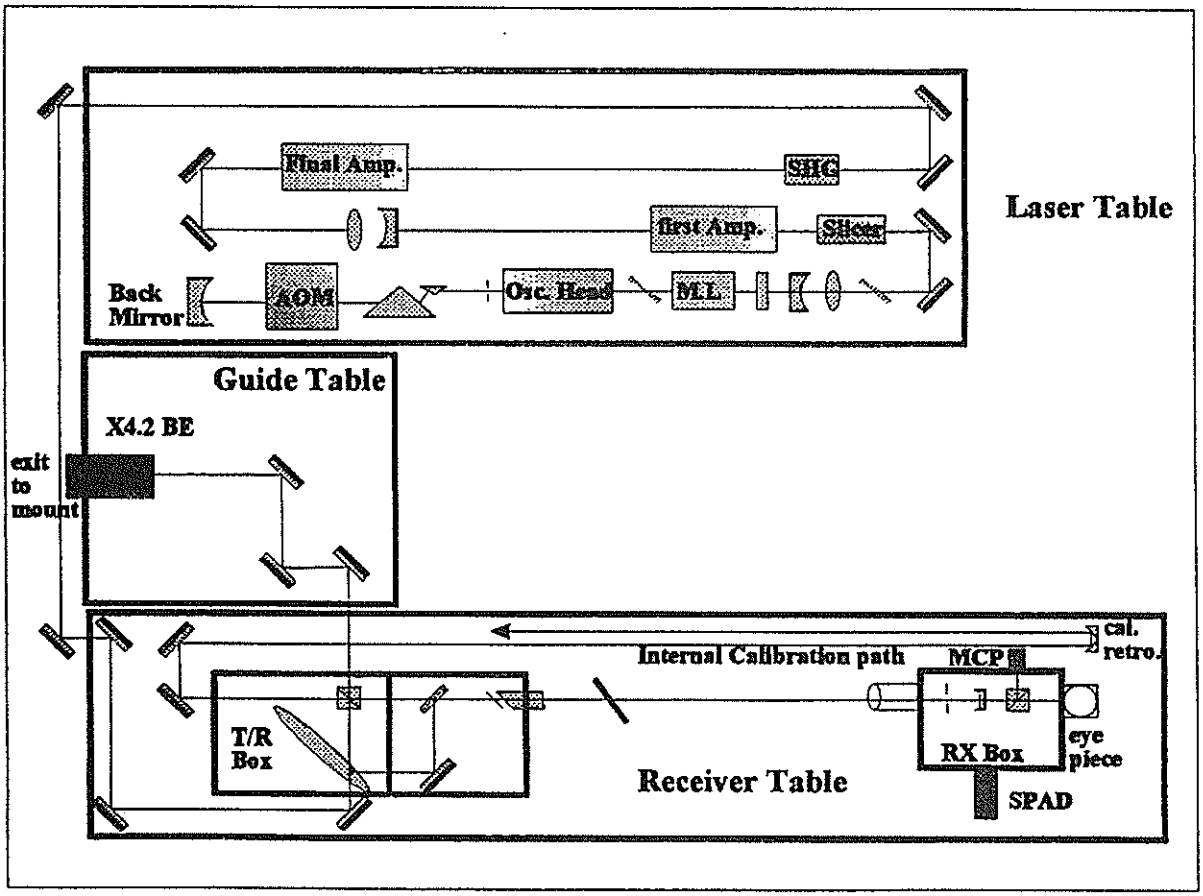

Figure ((5). Coude' Room Optical Layout

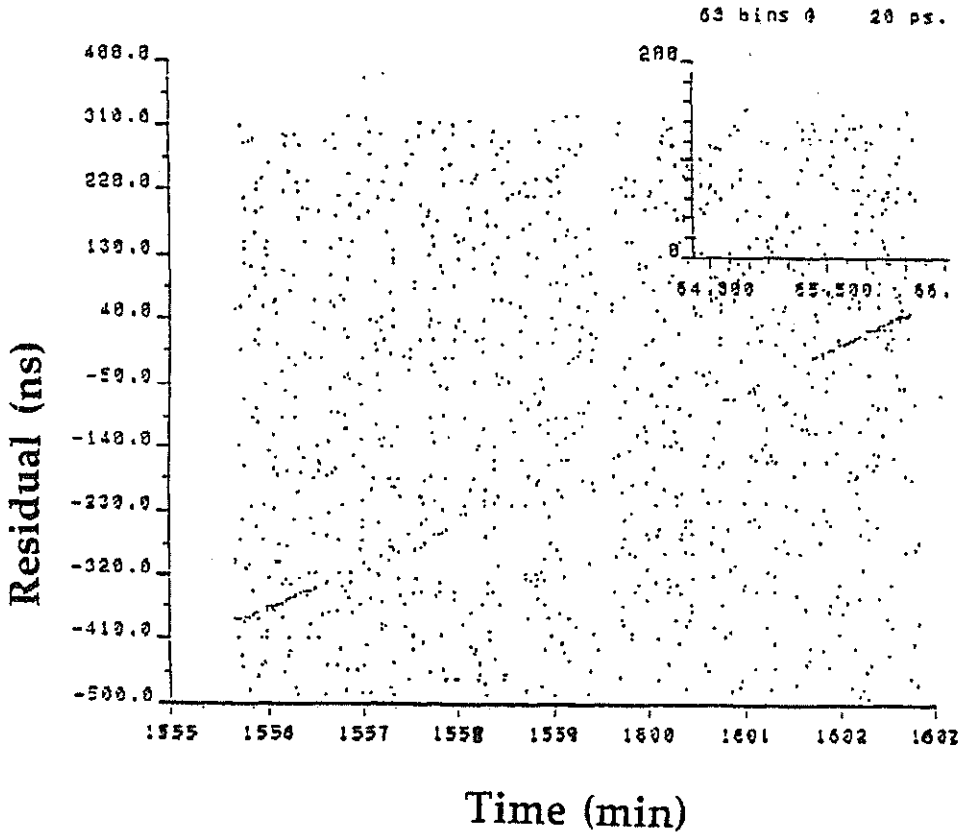

Figure (6.a). The data shows the first satellite ranging on the arabian Peninsula by SALRO. The data collected is from the LAGEOS-1 satellite using SPAD detection system.

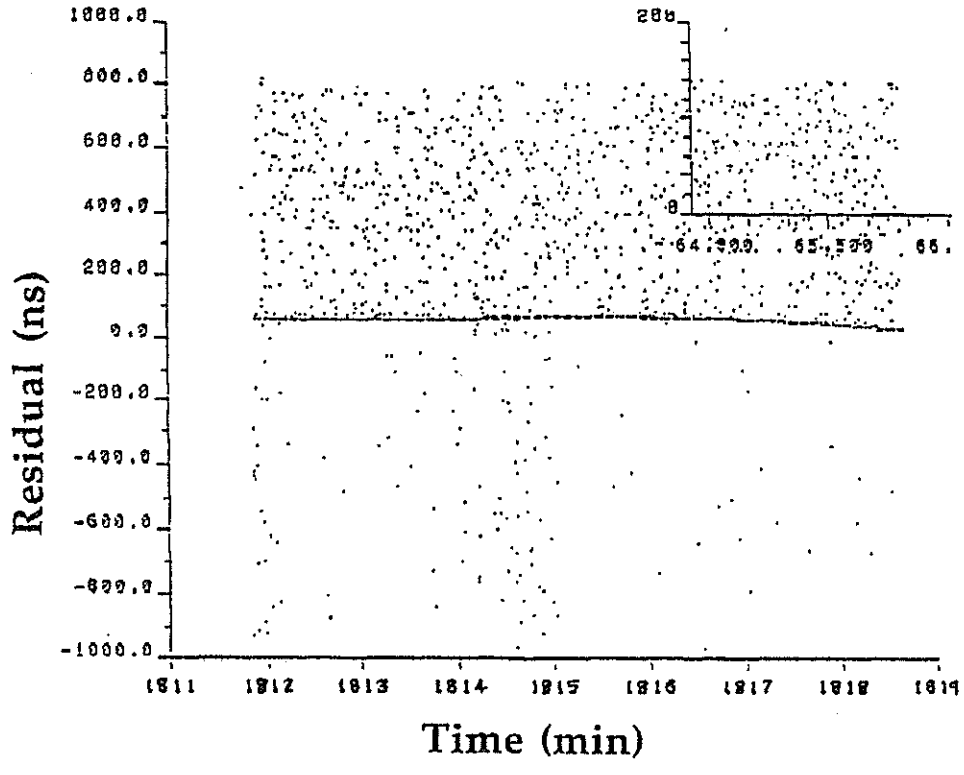

Figure (6.b). First data collected from AJISAI satellite by SALRO using SPAD detection system.

TIGO-Project: Concept-Status-Plans

P. Sperber, A. Böer, R. Dassing, H. Hase, W. Schlüter
Institut für Angewandte Geodäsie
Fundamentalstation Wettzell
D-93444 Kötzting

R. Kilger
Forschungseinrichtung Satellitengeodäsie der TU München
Fundamentalstation Wettzell
D-93444 Kötzting

Abstract: This paper will give a short overview about the concept, the actual status and the plans of the Transportable Integrated Geodetic Observatory (TIGO).

Currently all components of the observatory are assembled at the Fundamental Station Wettzell. During 1997 and 1998 the observatory will operate for a test period in Wettzell, then it will be used abroad as a fundamental station for the densification of the network of observatories realizing the terrestrial reference frame.

1. Introduction and Concept

TIGO is the acronym for "Transportable Integrated Geodetic Observatory". TIGO will consist of the relevant instruments for geodetic space techniques such as for VLBI, for SLR and GPS as well as other relevant sensors as a gravity meter, a seismograph and meteorological sensors. TIGO integrates the advantages of the different techniques and acts as a fundamental station /1,2,3,4,5/. The whole observatory is housed in standard sea-containers for transportation. During 1995 a platform for TIGO has been built at the Fundamental Station Wettzell (figure 1) in order to assemble and to test the whole equipment. In 1995 the 6 m-radiotelescope and 4 of 5 transport and laboratory containers (figure 2, 3) have been delivered. As soon as the MK IV Data Acquisition Terminal (DAT) becomes available in 1997 the VLBI module will be operational.

The motivation to build a transportable fundamental station for geodesy and geodynamics results from the need for a better global distribution of reference stations that are representing the terrestrial reference frame. The objective is to densify the terrestrial reference frame and to optimize the geographical distribution by transportable devices.

For geodynamical research a globally distributed network of fundamental stations is required to obtain precise and reliable results. This coordinated network of Fundamental Stations will define and realize a terrestrial reference frame and maintain the reference frame with respect to the extraterrestrial reference frame represented by quasars. Therefore it is possible to determine the position and the motion of Earth in the Universe. For this purpose a permanent, complementary and redundant spectrum of observable being sensitive to the rotation of Earth and the crustal motion have to be provided. TIGO is designed to make measurements on sites in the southern hemisphere (for at least 1-2 years per site) with all actual available geodetic sensors. Each module is new designed with a high degree of automatisation.

2. Status

2.1. Platform for TIGO

TIGO requires a prepared platform, in order to mount the radiotelescope on it and to setup the SLR-telescope. A platform was built at Wettzell within 6 weeks in 1995. The specification of the platform consists of:

- concrete fundament (10 x 10 x 1,5 m^3) for the radiotelescope containing a special steel construction to fix the radiotelescope,
- concrete fundament (3.5 x 3.5 x 1.5 m^3) for the SLR module,
- concrete fundament to setup 5 TIGO containers,
- separated underground cable channels for either power or signal cables,
- grounding network to earth all instruments and containers,
- dehydration tubes.

The sixth container with six 25 kW power generators will be located in a sufficient distance to minimize problems due to the emission and vibration of the generators.

2.2. VLBI Module

The 6m Offset antenna for the VLBI module (specifications in Table 1) was delivered in 1995 and tested in 1996. Due to the delay of the Mark IV Data Acquisition Terminal until 1997, the telescope is tested with parts of the Mark III terminal of the Wettzell VLBI System.

OFFSET ANTENNA with S/X-FEEDHORN

Diameter	6 m single offset
f/D	0.3629
Surface Accuracy	0.4 mm
Azimuth velocity	6 deg. per second
Elevation velocity	3 deg. per second

	Frequencies	Efficiency
S-Band	2.216 ... 2.350 GHz	64% (spec.) ... 67%
X-Band	8.108 ... 9.036 GHz	68% (spec.) ... 71%

Antenna Noise Temperature (45 deg. El., clear sky, 300K)

Antenna Noise	27K (S-Band)	24K (X-Band)
Ohmic Noise	26K (S-Band)	26K (X-Band)
Total Noise	53K (S-Band)	50K (X-Band)

Helium Cooled S/X-Receiver via NASA-GSFC
MK IV Data Acquisition Terminal and Field Unit via NASA
Set up time in Field < 2 days
Antenna, Receiver delivered in 1996 # MK IV expected in 1997

Table 1: Specifications of the TIGO VLBI Module

2.3. Basic Module

Three containers of TIGO are used for the basic module, in which five subsystems, which are important for the operation of the main modules or give additional information for the data analysis, are integrated.

Precise Satellite Microwave Systems, which includes 5 GPS receivers (IGS standard receiver and a GPS array around TIGO for local control survey). GLONASS, PRARE and Doris receivers will be placed on request.

- In Situ Observations consisting of a superconducting gravity meter, seismometer, meteorology sensors (pressure, humidity, temperature, rain, wind speed, water vapour radiometer) and a time & frequency system (hydrogen-masers and cesium-clocks).

- The central control computer will directly control most of the subsystems of the basic module and work as data storage and distribution system for all modules.

- LAN and WAN communication facilities will be available. All modules will be connected over a LAN to exchange of data and to control/operate TIGO from one terminal. Dependent on the possibilities of the site, the WAN will be realized by direct Internet connection, telephone line or INMARSAT data transmission.

- A powersystem consisting of six 25 kW Diesel generators and a solar power system (220 V, 48 V, 24 V, 12 V) will provide TIGO with electrical power in operation and standby mode.

2.3. SLR Module

The SLR module (specifications in Table 2) is currently in the final assembly and test status at TPD, TNO Institute of Applied Physics in Delft /6,7,8/. Telescope, Optics and Laser have passed the test procedures. These components are currently integrated and assembled with the control system consisting of the electronics, timing facilities and software.
Preparations are ongoing at the Technical University Delft to place the SLR-module on a pad for final testing and acceptance (Demonstration of ranging to all satellites). The delivery of the system to Wettzell is expected in summer 1997.
The telescope in the opened cart and the cart with telescope in the container (transport configuration) is shown in Figure 4, 5. The laser system is shown in Figure 6.

3. Operational Plans

After integration and test operation of the complete observatory at Wettzell in 1997/1998 the system will go into field operation. A small workshop at Wettzell is planned for 1997 to discuss the best sites for TIGO. The necessity for additional sites in the southern hemisphere is obviously shown in Figure 7, where the distance of SLR-, VLBI- and Fundamental Stations to their closest neighbour is plotted and the remote regions with distances of more than 4000 - 5000 km to the next station are marked with crosses /3/. In field TIGO has to be operated in close cooperation with a partner of the host country.

Overall Specifications	Telescope Specifications
Subcentimeter Ranging Accuracy	Folded Lens Telescope without central obscuration Diameter: 500 mm
Range from 0 up to 40000 km	Aberration Correction for 847 nm and 423.5 nm
Two-Color System	Max. Field of View: 4 arcmin
High Automatic Operation	Optical Efficiency: 75%
50cm Telescope for Transmit and Receive	Material: Static Part: Granite Tube : Stainless Steel Fixations : Titanium
High Efficiency in Transmit/Receive	Mass: 1700 kg
Internal and External Calibration	Pointing Accuracy: better than 2 arcsec RMS
Cr:LiSAF/Titan Sapphire Laser	Speed: 6 deg/s (Elevation) 15 deg/s (Azimuth)
3 Detector Ports (SPAD)	Encoders: 21 bit absolute accuracy: 0.8 arcsec
# Set up Time < 2 days # Delivery: begin 1997	Size of Mount: Height : 2 m Diameter: 1.3 m

Table 2: Specifications of the TIGO SLR Module

4. Summary

The Transportable Integrated Geodetic Observatory TIGO is currently assembled at Wettzell and will be ready for test operation in summer 1997. The observatory combines a complete set of state-of-the-art geodetic measurement techniques to form a fundamental station for geodesy and geodynamics.

The system will improve the global distribution of stations significantly when it starts field operation in the southern hemisphere.

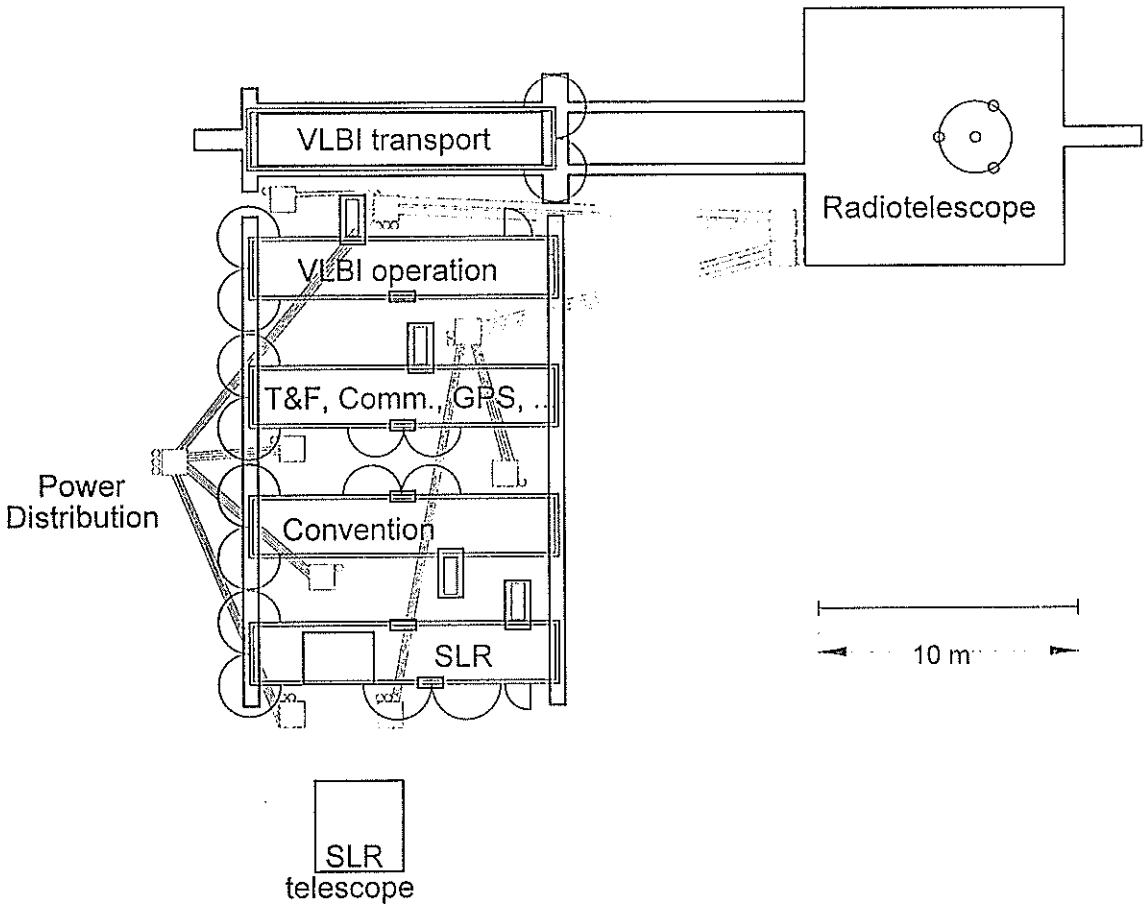

Figure 1: Schematic of the TIGO platform designed for Wettzell

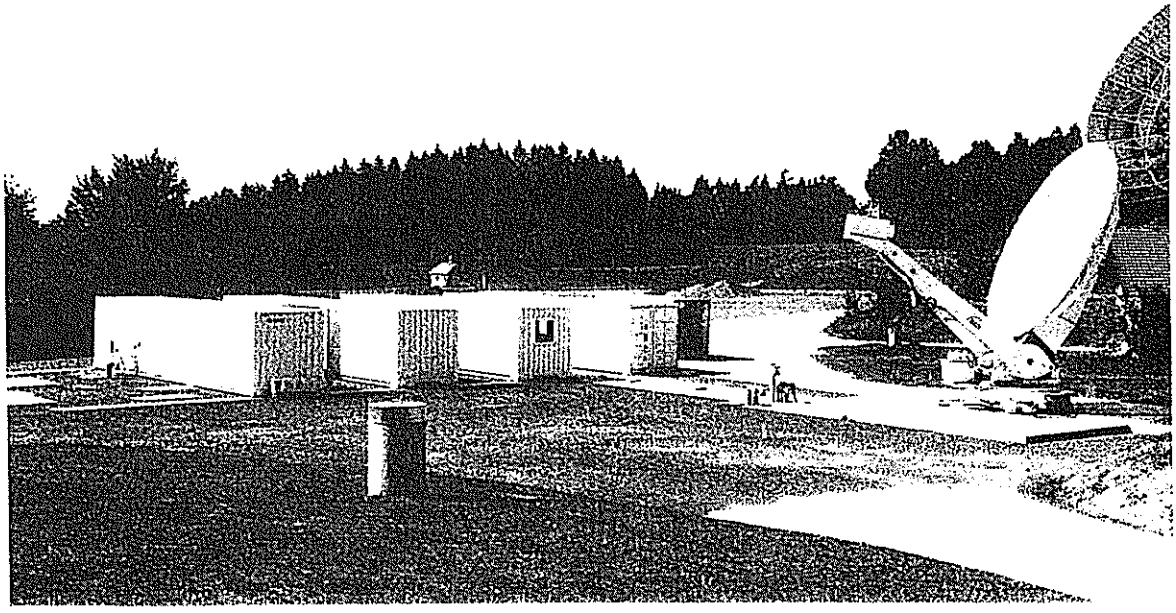

Figure 2: Four of five TIGO laboratory container and VLBI antenna

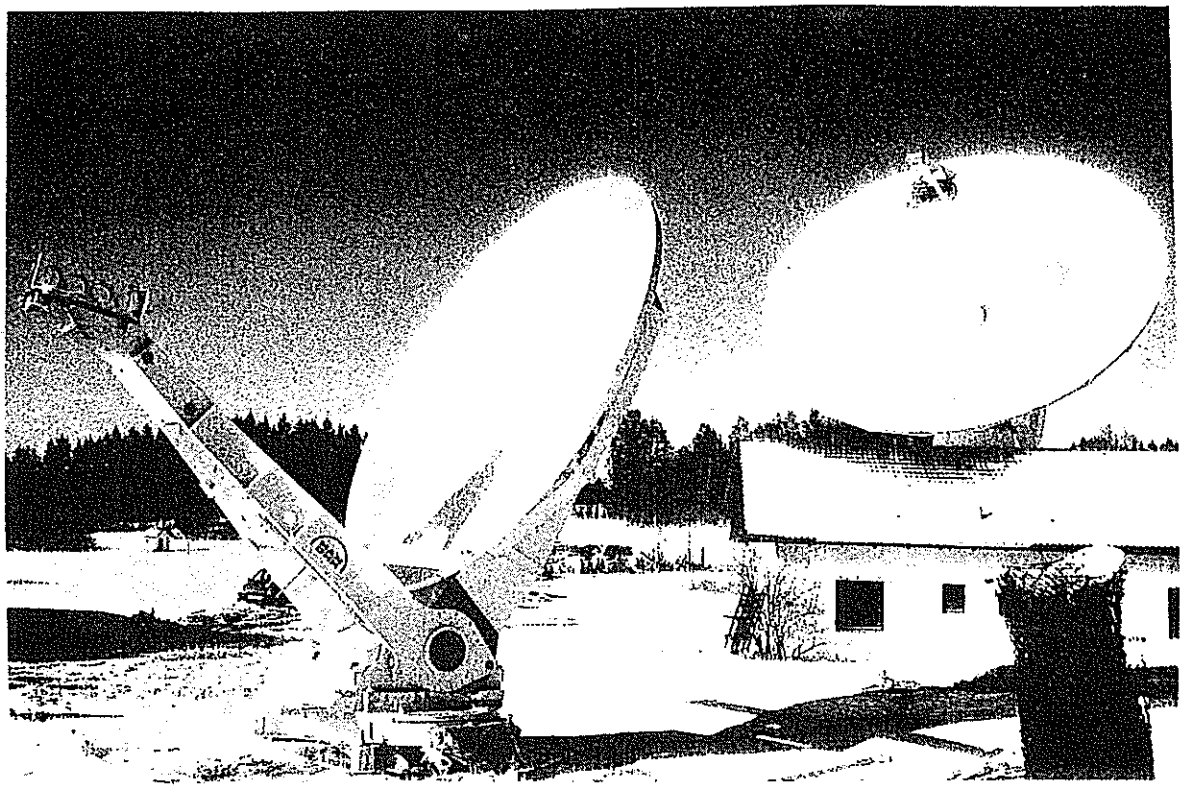

Figure 3: 6 m VLBI antenna in front of the 20 m VLBI antenna at Wettzell

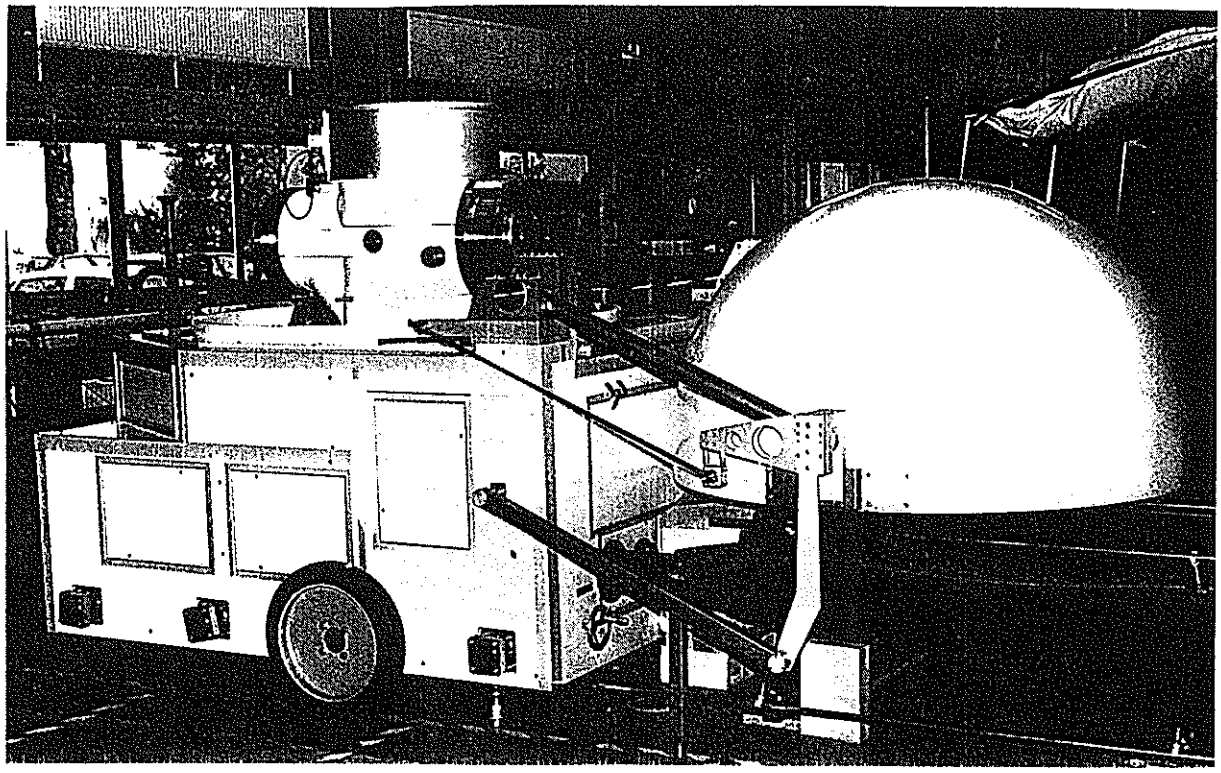

Figure 4: TIGO SLR Telescope in the open cart (ranging configuration)

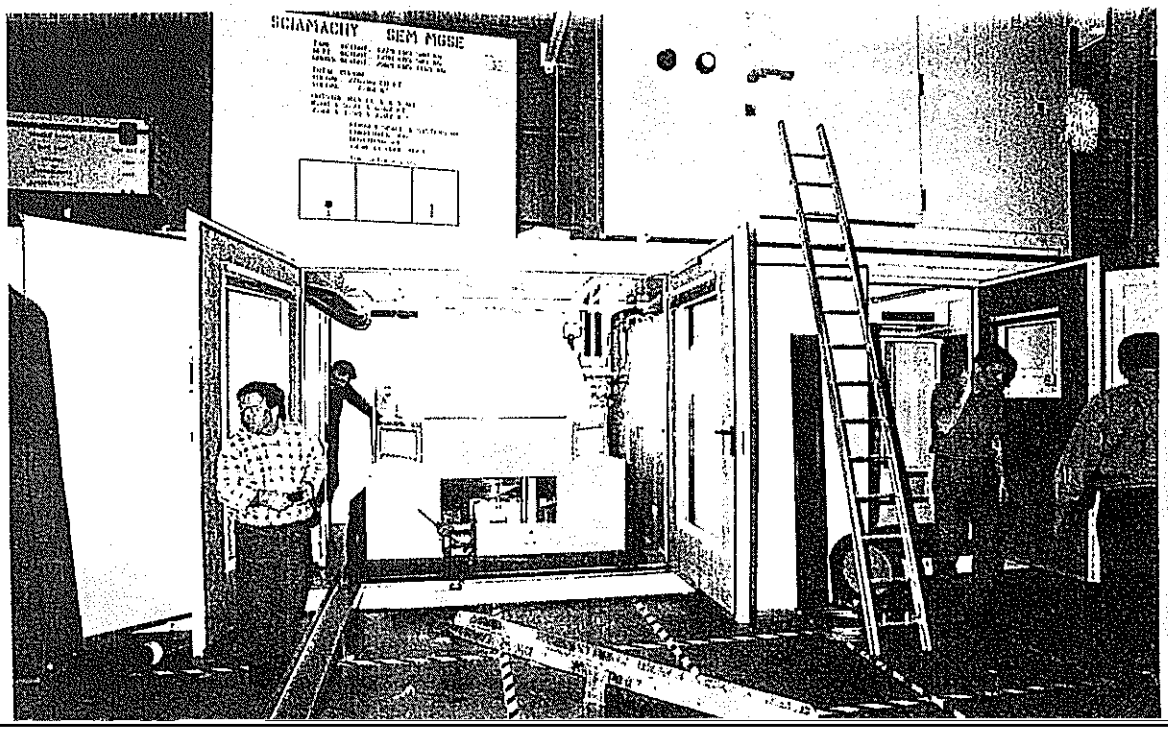
SCIAMACHY SEM MGSE

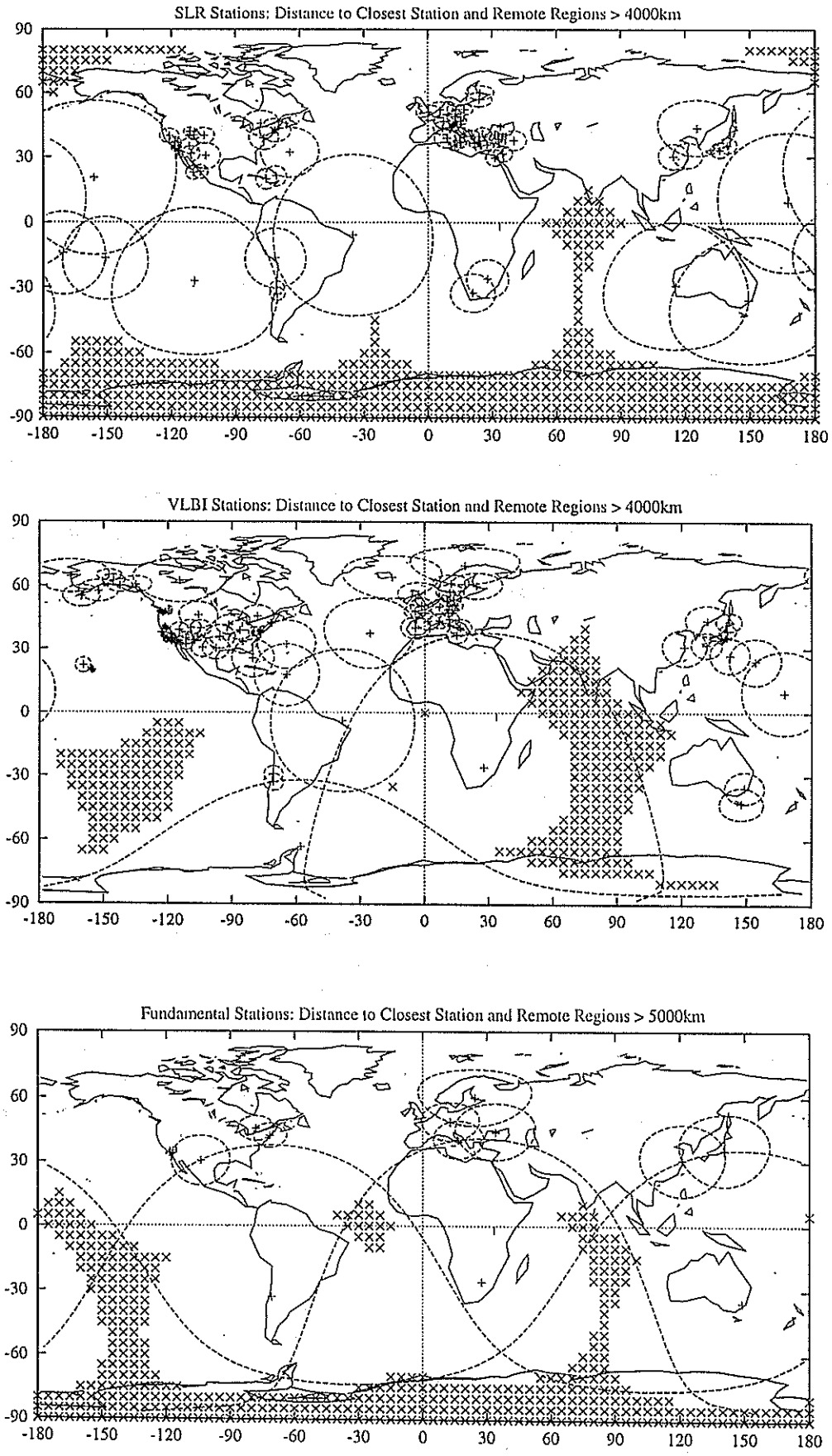

Figure 7: Worldwide distribution of SLR, VLBI and Fundamental Stations (ITRF 93) and their distance to the closest neighbour

References:

/1/ Seeger H., Schlüter W., Dassing R., Böer A., Hase H. Sperber P., Kilger R., TIGO Transportable Integrated Geodetic Observatory - A Fundamental Station for Geodetic Research, XXI General Assembly of the IUGG, Boulder (1995)

/2/ W. Schlüter, A. Böer, R. Dassing, H. Hase, P. Sperber, R. Kilger, "The Transportable Integrated Geodetic Observatory-Status of the System", Dynamics of Solid Earth (DOSE), Pasadena, (1995)

/3/ H. Hase, W. Schlüter, A. Böer, R. Dassing, P. Sperber, R. Kilger, "Status of the TIGO Project", Proceedings of the 4th Asia Pacific Telescope Workshop, Sydney, (1996) (in print)

/4/ W. Schlüter, A. Böer, R. Dassing, H. Hase, R. Kilger, E. Reinhart, B. Richter, W. Riepl, U. Schreiber, H. Seeger, P. Sperber, "Die Fundamentalstation Wettzell", Verlag des Instituts für Angewandte Geodäsie, Beiträge zum J. J. Baeyer-Symposium, Berlin-Köpenick; Deutsche Geodätische Kommission, Reihe E, Heft Nr. 25, (1996) 143

/5/ W. Schlüter, A. Böer, R. Dassing, H. Hase, R. Kilger, P. Sperber, "Status of the TIGO Project", IAG/CSTG working group on IUGG Fundamental Reference and Calibration Network, Baltimore, (1996)

/6/ P. Sperber, A. Böer, U. Hessels, W. Schlüter, "TIGO-SLR Module: Status", Proceedings of the 10th International Workshop on Laser Ranging Instrumentation, Shanghai (1996)

/7/ P. Sperber, A. Böer, F. Estable, F. Falcoz, E. Pop, L. Vigroux, "Cr:LiSAF/Ti:Sapphire based solid state Laser System for Two Color Satellite Laser Ranging", Proceedings of the 10th International Workshop on Laser Ranging Instrumentation, Shanghai, (1996)

/8/ P. Sperber, A. Böer, U. Hessels, U. Schreiber, "Two Color Satellite Laser Ranging using a Cr:LiSAF/Ti:Sapphire Picosecond Laser System", Society for Optical and Quantum Electronics, Proceedings of the Conference on Lasers'96, Portland, (1996), in print

TIGO SLR Modul: Status

P. Sperber, A. Böer, R. Dassing, U. Hessels, W. Schlüter
Institut für Angewandte Geodäsie
Fundamentalstation Wettzell
D-93444 Kötzting

Abstract. This paper gives a short overview about the status of the different subsystems of the new Satellite Laser Ranging Module for the Transportable Integrated Geodetic Observatory (TIGO).

In the moment the module is at TPD (Delft) for final assemblage and is expected to start with test ranging in spring 1997.

1. Introduction

During the last years Satellite Laser Ranging (SLR) using picosecond Nd:YAG Lasers achieved an accuracy of better than one cm. At this accuracy more emphasis has to be placed on the influence of satellite geometry and atmospheric dispersion causing errors up to a few cm. The control and refinement of these models can be done with multiple wavelength ranging /1, 2/. Taking into account the difference in the refractive index, the atmospheric transmission and the sensitivity of single photon detectors, best results are expected with wavelengths around 425 nm and in the near Infrared. This paper reports about the setup of a SLR system, expecially designed for two-color ranging.

The system is based on a Cr:LiSAF/Ti:Sapphire picosecond laser system, a 50 cm compact Lens Telescope and a flexible and powerful controlsystem realized on a Dec Alpha workstation and a transputer network. The whole SLR-Module is installed in a 40 ft standard seacontainer.

2. Overview

This chapter gives a short overview about the specifications and about the status of the different subsystem container, laser, telescope and control system.

2.1. The TIGO SLR Container

2.1.1 Mechanical description

The TIGO Satellite Laser Ranging module is installed in a standard 40 feet sea container (see figure 1). This allows an easy transportation by train, truck or ship without using a special vehicle.

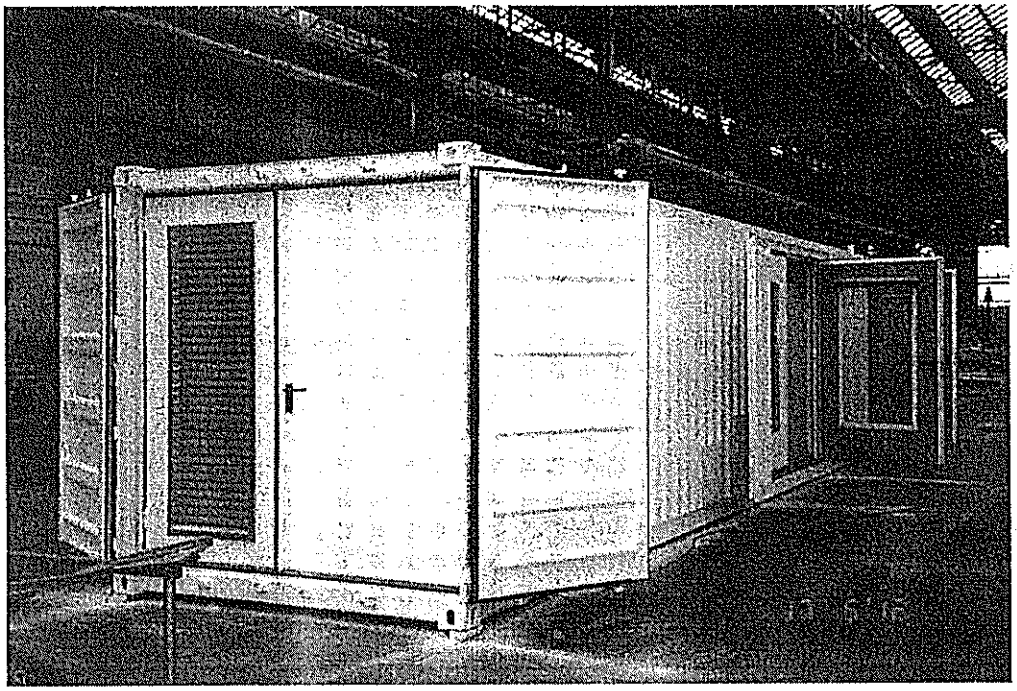

Figure 1: The SLR Container under construction

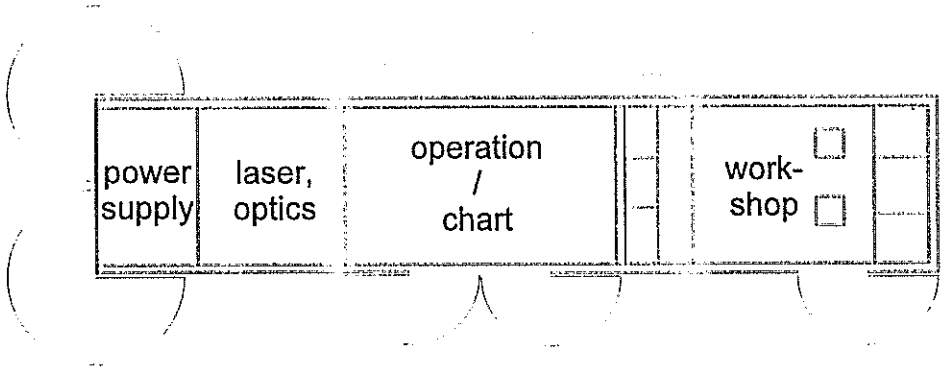

Figure 2: Sketch of the SLR container

The container is divided into four rooms as shown in figure 2. The first room is not air conditioned and houses the main electrical junction supply and the power supplies for the Ti:Sapphire laser. The Ti:Sapphire laser and the Transmit/Receive optics are

installed in the second room. As the requirements are constant temperature and dry and clean air, this room is highly isolated. An air condition provides nearly constant temperature and constant humidity. The air is kept clean by having a little over pressure in the room and by an additional air filter system. There are holes in the floor, which allows the laser table and the Transmit/Receive unit to stand on the concrete ground to avoid instability to the optics. The third room is the operators room with the controll system. This room is also air conditioned. A window in the door allows to observe the telescope during operation. When the SLR module has to be transported, the telescope is placed and fixed in this room. During operation, the telescope is placed in front of this room on a concrete plattform as shown in figure 3 /3/.

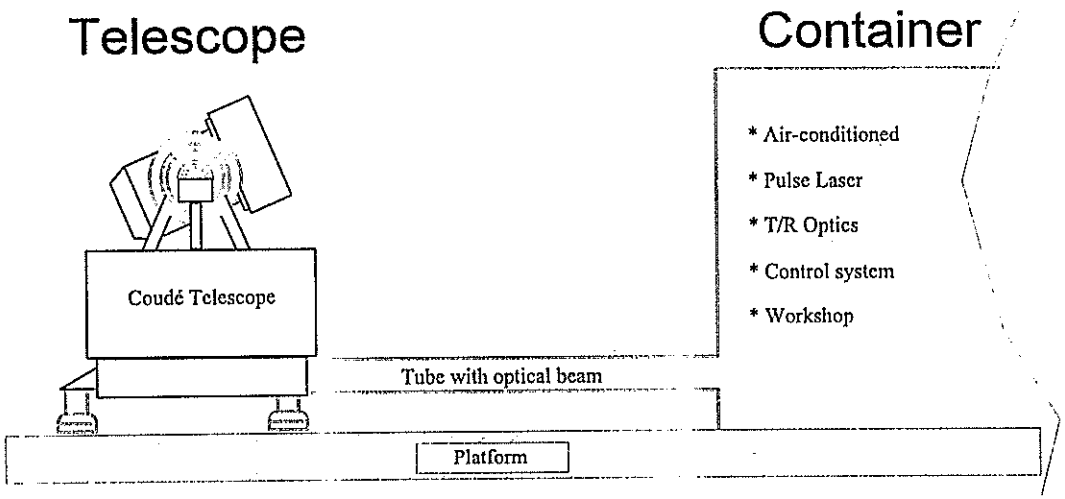

Figure 3: SLR configuration during operation

The last room is housing the air compressor and is used as a workshop and a storage room for spare parts and maintenance equipment.

2.1.2 Electronic description

In the SLR container three completely separated main power supplies are installed. One permanent, clean supply for sensitive instruments like detectors, clocks, encoder, etc. and one permanent supply for airconditioning, light, computers and other instruments producing noise in the net. The third supply is used for the direct measurement equipment like laser and telescope motors and is switched on only during measurement.

The whole power cabling is done with shielded cables. All circuits are protected against over voltage and over current to provide a safety and reliable operation.

2.2. Laser System

The Laser was especially designed for this application by B.M. Industries /4, 5/ in Paris/France. It is based on a diode pumped cw-modelocked Cr:LISAF oszillator generating pulses between 50 ps and 150 ps. A chain of Nd:YAG pumping Ti:Sapphire amplifiers. The system (figure 4) produces pulses with 10 Hz repetition rate at 847 nm and 423.5 nm with a pulse energy of 30 mJ at each wavelength.
The detailed optical setup is shown in figure 5, the specifications are summarized in Table 1.
The Cr:LiSAF Oszillator is longitudinally pumped by a Laser Diode, a Lyot Filter is used to adjust the wavelength, a Fabry Perot Etalon is used for the selection of the pulse duration (without Etalon the oszillator produces pulses below 20 ps). The pulses are amplified with 10 Hz repetitionrate in one regenerative and two multipass Ti:Sapphire amplifiers. The amplifiers are pumped by a two channel q-switched Nd:YAG Laser.
After second harmonic generation the pulses at 847 and 423.5 nm are sent to the telescope. The returned photons from the satellite are detected with three single photon avalanche diodes (two at 847 nm, and at 423.5 nm), (SPAD /6/).

The laser is operational since summer 1996.

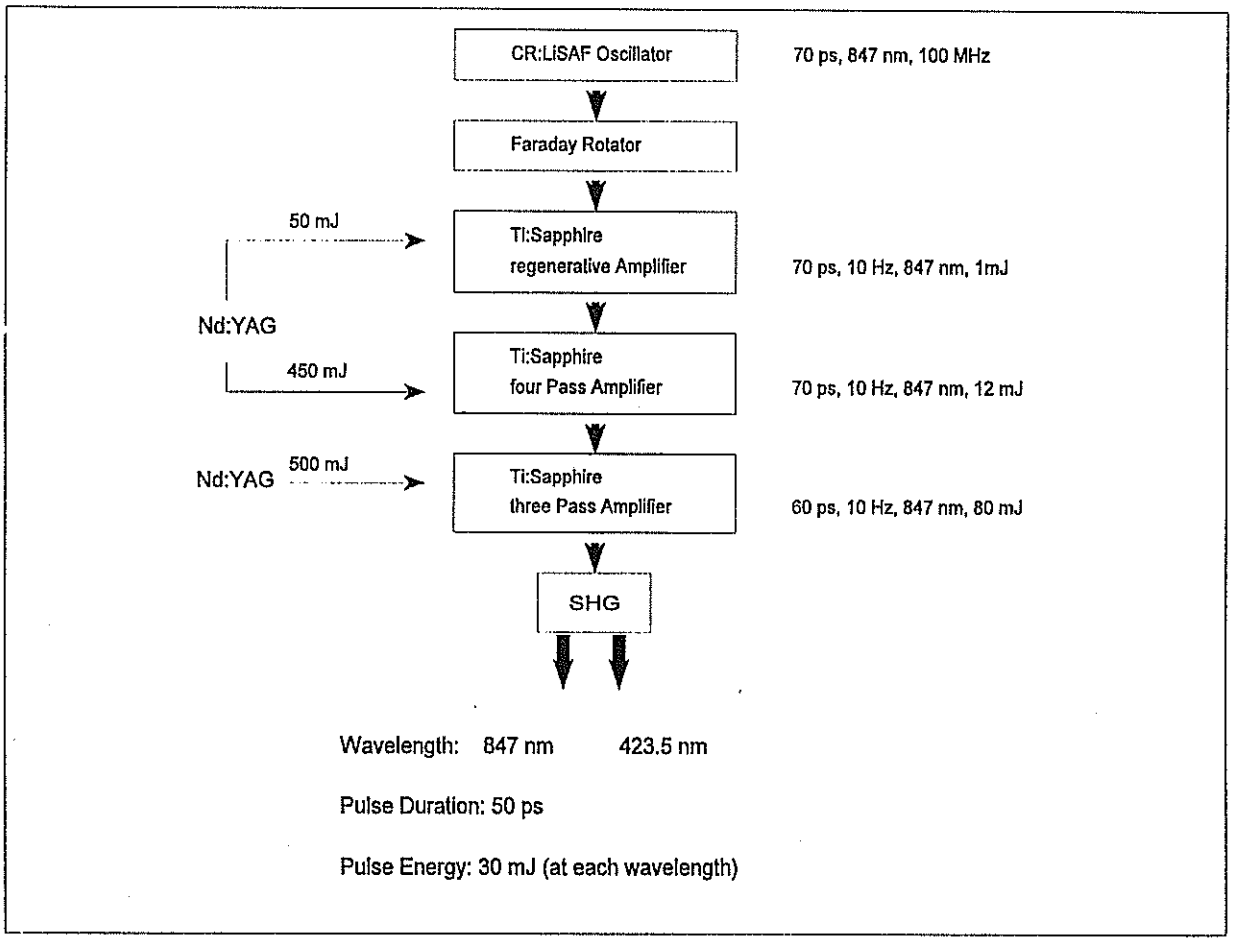

Figure 4: Block Diagram of the Cr:LiSAF/Ti:Sapphire Laser System

Cr:LiSAF oscillator	
Active medium	Cr^{3+}:LiSAF
Typical output power	> 5 mW
Tuning range	820 - 900 nm
Operating wavelength	847/846* nm
Spectral width	< 0.5 A
Repetition rate	100 MHz
Spatial mode	TEM_{oo}
Polarisation	Linear horizontal
Pulse duration	variable 60/100* ps

Regenerative amplifier	
Active medium	Titanium:Sapphire (Ti^{3+}:Al_2O_3)
Tuning range	750 - 850 nm
Operating wavelength	847/846* nm
Repetition rate	10 Hz
Pump energy	40 mJ
Output energy (1)	> 2 mJ at 10 Hz
Spatial mode	TEM_{oo}
Beam divergence	< 1.5 mrad
Pulse duration (FWHM) (2)	< 100 ps
Output polarisation	Linear vertical

(1) Measured just at the output of the regenerative oscillator. The cavity is then unseeded.
(2) For the seeded cavity only. This specification depends on the oscillator specifications.

Multipass preamplifier	
Active medium	Titanium:Sapphire
Tuning range	750 - 850 nm
Operating wavelenght	847/846* nm
Repetition rate	10 Hz
Pass number	4
Pump energy	200 mJ
Input energy	> 2 mJ
Output energy	> 25 mJ
Typical average power	> 250 mW at 10 Hz
Spatial mode	Single transverse
Beam divergence	< 1 mrad
Pulse duration (2)	< 100 ps
Output polarisation	Linear horizontal

Multipass amplifier	
Active medium	Titanium:Sapphire
Tuning range	750 - 850 nm
Operating wavelenght	847/846* nm
Repetition rate	10 Hz
Pass number	3
Pump energy	400 mJ
Input energy	> 25 mJ
Output energy	> 65 mJ
Typical average power	> 650 mW at 10 Hz
Spatial mode	Single transverse
Beam divergence	< 1 mrad
Pulse duration (2)	< 100 ps
Output polarisation	Linear horizontal

(2) Specification depends on the oscillator specifications

Table1: Specifications of the Cr:LiSAF/Ti:Sapphire Laser System

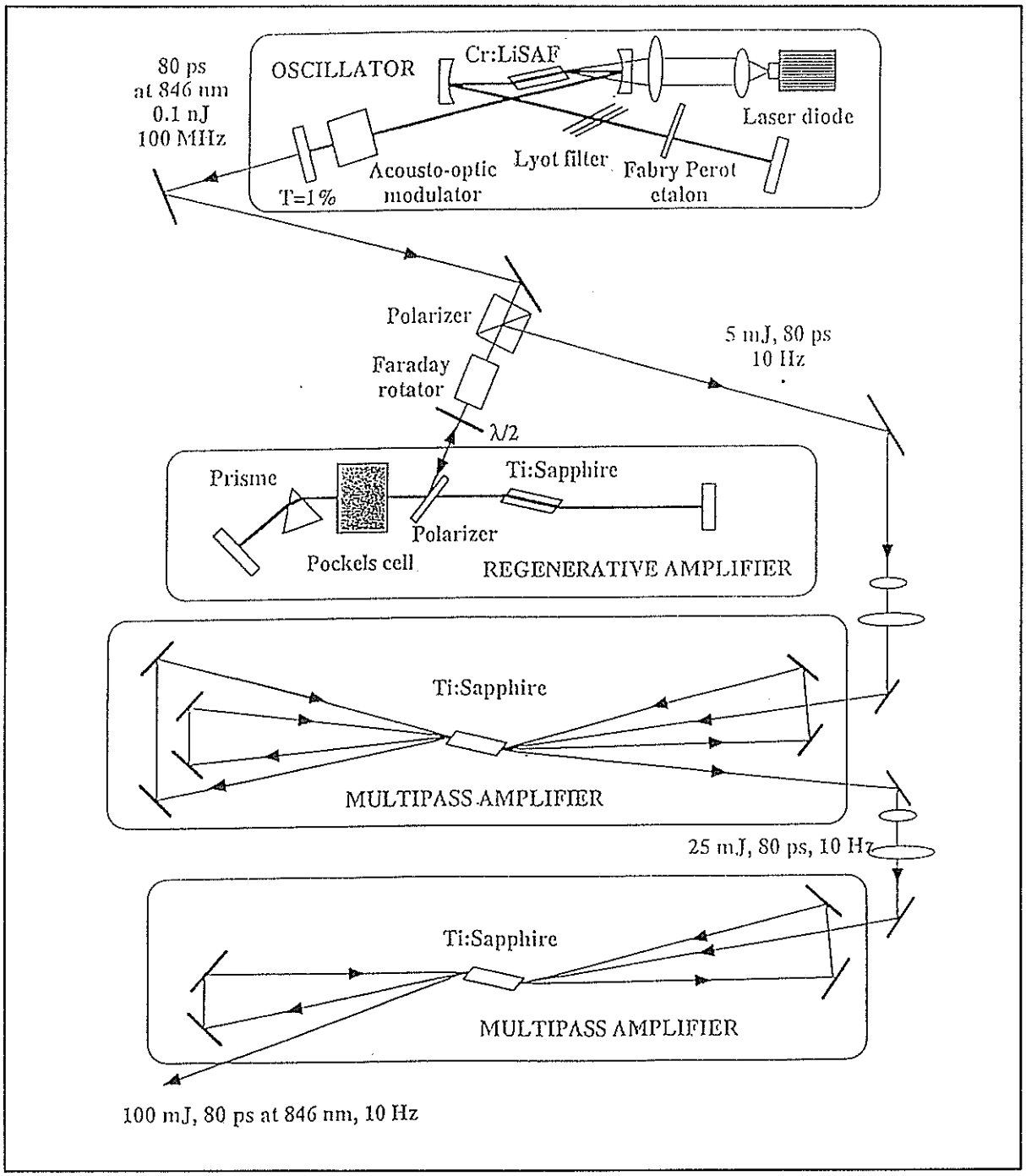

Figure 5: Detailed optical setup of the Laser System

2.3. Telescope

The design of the telescope is based on a further development of the MTLRS-1 telescope /3, 7/.
The 50 cm lens telescope with excellent optical efficiency is installed in a small cart. During transport this cart is fixed in the container, during measurement the cart with the telescope is moved to a concrete pad near the container.

Due to the design of the folded lens telescope (figure 6), central obscuration of the beam is avoided. The transmit / receive switch is realized by aperture sharing, this means the laser is fired through the central part of the telescope (18 % of telescope area), the outer circle (82 % of telescope area) is used for receiving photons.

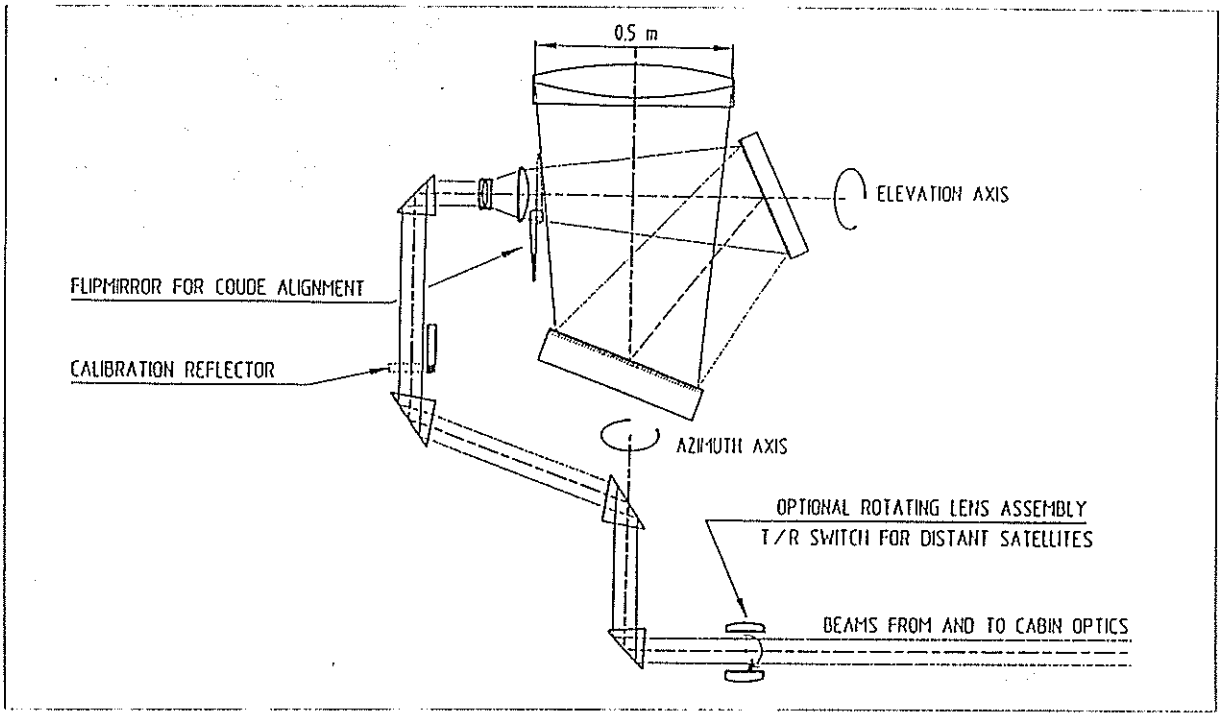

Figure 6: Telescope Optics

The telescope is supported by three adjustable feet on the TIGO platform. These three feet are mounted on a large ring-shaped granite component (out of one single block of granite), that forms the main part of the static structure of the telescope mount.

The main advantages of the granite component in the static part of the mount are:

- good top surface finish and flatness (better than 4 µm over the entire diameter) to form the static part of an air-bearing that determines the direction of the azimuth axis of the telescope
- good stiffness
- good thermal and temporal stability
- corrosion resistant.

The telescope and cart in operational and transport configuration is shown in figure 7. The telescope was finished in december 1996 with the installation of the big coated optics.

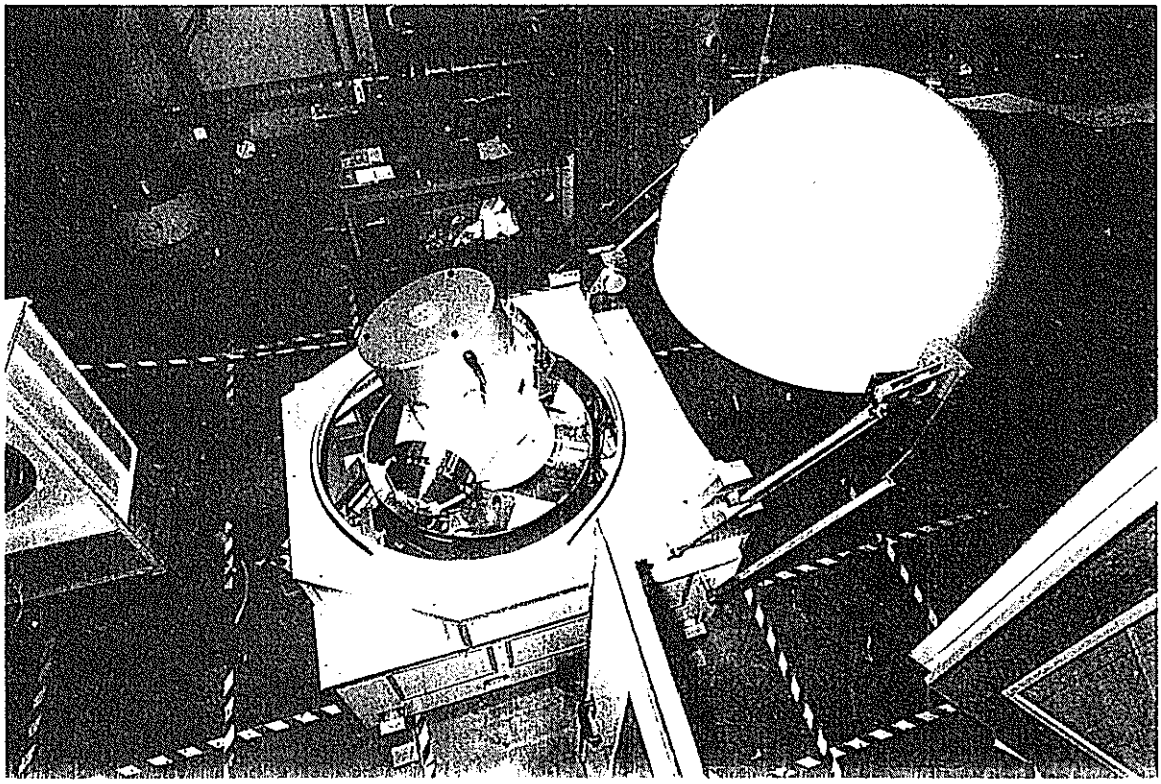

Figure 7a: TIGO SLR Telescope in the open cart (ranging configuration)

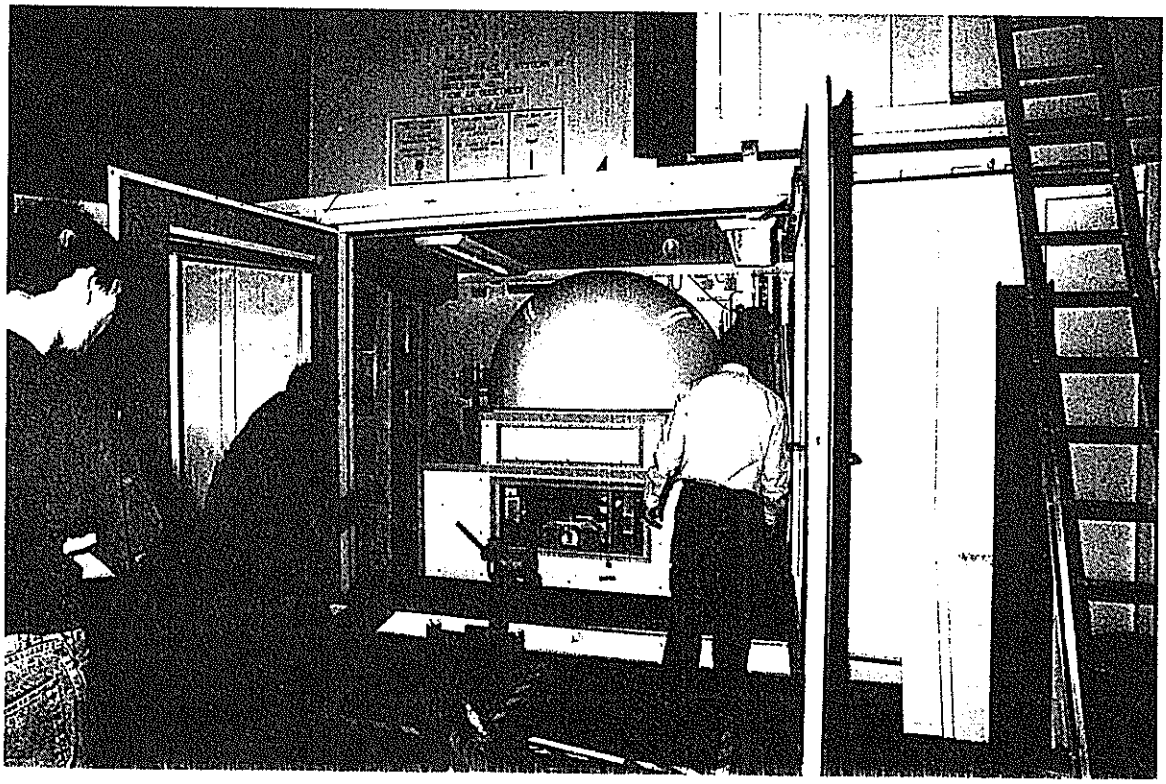

Figure 7b: TIGO SLR cart in the container (transport configuration)

2.4 The Control System

2.4.1 System Architecture

The control system for the Tigo SLR module consists of a workstation and a real time controller /8/. The operator uses a completely graphical program to work with the laser ranging system. The real time controller controlls directly all functions of the instrument. An overview of the global architecture is given in figure 8.

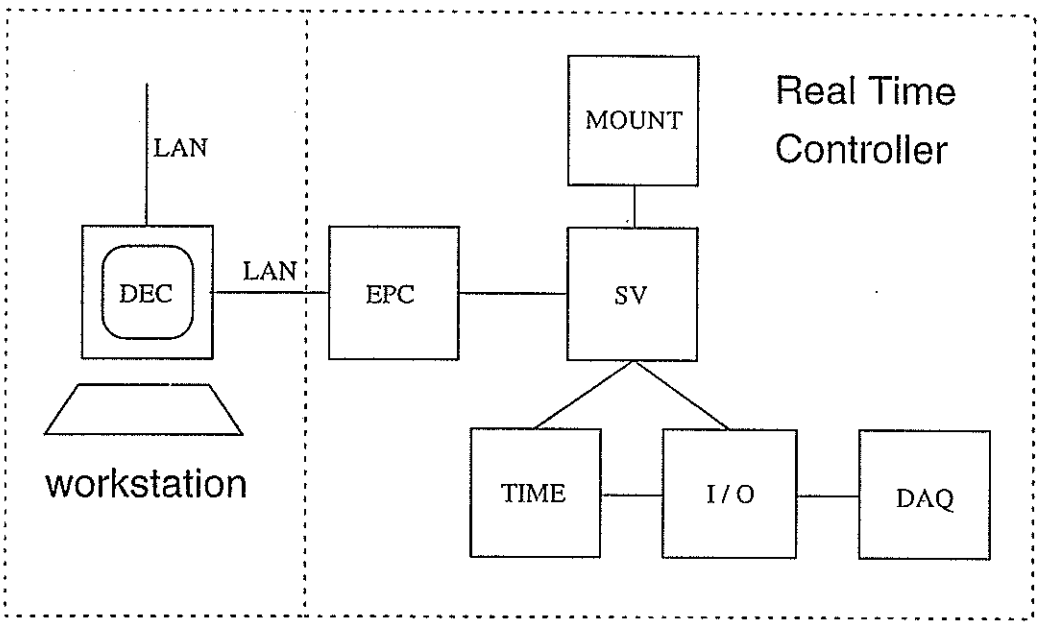

Figure 8: Architecture overview of the SLR controller

2.4.2 The workstation

The main task for the workstation is to run the graphical user interface program. This user interface provides everything to operate the complete SLR module. That means it is not only used to do the real tracking work, but also takes care on nearly all other tasks for Satellite Laser Ranging.

The first thing which must be done, is to setup the parameters for initialisation and installation. Therefor a window based, especially developed editor can be used to edit the associated data bases. Furtheron a star observation program is implemented to do the site installation and to determine the mount model (figure 9).

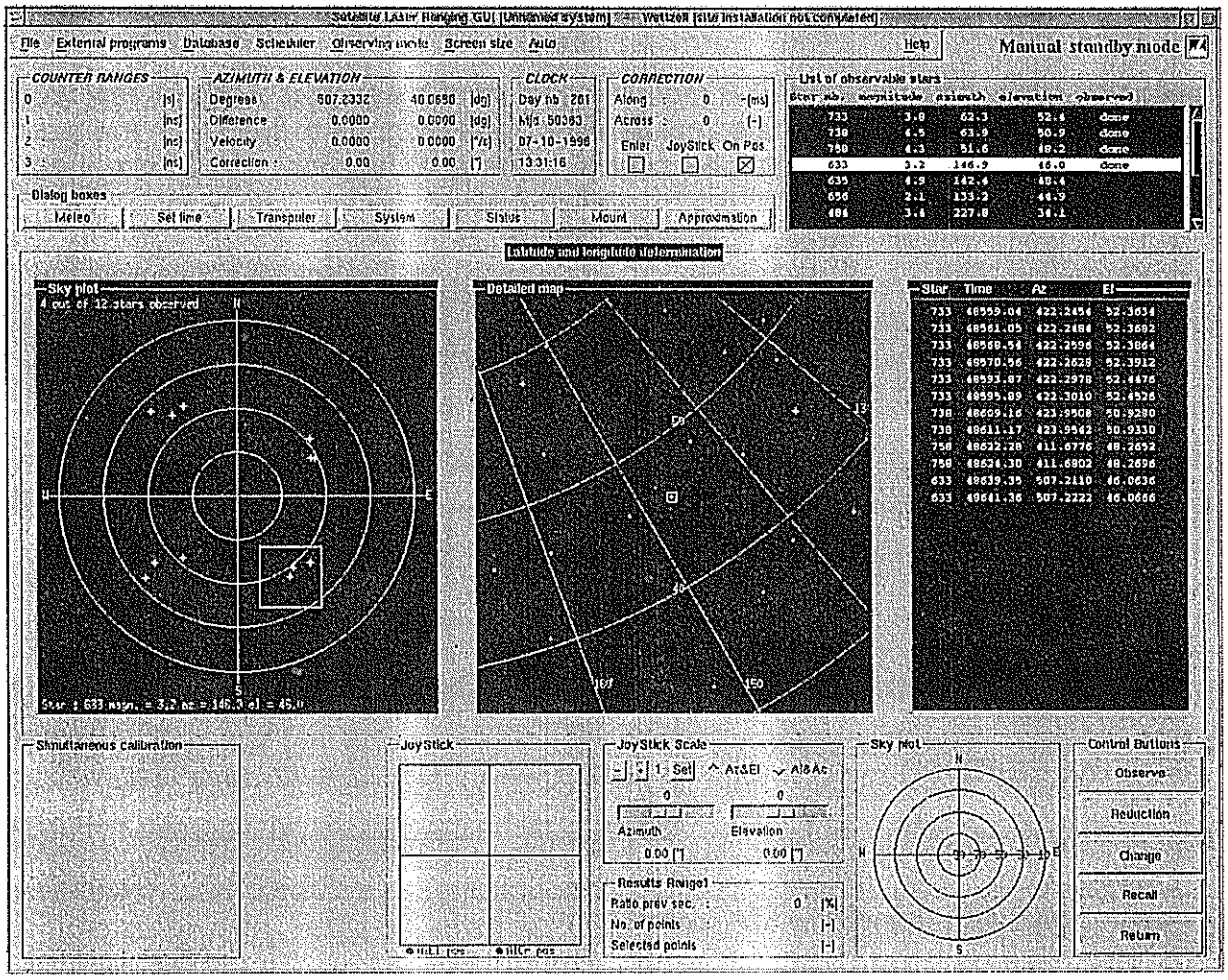

Figure 9: The graphical user interface during site installation

It is very convenient to use the implemented backgroud tasks, which automatically provides the latest IRV values and calculates the predictions. During real tracking the operator can switch between two displays. One showes the detected photons in the expected time gate and the other displays the values in histograms to have a "real time impression" on the quality of the data. See figure 10 and 11.

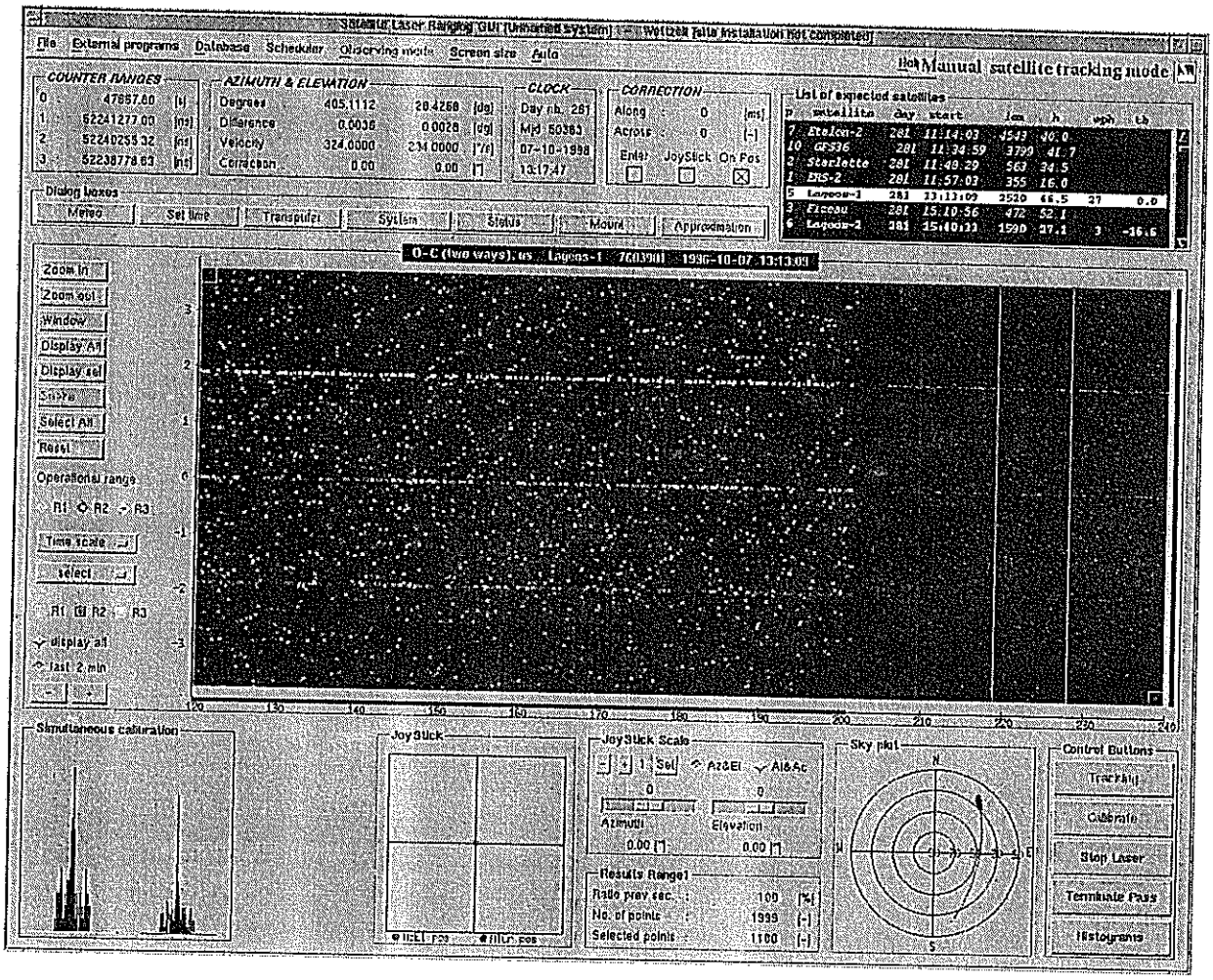

Figure 10: The graphical user interface in normal tracking mode

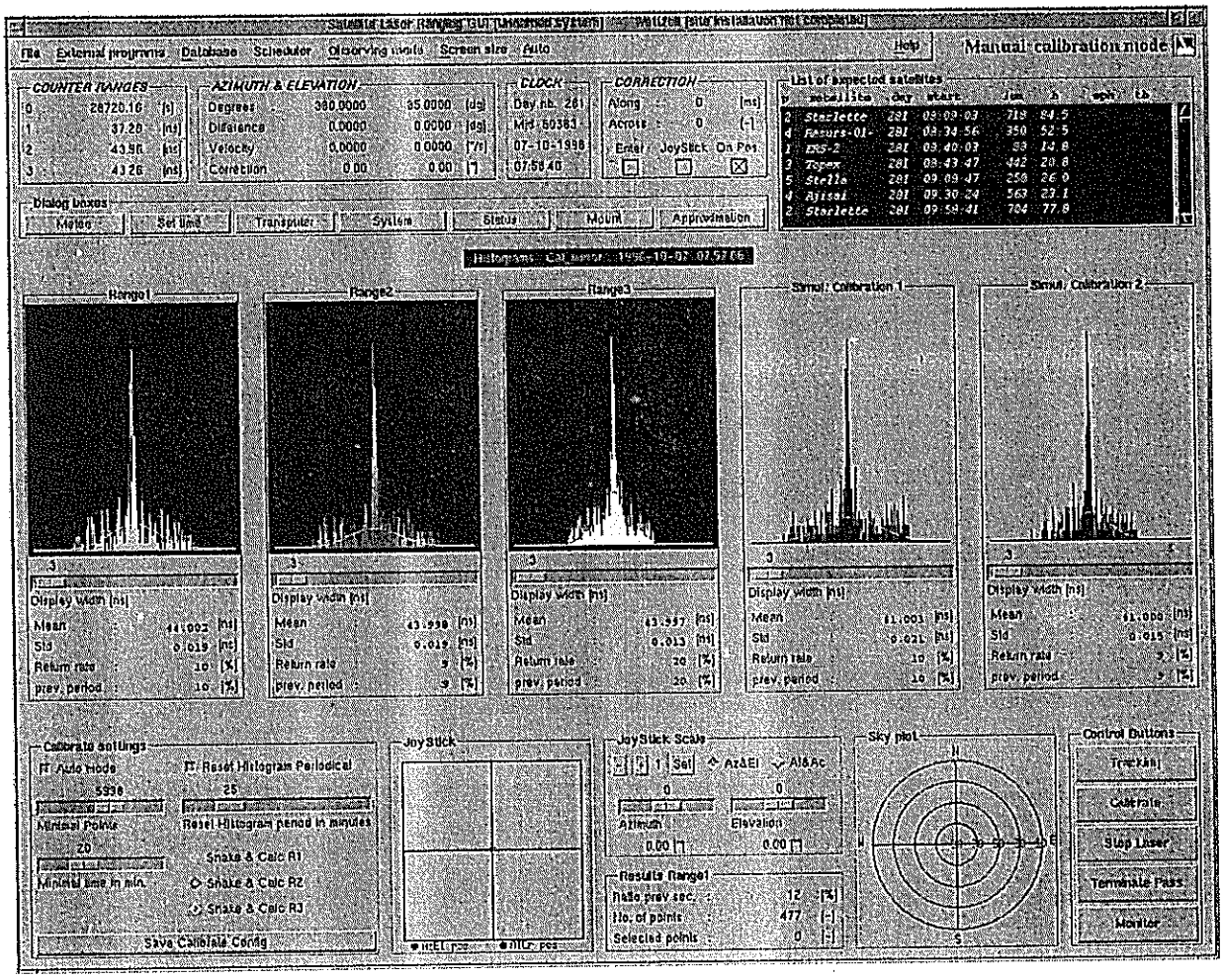

Figure 11: Measured data in form of histogramms

After tracking the grahpical user interface program can be used to evaluate the measured data. The purpose of this graghical user interface is to make the normal "tracking work" as easy as possible. The administration of the system however requires the knowlegde of an expert.

2.4.3 The Real Time Controller

The Real Time Controller controls directly all functions of the instrument. It is implemented by using five transputer boards and an embedded Personal Computer (PC). One transputer board, the supervisor board, has global tasks and routes the communication stream from the user interface on the workstation to each transputer board. The other four transputer boards, the time board, the mount board, the I/O board and the data aquisition board are controlling special functions of the instrument. On the time board all tasks are executed that are associated with the measurement of accurate time intervals. The software controls and reads out the hardware status that is needed for the generation of signals with very accurate timing. On the mount board all tasks, related with the positioning of the telescope are executed. The I/O board carries out the sysnchronous tasks which have strict timing constraints, like controlling the counters or the photo detectors. On the data aquisition board all asynchronous tasks with no strict timing constraints are executed such as reading out the temperatur sensors.

The embedded PC acts as an interface between the graphical user interface running on the workstation and the real time control system of the instrument. It contains the boot code for the real time controller and performs some elementary maintenance functions by using a touch screen. The embedded PC can also maintain a system log with all command issued to and responsed from the real time controller. The communication between the PC and the workstation is done by an ethernet interface, using the TCP/IP protocol. To transfer the data transfer from the PC to the real time controller and vice versa a special interface with a special serial transputer protocol is used.

3. Overall System Status

All the main subsystems except the control software (data analysis and tracking routines are not yet implemented) were ready and tested in Dec. 1996. The final assemblage started in Oct. 1996 and should be finished at the beginning of 1997. In Nov./Dec. 1996 the system was able to make the first calibration measurements at 423.5 nm (figure 12), showing the good operation of laser, electronics, optics and detectors. The system will by moved to a test pad in Delft in spring 1997 to perform the acceptance test (ranging to all satellites), the delivery to Wettzell is expected in summer 1997.

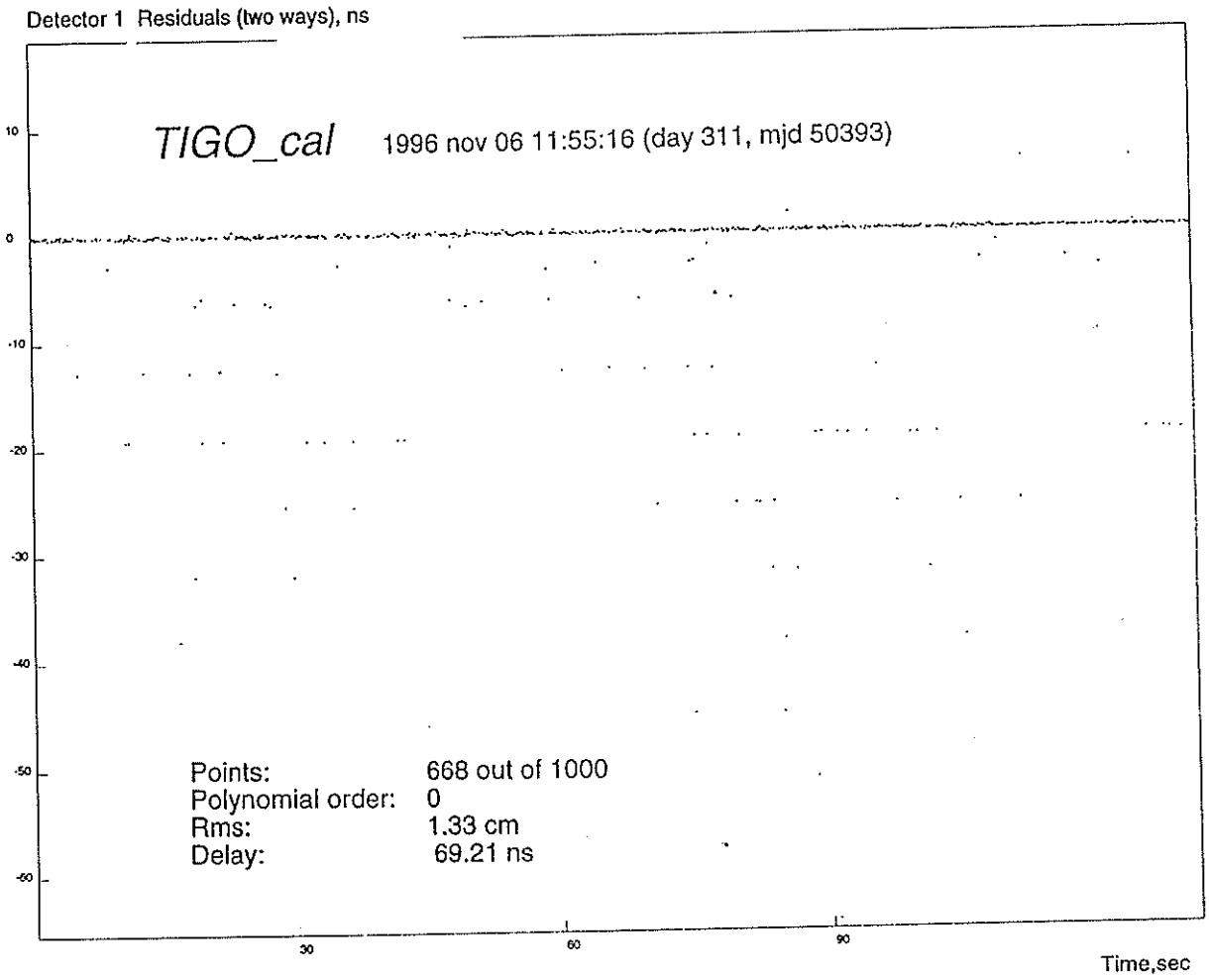

Figure 12: First Calibration at 423.5 nm with the TIGO SLR Module

References:

/1/ Kirchner G., Koidl F., Hamal K., Prochazka I., Multiple Wavelength Ranging in Graz, Australian Government Publishing Service, Proceedings of the 9th International Workshop on Laser Ranging Instrumentation, Canberra (1994) 609

/2/ Degnan I. I., Millimeter Accurancy Satellite Laser Ranging: A Review, Geodynamics Series Vol. 25, Contributions of Space Geodesy to Geodynamics, Americal Geophysical Union, Washington (1993) 125

/3/ Braakman H., van der Kraan M., Visser H., van der Zwaan B., Sperber P., TIGO-SLR Opto-Mechanical Configuration, Australian Government Publishing Service, Proceedings of the 9th International Workshop on Laser Ranging Instrumentation, Canberra (1994) 198-206

/4/ P. Sperber, A. Böer, F. Estable, F. Falcoz, E. Pop, L. Vigroux, "Cr:LiSAF/Ti:Sapphire based solid state Laser System for Two Color Satellite Laser Ranging", Proceedings of the 10th International Workshop on Laser Ranging Instrumentation, Shanghai (1996)

/5/ P. Sperber, A. Böer, U. Hessels, U. Schreiber, "Two Color Satellite Laser Ranging using a Cr:LiSAF/Ti:Sapphire Picosecond Laser System", Society for Optical and Quantum Electronics, Proceedings of the Conference on Laser'96, Portland (1996), in print

/6/ Prochazka, K. Hamal, B. Sopko, G. Kirchner in Conference on Lasers and Electro-Optics, Vol. 7, 1990 OSA Technical Digest Series (Optical Society of America, Washington, DC, 1990)

/7/ Braakman H., van der Kraan M., Visser H., van der Zwaan B., Sperber P., Transmit / Receive Two-Color Unit for TIGO, Australian Government Publishing Service, Proceedings of the 9th International Workshop on Laser Ranging Instrumentation, Canberra (1994) 407-415

/8/ Vermaat E., Offierski J. W., Otten K. H., Beek W., van ES C., Sperber P., Transputer Based Control System for MTLRS, NASA Conference Publication 3214, Proceedings of the 8th International Workshop on Laser Ranging Instrumentation, Annapolis (1992) 12-40

A Transportable Laser Ranging System in China (CTLRS)

Xia Zhizhong, Cai Qingfu, Ye Wenwei,
Guo Tangyong, Wang Linhua
Institute of Seismology,State Seismological Bureau
Xiao Hong Shan, Wuhan 430071,China

Abstract

In order to set up a state geodesy control network and to monitor crustal movement, since 1993 Institute of Seismology, State Seismological Bureau and Xi'an Institute of Surveying and Mapping have cooperated to develop a transportable satellite laser ranging system. The system is composed of a Nd:YAG mode-locked laser, a telescope mount, receiving electronics equipment, time and frequency standard, and a computer etc. The repetition rate of the laser is 1-5pps, the wavelength is 532nm and the main pulse energy is 30mj. The diameter of the receiving telescope is 35cm. All these equipments can be installed in a vehicle consisted of two rooms, its loaded weight is 3.5 tons. The single shot ranging accuracy of the system will reach 2-4cm for LAGEOS and other satellites. The system will be completed in 1996 and put into operation in 1997. This paper provided with the technical details of the system and the results of the testing observation.

Key words: Satellite laser ranging-TLRS

Introduction

Since 1980's, the 3rd generation satellite laser ringing network has been set up in Shanghai, Wuhan, Changchun, and Beijing in China. Each station can observe satellite ETALON, LAGEOS, ERS-1, TOPEX, etc. in generally, the single shot accuracy can reach 5cm. All stations joined the international cooperative project of NASA and WPLTN. But the geographical distribution of the stations is not even, there aren't observation station in the western part of China. Thus, in order to set up a space geodesy network with reasonable distribution and monitor crustal movement beneficially in China. Since 1993 Institute of Seismology and Xi'an Institute of surveying and mapping have cooperated to develop a transportable laser ranging system which is suitable for China. The system can observe LAGEOS etc. We hope the ranging precision can reach 2-4cm. In 1995 the CTLRS has been entered in to the stage of the assembly and the adjustment. It is estimated that the system will be completed in 1996 and come into operation in next year.

System Configurations

1. Laser

The laser is a frequency doubled and passively mode-locked (SFUR) Nd:YAG system that produces a mode-locked pulse train with a repetition rate of 1-5pps. The Laser consist of a pumping oscillator followed by a pulse slicer, an amplifier and an optical second-harmonic. The oscillator transmits a mode-loked pulse train which included five to seven pulses, the slicer selects 2-3 pulse from the pulse train. The main pulse has 30 mj energy with wavelength 532nm and about 60ps width. The diameter of the output laser beam is 8mm. The laser transmitter assembly is located on a table under the mount, the volume of the table is 320x260x1320mm. This laser is developed by Shanghai Institute of Optics and Fine Mechanics.

The optical diagram of the laser is given in figure 1.

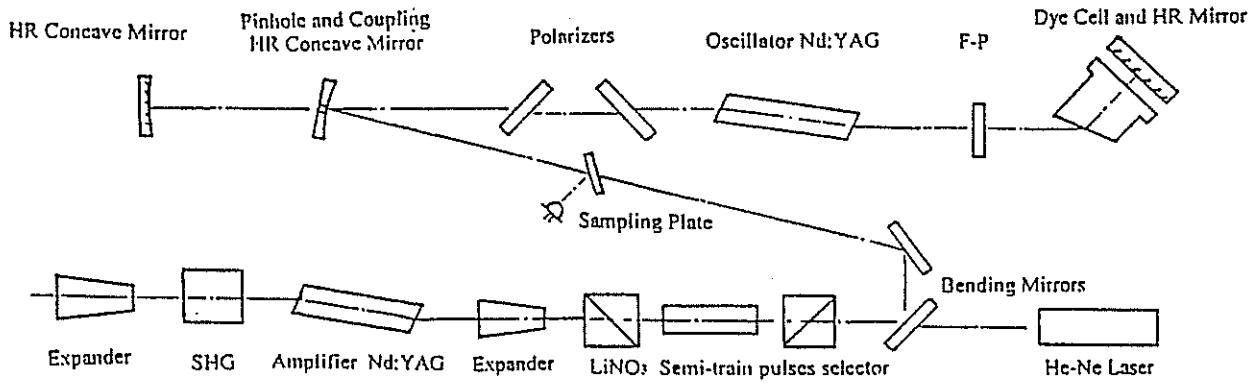

Fig.1 The optical diagram of the Nd:YAG laser

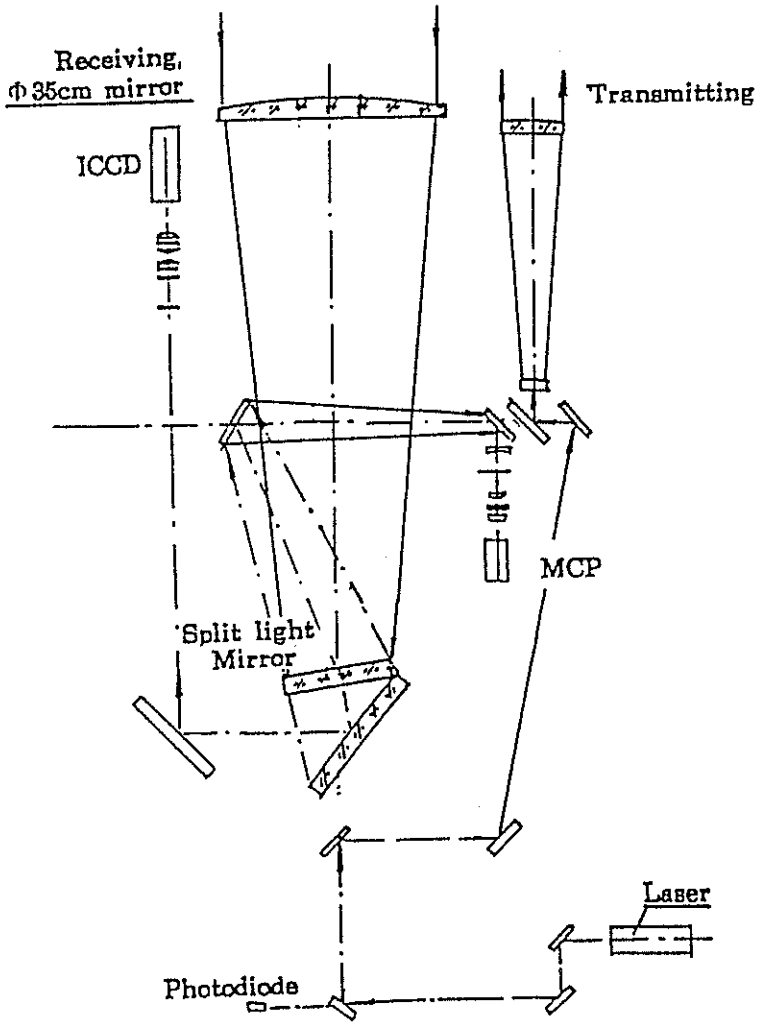

Fig.2 The optical block diagram of the system

2.mount

A horizontal structure with two axes is used for the mount. The optical block diagram of the system is shown in figure 2. The elevation and the azimuth axes are driven by DC-torque motor and controlled by both a tachometer and a synchronistic inductor (resolution 1 arcsec). The ranges of the azimuth and the elevation axes are ± 270 deg. and -10 deg. to +190 deg. respectively. The tracking angular velocities are from sidereal to 2 deg/s for elevation and 15 deg/s for azimuth. The estimation of the tracking accuracy is within 10 arcsec.

2.1 Transmitting optics

The laser pulse beam transmitted from Nd:YAG laser with diameter 8mm is expanded to about 80mm by two beam expanders and reflected in a Coude path along the azimuth and elevation axes by the mirrors. The divergence for output laser light is controlled from 100 μ rd to 1 mrd by a motor. In order to measure the ground target for calibration, an attenuator for output laser beam is installed in the Coude path.

2.2 Receiving optics

The aperture of the receiving telescope is 35cm and the focal length is 2.3m. The returned light from satellite is splitted in two ways by a split mirror. One light beam with the wavelength 532nm goes to a micro-channel-plate photomultiplier tube along the Coude path and the another (except 532nm) goes to a television with an image intensifier for guiding satellite.

3. Receiving electronics equipment

In order to detect returned signal and to measure the flight time, the receiving electronics equipment includes a MCP photomultiplier, (Hamamatsu R2566U-07) two amplifiers(B&H DC3003A), a constant fraction discriminator (TENNELEC TC454) and a time interval counter (Stanford Research system SR620 resolution 25ps). The external frequency standard of the counter is provided by a Rubidium clock. The MCP-PMT has a gain of 5x10E5 (TYP) and a rise time of 100ps, the quantum efficiency is 6% at 532nm of the wavelength. The start pulse is detected by a photodiode (Hamamatsu S-2381 with 200ps risetime) behind the first mirror in the Coude path.

4. time and frequency standard

A model TTR-6A NAVSTAR GPS Synchronized Time and Frequency standard (Allen Osborne Associates, Inc) is used as time and frequency standard for TLRS. This equipment contains a Rubidium clock which supplies a 10 MHz signal with the stability of 1x10E-11, the timing accuracy of corrected 1pps output is about 100ns. The TTR-6A GPS receiver also includes a navigation, or position and program for refining local coordinates.

5. Control and computer

An IBM PC 486 computer has been used in the transportable laser ranging system as control center. Real-time clock range gate controller, data acquisition and laser shooting controller etc. are integrated on two extending circuit boards to be installed on the extension slots of IBM PC computer. Software regarding calculation of prediction, data processing, numerical track guiding,software managing etc. are all transplanted to this computer. While working , the telescope isautomatically guided towards the satellite by the track control part with the calculating

result from ephemeris. In order to improve tracking accuracy, the tracking parameter (UTC time, azimuth, elevation O-C etc.) can be displayed and corrected in real-time during the observation, so that some of the status of the system and computed results are shown on the CRT colorfully and in picture.

6. Transportable manner

All equipments of CTLRS are installed in a vehicle which has loading capacity of 3.5 tons. This vehicle is divided into two rooms. The receiving electronic control and computer, time and frequency standard equipments etc. are set up in the front room with a air conditioner. The mount and laser are installed in the another one located at the back the vehicle. While working, the roof of the vehicle can be moved off and the mount and laser are jacked up by four jacks. The size of the vehicle is 2.3x3.0x6.4m. Figure 3 shows the schematic diagram of the mobile SLR system.

The overview of the mount and receiving electronics, control computer, time and frequency standard equipments of CTLRS are given in figure 4.

Testing observation of the CTLRS

Since 1995 the CTLRS has been entered into the stage of the assembly and the adjustment. the first returns from TOPEX were obtained in July 24,1996. The number of ranges is about 205 and the RMS of residuals to observation range minus prediction range for polynomials fitting is 6.1cm(Fig.5). We also have observed successfully LAGEOS satellite in Aug.5. The number of ranges for this pass and the ranging accuracy is about 122 and 6.5cm respectively(Fig.6). Because we are afraid to damage the MCP photomultiplier, the PM2233 PMT is used in the testing stage as a receiving equipment, so the ranging accuracy only reached about 6-7cm.

Now the improvement of this system is further carried on by us. It can estimate that the all equipments will be completed in 1996 and put into the operation in next year.

Reference

[1] Xia Zhizhong et al. A Technical Scheme for The Transportable Satellite laser ranging system. 1992.12 Wuhan (in Chinese)

[2] Xia Zhizhong et al. New progress of Ranging Technology at Wuhan SLR station. Proceedings of Symposium on Eight International Workshop on Laser Ranging Instrumentation Annapolis U.S.May,1992.

[3] Sasaki M. Completion of a transportable laser ranging station (HTLRS). Data Report of Hydrographic Observation. Maritime Safety Agency Tokyo. Japan No.1,March 1988.

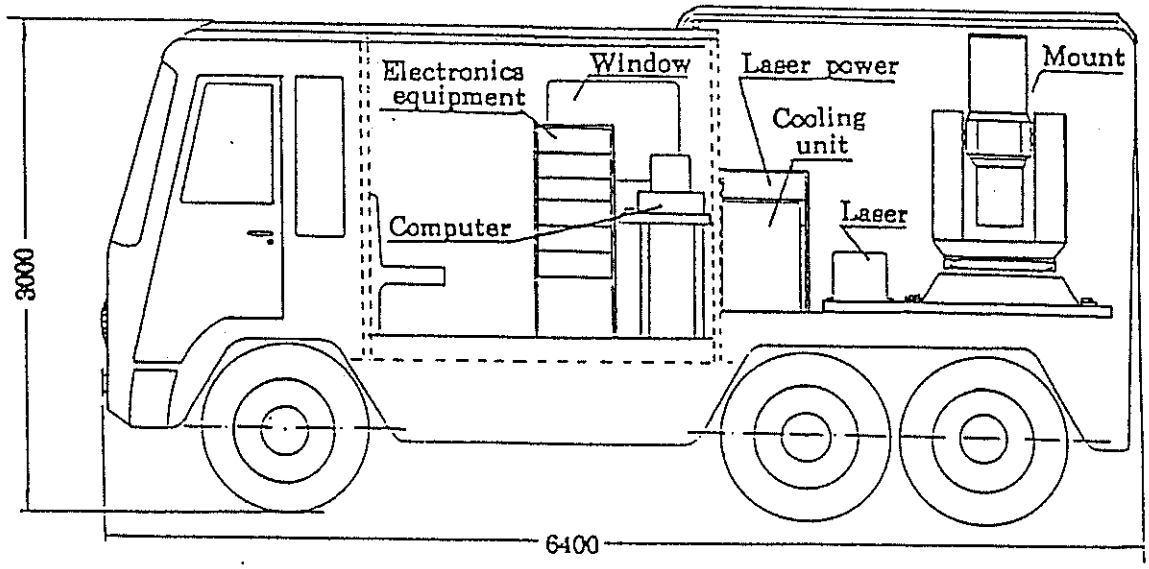

Fig. 3 The schematic diagram of the CTLRS

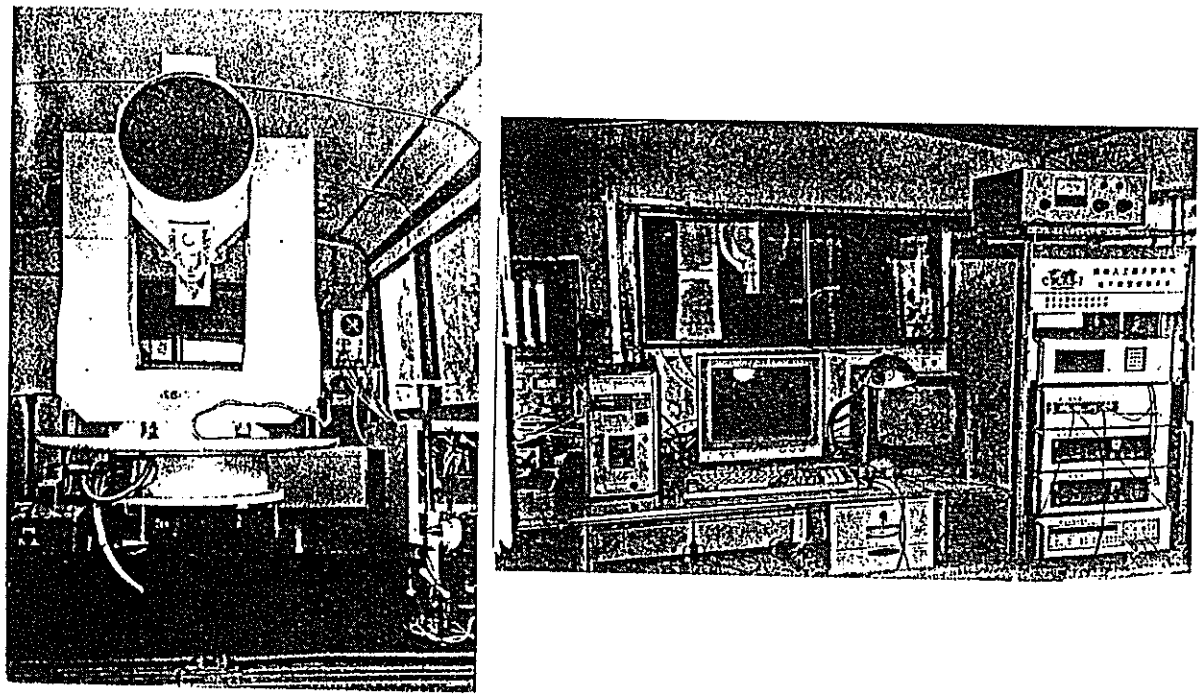

Fig.4 The overview of the mount and receiving electronics, control computer, time and frequency standard equipments of CTLRS

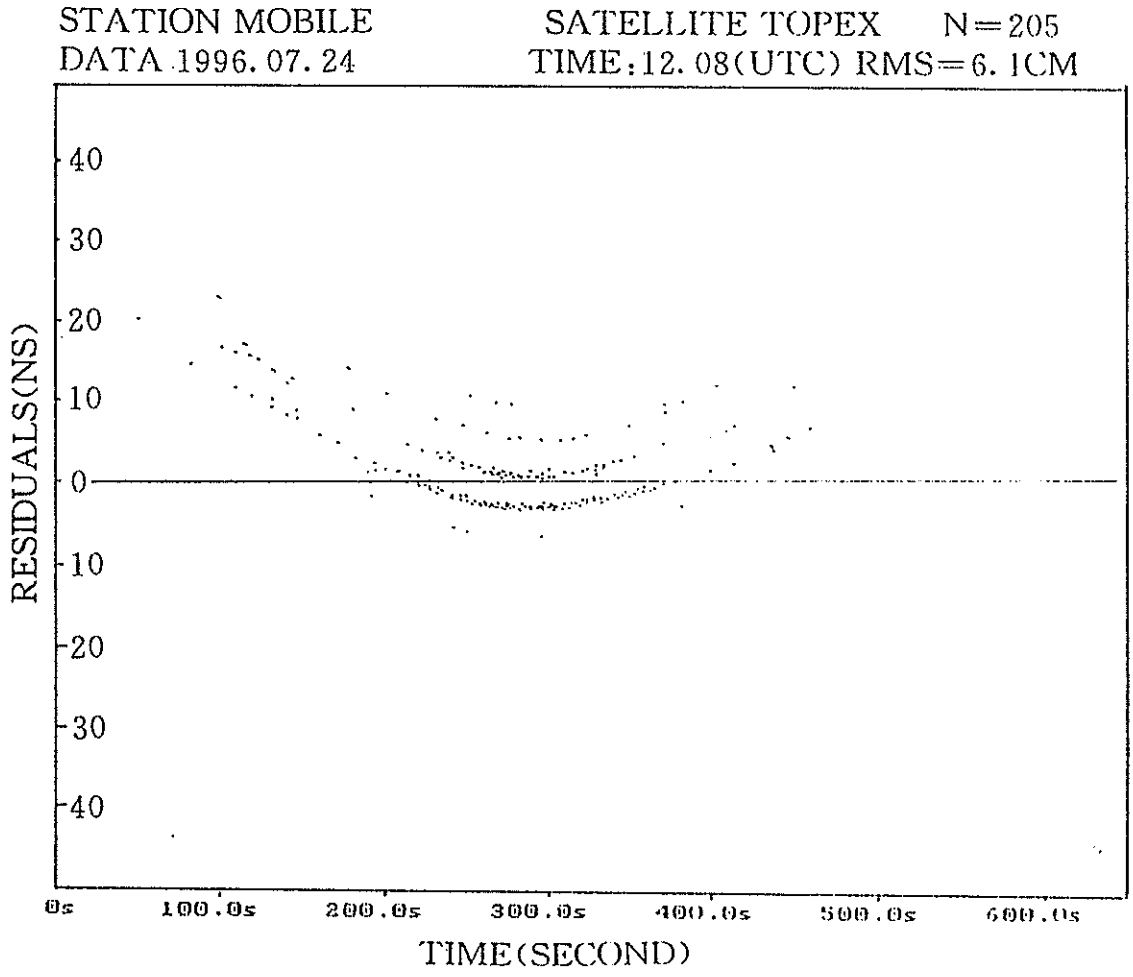

Fig.5 Testing results of ranging to TOPEX

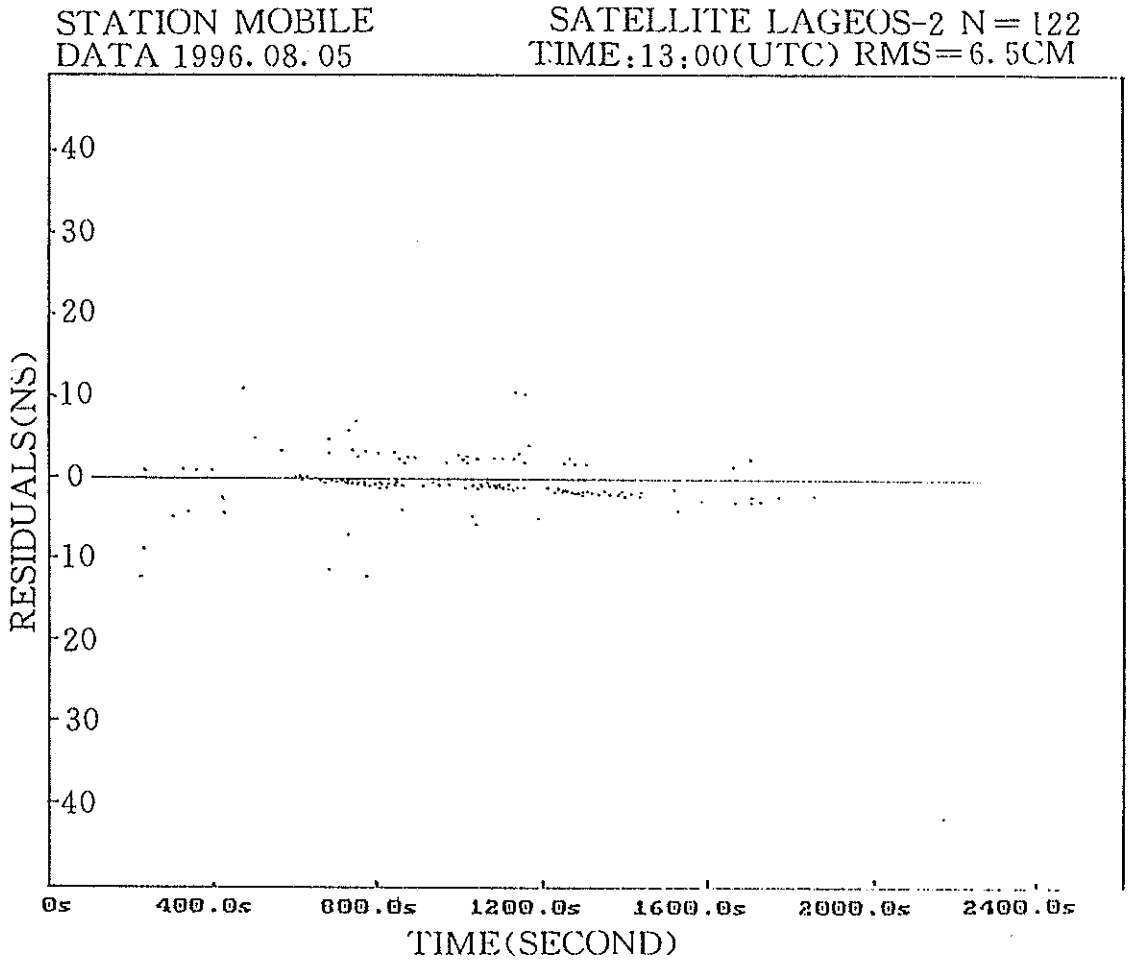

Fig.6 Testing results of ranging to LASEOS-2

Lunar Laser Ranging

Adaptive Ridge Regression: the Multicollinearity and its Remedy – a Case in Lunar Laser Ranging

[1] Chengli HUANG , Wenjing JIN, and Huaguan XU

Shanghai Observatory, Academia Sinica,
80 Nandan Road, Shanghai 200030, P.R.China
E-mail:jwj@center.shao.ac.cn

Abstract. The multicollinearity among regression variables is a common phenomenon in astronomy data reduction. The case of determining Earth Orientation Parameters by Lunar Laser Ranging(LLR) is discussed in this paper. It is pointed out that there exists serious multicollinearity between these two regression variables at the last stage of LLR data reduction in which the Universal Time(UT) and the variation of latitude ($\Delta\phi$) at observing site are solved from the post-fit residuals. As a remedy, a new method, Adaptive Ridge Regression(ARR), as well as the method to choose the departure constant θ, is suggested and applied in this paper. It is proved that ARR method is effective to reduce the multicollinearity and makes the regression coefficients more stable than that by standard least square fits, especially when there is serious multicollinearity.

Key words: adaptive ridge regression — multicollinearity — lunar laser ranging

1. Introduction

As one of the new techniques to determine Earth Orientation Parameter(EOP), Lunar Laser Ranging(LLR) can provide highly accurate Universal Time(UT) frequently and regularly. The accuracy of UT from LLR depends upon not only the measurements but also the mathematical method and physical models adopted in the reduction (*Huang 1992*). The difference of the UT results by pre-residual and post-residual has been discussed by *Wang (1985)*. In order to overcome the imperfections of adopted physical models in calculating the theoretical delay and the uncertainty of the adopted initial value which can induce an obvious systematic deviation in UT, the post-residual are used for solving UT and $\Delta\phi$ except for rapid service. And the related problem on the terrestrial and lunar reference frame has also been discussed by *Huang et al. (1996)*. Because there are only four LLR stations and the common observation of more than two stations is rare, it is common to use LLR data obtained at a single station data for solving UT and $\Delta\phi$.

Nevertheless, the number of normal points of a single station is small and their time span of observation at one night is short, the parameters to be solved are usually related to each other(*Huang, et al., 1993*). At this time, we say that there exists multicollinearity among the regression parameters to be estimated, and then we should be careful in chosing the proper parameters into the observation equa-

[1] *Correspondence to:* Chengli HUANG

tions.

In fact, the multicollinearity among regressors is a common phenomenon in astronomy data reduction, and there are different methods to solve the problem in different fields. In this paper, we discuss the case of LLR and introduce the Adaptive Ridge Regression (ARR) method in the following sections. It is proved that ARR is an effective method to reduce the multicollinearity and makes the regression coefficients more stable.

2. LLR data reduction

Generally, LLR data can be processed by two steps. First, corrections of more than fifty parameters and post-fit residuals are obtained from least square adjustment of the whole available measurements. These parameters include geocentric coordinates of observatories, precession, nutation, the orbit of the Moon around the Earth and some lunar parameters such as third-degree potential harmonics, Love number, fractional moment of inertia differences, rotation dissipation and selenocentric coordinates of reflectors. In the second step, UT and the variation of latitude $\Delta\phi$ at observing site are solved from the post-fit residuals at a single station. The observation equation in the second step can be written as(*Jin et al.,1985*)

$$\Delta\rho_i = (\frac{\partial\rho}{\partial UT})_i\Delta UT + (\frac{\partial\rho}{\partial\phi})_i\Delta\phi + \sum_j(\frac{\partial\rho}{\partial K_j})\Delta K_j \tag{1}$$

Where, the partial derivatives:

$$\begin{cases} (\frac{\partial\rho}{\partial UT})_i = Rcos\phi cos\delta_i sinH_i \\ (\frac{\partial\rho}{\partial\phi})_i = R(sin\phi cos\delta_i cosH_i - cos\phi sin\delta_i) \end{cases} \tag{2}$$

in which (R,ϕ) are the geocentric radius and latitude of station, and (δ_i, H_i) are the declination and time angle of the Moon at time t_i.

The time span used in the second step is short (about 3 hours), so the last term in equation (1) can be considered as a constant.

3. The multicollinearity between regressors, ΔUT and $\Delta\phi$

During the past two decades, the problem of multicollinearity has received considerable attention. Multicollinearity exists when the multiple regressor variables are truly not independent, but rather, display redundant information(*Myers 1986*). Generally, we write the observation equation as follows:

$$Y = XB + E \tag{3}$$

where, Y, X, B and E denote weighted vector of observations (O-C), weighted design matrix, vector of the coefficients to be estimated and error term respectively.

It is well known that if X is less than full rank in the weighted least-squares fit, the matrix $X'X$ is singular and the normal equations no longer have a unique solution. In practice, this case of exact multicollinear data rarely occurs, but due to the presence of a near linear relationship among the multiple regressors, the near-multicollinear data frequently arises(*Souchay et al., 1995*).

Consequently, there are two important effects of multicollinearity, not readily illustrated by the foregoing. One is the instability of the regression coefficients which are very much dependent on the particular data set which generated them; the other is that the estimated coefficients may vary by large amounts and perhaps change sign.

When more than two regressors are taken into account, the simple correlations could be low and yet multicollinearity could be serious due to intercorrelations. Nonetheless, when only two regressors are considered, as is the case here, their multicollinearity degenerates into collineation.

In practice, there are many quantities which serve as multicollinearity diagnoses and evaluate the extent of the multicollinearity problem. For example, the simple correlations coefficients among the regressor variables is the most simple diagnosis and is often used; variance inflation factors(VIFs) represent the extent of inflation that each regression coefficient goes beyond the ideal condition in which the correlation matrix is a unit. So, VIFs are more accurate, at certain extent, than the simple correlations coefficients. In addition, the system of eigenvalues of $X'X$, including the eigenvalues, eigenvectors and the related condition numbers of the correlation matrix(*Maddala,1977*), is also a formal diagnostic tool. At times, the functions of these three diagnoses are equivalent to each other. In this paper, the simple correlation coefficients and VIFs are used to show the severity of collineation between ΔUT and $\Delta\phi$.

3.1. The simple correlation coefficients in a simulated observation

Assuming that the declination of the Moon, δ, is constant in the time span of observation, the simple correlation between ΔUT and $\Delta\phi$ can be obtained from equation (2):

$$r_{12} = \frac{\sum_{k=1}^{NP}(\sin H_k - \overline{\sin H})(\cos H_k - \overline{\cos H})}{\sqrt{\sum_{k=1}^{NP}(\sin H_k - \overline{\sin H})^2}\sqrt{\sum_{k=1}^{NP}(\cos H_k - \overline{\cos H})^2}} \tag{4}$$

Where, NP is the total number of normal points obteained from one telescope per night.

From equation (4), r_{12} is related to the time angles of retro-reflector H_k. If all observations are strictly symmetric with respect to meridian, it can be proved that r_{12} is always equal to 0.0, or r_{12} lies on (-1.0 +1.0).

A simulated observation is presented in this paper: Supposing there are five well-distributed normal points (NP=5), the time angle of the middle observation $H_0 = -0^h.10$, the total time span is 1 hour, then the time angle of other four observations are $H_{-2} = -0^h.60$, $H_{-1} = -0^h.35$, $H_{+1} = +0^h.15$ and $H_{+2} = +0^h.40$, the simple correlations,r_{12}, between ΔUT and $\Delta\phi$ is then calculated to be 0.56. Similarly, taking different central time angle H_0 and different time span of observation, the corresponding correlation coefficients r_{12} are listed in Table I.

Table I. The correlation coefficients of different H_0 and different observation span (NP=5)

$H_0(hour)$	S P A N (hour)										
	1.0	1.2	1.4	1.6	1.8	2.0	2.2	2.4	2.6	2.8	3.0
-0.1	0.56	0.49	0.43	0.39	0.35	0.32	0.29	0.27	0.25	0.23	0.22
-0.2	0.80	0.75	0.69	0.64	0.60	0.56	0.52	0.49	0.45	0.43	0.40
-0.3	0.90	0.86	0.82	0.78	0.74	0.71	0.67	0.64	0.61	0.58	0.55
-0.5	0.96	0.94	0.92	0.90	0.88	0.86	0.83	0.81	0.78	0.76	0.74
-0.7	0.98	0.97	0.96	0.94	0.93	0.92	0.90	0.89	0.87	0.85	0.83
-1.0	0.99	0.98	0.98	0.97	0.96	0.95	0.95	0.94	0.93	0.91	0.90
-1.5	0.99	0.99	0.99	0.98	0.98	0.98	0.97	0.97	0.96	0.95	0.95
-2.0	1.00	0.99	0.99	0.99	0.99	0.98	0.98	0.98	0.97	0.97	0.96
-2.5	1.00	1.00	0.99	0.99	0.99	0.99	0.98	0.98	0.98	0.97	0.97
-3.0	1.00	1.00	0.99	0.99	0.99	0.99	0.99	0.98	0.98	0.98	0.97

It can be concluded from Table I that

(1) the farther the distance between the central time angle of observation H_0 and meridian is, the larger r_{12}; and

(2) the longer the time span is, the smaller r_{12}.

Additionally, with the same time span and the same central time angle of observation, increasing or decreasing the number of normal points NP makes r_{12} vary little; making the central time angle of observation the opposite sign with the same other conditions makes r_{12} the opposite sign, too.

Nonetheless, because the practical observations are far from symmetric and well-distributed and the central time angles are also usually far from meridian, the practical correlation coefficients are often very large. This can be reflected in the VIFs of practical observation data in the following section.

3.2. Variance Inflation Factors(VIF)

The VIF of the ith coefficient is defined by (*Neter et al,1983*)

$$(VIF)_i = (1 - r_i^2)^{-1} \qquad (i = 1, 2, ..., p-1) \tag{5}$$

where, r_i^2 is the complex coefficient of the regressor variable x_i against the remain (p-2) regressor variables, the $x_j (j \neq i)$.

It is easy to see that VIF involves the notion of multiple association. If the ith regressor variable has a strong linear association with the remaining regressors, r_i^2 is near unity, $(VIF)_i$ will be very large. They supply us with a numerical indication of which coefficients are adversely affected and of how the extent is, so VIFs represent a considerably more productive approach for detection than do the simple correlation values.

When $p - 1 = 2$, i.e., there are only two regressor variables, as the case here, the situation becomes clear and easy to deal with. At this time, r_i becomes the simple correlation coefficient r_{12} between $\Delta\phi$ and ΔUT. The relationship between VIFs and r_{12} is

$$(VIF)_1 = (VIF)_2 = 1/(1 - r_{12}^2) \tag{6}$$

Unfortunately, there is not a universal value of VIF which can tell us whether there is multicollinearity, but it is practically believed that if any VIF exceeds 10(equally, r_{12} larger than 0.95), there is reason for at least concern.

As an example and a test, the 1060 LLR normal points during Jan.7, 1995 and Dec.27,1995 are used, they are divided into 206 groups which were observed at the same telescope and retro-reflector in the same night, while about half groups are deleted because they are fewer than three normal points or they are obvious outliers. As a result, only 104 groups remained. Finally, their VIFs of ΔUT or $\Delta\phi$ are plotted in Figure I.

It is necessary to point out here that, in order to reduce the truncation error in the calculation of $(X'X)^{-1}$, the variables(X_1 and X_2) and Y have been previously transformed to X_1', X_2' and Y', by related transformation:

$$\begin{aligned} Y_i' &= \frac{1}{\sqrt{n-1}}\left(\frac{Y_i - \overline{Y}}{S_y}\right) \\ X_{i1}' &= \frac{1}{\sqrt{n-1}}\left(\frac{X_{i1} - \overline{X_1}}{S_1}\right) \\ X_{i2}' &= \frac{1}{\sqrt{n-1}}\left(\frac{X_{i2} - \overline{X_2}}{S_2}\right) \end{aligned} \tag{7}$$

where, the values under overline represent their mean value, and the S_y, S_1 and S_2 are the root mean square error of Y, X_1 and X_2 respectively.

It is shown from figure I that many of the VIFs are greater than 100 (equally, the simple correlation coefficients r_{12} are greater than 0.99). So, the collineation should be regarded as serious.

4. Adaptive Ridge Regression: The Method and Its Result

In order to overcome the so-called ill-condition situations where correlations between the various parameters in the model cause the $X'X$ matrix in equation (3) to be close to singular, giving rise to an unstable parameter estimates which, for example, have the wrong sign or are much larger than physical or practical considerations, there are several numerical methods available to obtain a better conditioning and to reduce the model to one of full rank. For example, there are principal component regression(*Hotelling et al., 1939*), latent root regression(*Webster et al., 1974*), stepwise regression(*Berk, 1977*), ridge regression(RR)(*Hoerl 1962; Weisberg 1985*) and so on. *Huang et al.(1993)* has attemoted for the first time to adopt RR method in LLR, which is proved to be effective.

Generally, in the RR method, another matrix, $(X'X + \theta I_t)$, is used to replace the original normal equations coefficient matrix $X'X$, where θ is the departure constant and positive, in practice, it usually lies on (0,1); I_t is the normalized matrix. RR becomes the least square estimation when $\theta = 0.0$. Consequently, the ridge regression estimation of the parameters **B** is

$$\beta = (X'X + \theta I_t)^{-1} Y \tag{8}$$

In fact, RR is a biased estimation. Alternately, it adds a constraint to the parameter estimation, so RR is somewhat controversial and, indeed, is often criticized by many statistical researchers, especially concerning its usage. Sometimes, the use of RR is unnecessary and even incorrect. But there is a situation in which RR can be used as a useful and exactly appropriate treatment of the problem. This situation is that the values of the regression parameters are unlikely to be large from prior theoretical knowledge or from a practical point of view (*Draper & Smith 1981*). Furthermore, people will probably prefer to use an estimation which is of small bias with high precision rather than to use one which is unbiased with very low precision because the probability of the former, with which the estimation distributes in the confidence region of the true value, is far greater than that of the latter.

Our LLR data reduction is just this case. We adopt the EOP(UT and polar coordinates) series from IERS Bulletin as initial values, so the regressor variables to be estimated are the deviations of UT from the IERS values. From a practical and theoretical point of view, the initial EOP value of IERS can be considered as appropriate "true" value. Their discrepancy should not be very large, especially when there is serious multicollinearity. So, now that it has been detected that there is serious multicollinearity, adding a constraint to the parameter estimation and adopting RR method are reasonable and appropriate.

However, it is difficult in RR to choose the value of θ. The choice of θ is essentially equivalent to an expression of how big one believes those parameters to be.

So, as for this problem, the benevolent see benevolence and the wise see wisdom– different people have different views, and it depends on the condition, under which the problem is discussed. Usually, it is determined by experience or manually with certain arbitrariness.

Here, we put an adaptive method for choice of θ:

$$\theta_k = (p-1)(rms)_{k-1} / \sum_{i=1}^{p-1} (\sigma_i^2 \beta_i^2)_{k-1} \tag{9}$$

Where, (p-1) is the number of parameters in the model which is 2 in this case, θ_k is the departure constant in the kth iteration; $(rms)_{k-1}, \sigma_{k-1}$ and β_{k-1} are the root mean square of residual, root mean square error and the estimated value of parameter β_i in the *(k-1)*th iteration, respectively. It is an iterative process, the criteria to end the iteration is determined by the author for various special purposes; for instance, the resulted root mean square error of estimated parameter may be asked by an author to be smaller than a value. If $k = 1$, the iteration is processed only once, this is just the general RR method based on the standard weighted least squares fit.

There are two benefits from equation (9):

(1) the intensity of constraint can vary according to the severity of multicollinearity. The more Severe the multicollinearity is, the more the constraint; by contrast, if there is not multicollinearity, θ will be zero, it returns to general least square estimation. This is just the concept of RR method, and

(2) the information of the resulted *rms* and root mean square error of estimated parameters can serve as feedback information for the choice of θ directly and in time.

4.1. Results

The LLR post-residuals during 1995 are used again to calculate the UT and $\Delta\phi$ by ARR model. The root mean square deviation(RMSD) of estimated UT by standard least squares fit(LS) and by ARR model are plotted in Figure (2a) and (2b), respectively. The deviation of UT results, by LS and by ARR, from the UT value of EOP(IERS)C04 are also plotted in Figure (2c) and (2d), respectively. It is obvious that

(1) the RMSD of the results by ARR model is smaller than that by LS, so, ARR is effective to reduce the RMSD, especially when RMSD is too large in which the multicollinearity usually occurs and

(2) the deviation of UT from EOP(IERS)C04 by ARR are smaller than that by LS.

So, ARR can make the results more stable and make the probability, with which the resulted UT locates inside the distribution region of EOP(IERS)C04, greater than that by LS, especially when there is serious multicollinearity.

5. Concluding Remarks

Adding a constraint will make the resulting system have a rotation. Generally speaking, all observation and reduction are biased. There is not any system which is absolute. There may be a departure with a constant term and a liner term or some periodic terms between two different systems. These two systems can be linked by transformation, so it is irrelevant whether one system is regared as effective as the preferred system. Additionally, in order to evaluate one system, it is not enough to note only the difference between this system and another reference system, even though the latter is considered as an absolute one; it is also necessary to investigate the internal stability of this system.

The correlation coefficients of simulation and VIFs of practical observation have shown the existence of serious collineation problems, which makes the result instable and unreliable. As a proper remedy, the ARR method, an improved form of RR, as well as the method to choose the departure constant θ, is suggested in this paper. It is proved that ARR is effective to reduce the multicollinearity and get satisfied results.

Acknowldgement

We should like to pay our respects to all the people who have been making the daily maintenance of the LLR equipment and the regular data storage during the long period of continuous registrations, especially under the present poor fund circumstances. We also thank the geodetic group of JPL for their kindness in providing us lunar and planetary ephemeris.

Reference

Berk, K., 1977, Tolerance and condition in regression computations, *J. Am. Statist. Assoc.*, **72**, 863-866

Draper, N.R. and Smith, H., 1981, Applied Regression analysis, John Wiley & Sons, Inc., New York, 313-324

Hoerl, A.E., 1962, Application of ridge analysis to regression problems, *Chem. Eng. Prog.*, **58**, 54-59

Hoerl, A.E., Kennard, R.W., and Baldwin, K.F., 1975, Ridge regression: some simulations, *Comm. Statist.*, **4**, 105-123

Hotelling, H., 1933, Analysis of a complex of statistical variables into principal components, *J. Ed. Psych.*, **24**, 417-441, 489-520

Huang, C.L.,1992, Improvment of the models in lunar laser ranging, M.S. Degree Thesis

Huang, C.L., Xu H.G., and Jin W.J., 1993, On the methods of determination of UT from LLR, *Annals of Shanghai Observatory, Academia Sinica*, **14**, 110-117

Huang, C.L., Jin, W.J., and Xu, H.G., 1996, The terrestrial and lunar reference frame in lunar laser ranging, *Journal of Geodesy* (accepted)

Jin, W.J., and Wang Q.G., 1985, Determination of ERP with LLR and discussion of the influence of the adopted parameters, *Proceedings of the international conference on earth ratation and terrestrial reference frame*, 287

Maddala, G.S., 1977, Econometrics, eds. Mc Graw Hill

Myers , R.H., 1986, Classical and moden regression with applications, PWS Publishers, Boston, 218-275

Neter, J., Wasserman, W., and Kutner, M.H, 1983, Applied Linear regression models, Richard D.Irwin, Inc.,

Souchay, J., Feissel, M., Bizouard C., Capitaine N., and Bougeard, M., 1995, Precession and nutation for a non-rigid earth: comparison between theory and VLBI observation, *Astron. Astrophys.*, **299**, 277-287

Wang, 1985, M.S. degree thesis.

Webster, J.T., Gunst, R.F., and Mason, R.L., 1974, Latent root regression analysis, *Technometrics*, **16**, 513-522

Weisberg, S., 1985, Applied Linear regression, John Wiley & Sons, Inc., New York, 196-225

Xu H.G., Jin W.J., and Huang C.L., 1996, The secular acceleration of the Moon determined from lunar laser ranging data, *Earth, Moon and Planets*, **73**, 101-106

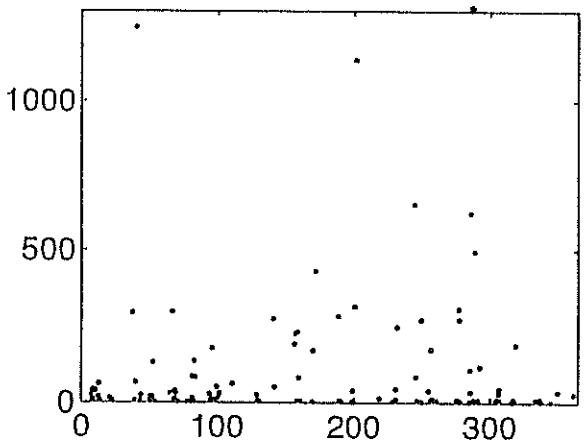

Figure I. VIF of UT

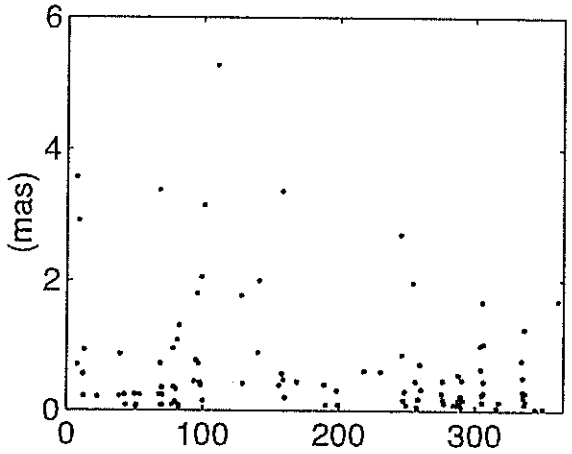

(2a) RMSD of UT by LS

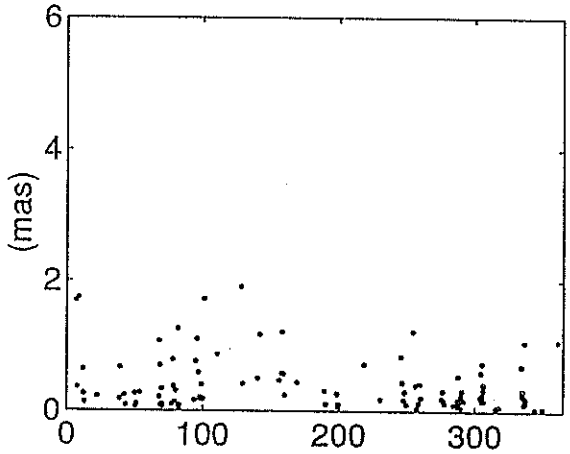

(2b) RMSD of UT by ARR

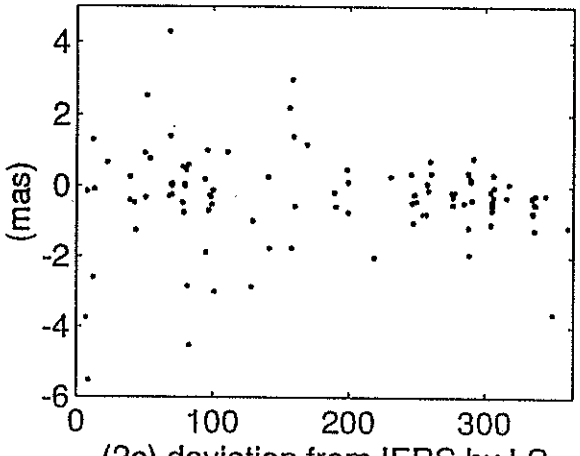

(2c) deviation from IERS by LS

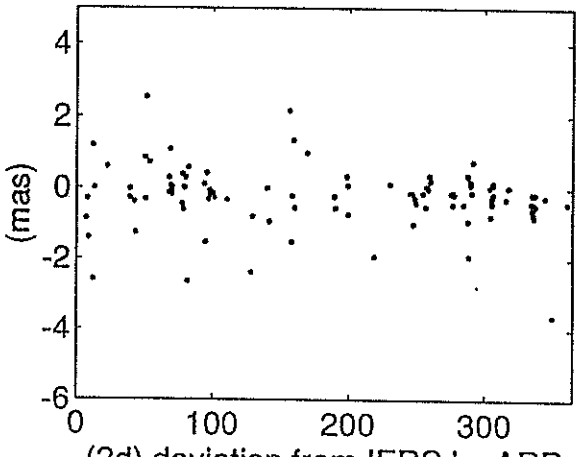

(2d) deviation from IERS by ARR

Expected Results from the Analysis of LLR Data

J. Müller
Institut für Astronomische und Physikalische Geodäsie
Technische Universität München
D-80290 München, Germany
Email: jxmx@alpha.fesg.tu-muenchen.de

U. Schreiber
Forschungseinrichtung Satellitengeodäsie
Fundamentalstation Wettzell
D-93444 Kötzting, Germany

Abstract

Lunar Laser Ranging provides an excellent tool for testing metric theories of gravitation. Remarkable results have been obtained by analyzing the lunar observations over the past 27 years. However the realistic errors of the relativistic parameters (of others too) are by a factor 3 (or more) larger than the formal standard errors resulting from the global fit. This discrepancy can be reduced by an improved observation strategy and by a more accurate analysis model.

1. Introduction

Since the beginnig of Lunar Laser Ranging (LLR) in 1969, the data have been used for the determination of relativistic quantities and parameters describing the dynamics of the Earth-Moon system. In fact, one important reason for setting up the LLR experiment has been the chance to test EINSTEIN's theory: if there exists a violation of the strong equivalence principle, the lunar orbit about the Earth would be polarised towards the Sun (NORDTVEDT effect) which can be measured by LLR ([1]).
Several analysis centers determined relativistic quantities like the NORDTVEDT parameter η, metric parameters (γ, β, α_1), a time variation of the gravitational constant $\dot{G}/G$ and others (see e.g. [5], [4], [2], [3]). It is obvious that the realistic errors derived in some tricky way are much larger than the formal errors obtained from the adjustment of the unknown parameters. The results for the relativistic quantities determined at our institute are given in table 1. The realistic errors are up to a factor 3 - 5 (one about 10) worse compared to the formal ones. The reason for the difference is the insufficient theoretical model, but also the non-ideal distribution of the observations. Therefore both analysts and observers can contribute to an improvement of the LLR results. This will be shown for the NORDTVEDT effect.

Table 1: Realistic errors for the relativistic quantities

parameter	realistic error
geod. prec. Ω_{GP} ["/cy]	$\leq 1.5 \cdot 10^{-2}$
metric par. γ	$\leq 6 \cdot 10^{-3}$
metric par. β	$\leq 5 \cdot 10^{-3}$
Nordtvedt par. η	$\leq 1 \cdot 10^{-3}$
time var. grav.const. $\dot{G}/G$ [yr^{-1}]	$\leq 5 \cdot 10^{-12}$
Yuk. coupl.const. $\alpha_{\lambda=4\cdot10^5\,\mathrm{km}}$	$\leq 1 \cdot 10^{-11}$
spec. relativity $\zeta_1 - \zeta_0 - 1$	$\leq 1.5 \cdot 10^{-4}$
infl. of dark matter δg_c [$\mathrm{cm/s}^2$]	$\leq 3 \cdot 10^{-14}$
preferred frame effect: α_1	$\leq 9 \cdot 10^{-5}$
preferred frame effect: α_2	$\leq 2.5 \cdot 10^{-5}$

Furthermore, the precision of the observations has improved remarkably[1] since the beginning in 1969 (figure 1). One goal should be to transfer this increase of accuracy as good as possible to the quantities to be determined by the analysis of LLR data.

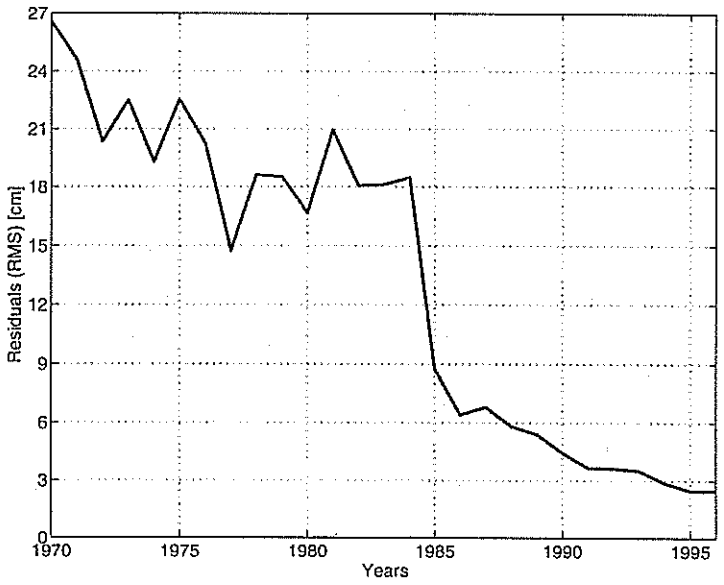

Figure 1: RMS Residuals (observed - computed Earth-Moon distance)

2. Expected results for the NORDTVEDT parameter

The NORDTVEDT effect which describes how a violation of the strong equivalence priniple would appear in the Earth-Moon system, can be understood as follows: the silicate Moon is attracted by the Sun in a different way as the nickel-iron Earth which leads to a shift of the lunar orbit towards the Sun[2]; see figure 2.

[1] A precision of 3 mm for a single normal point seems possible.

[2] In contrast, EINSTEIN, also NEWTON state that all bodies/matter will be attracted gravitationally in

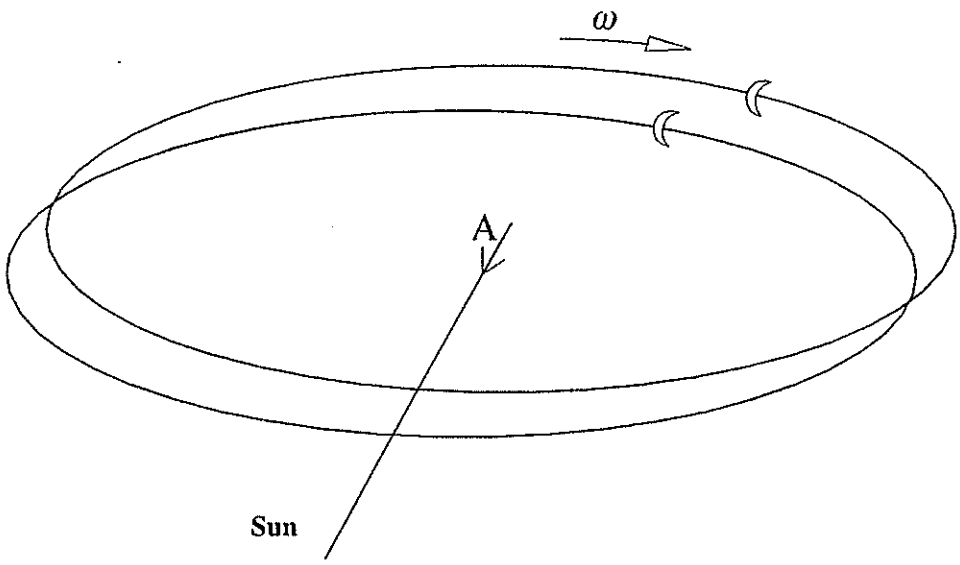

Figure 2: NORDTVEDT effect

This effect can be modelled by

$$\Delta r_{Earth-Moon} = 12.8\,\eta\cos(\omega\ t)\ [\mathrm{m}] = \mathrm{A}\cos(\omega\ \mathrm{t}). \tag{1}$$

ω is the synodic frequency (angular velocity of the Moon). The amplitude A can be determined with a realistic error of 1.3 cm, whereas the formal error becomes only about 3 mm. One should try to achieve this 3 mm as realistic error. To see how to reach this goal one can look on figure 3.
There the lunar residuals (observed - computed Earth-Moon distance) are plotted as a function of their angular distance from the nearest New Moon[3]. The residuals are weighted and averaged over 10 degree blocks. E.g. for 25° we took observations between 20° and 30°. The residuals plotted at 175° are based theoretically on measurements between 170° and 180°. In fact there are only observations available which were performed during some lunar eclipse (Full Moon) which means they belong all to 179,...°.
What can be seen? The residuals are much worse near New and Full Moon. But the observations during lunar eclipses are better than those taken for 165° (much noise by reflected photons from the surface of the Moon). Bad residuals can mean bad theoretical model or bad observations or both.
The smoother curve (dashed) is designated with 'Nordtvedt effect'. It shows how the NORDTVEDT effect appears in such a plot, if one does not model it in the analysis program resp. does not solve for the amplitude of the synodic frequency. It was computed by adding a signal as (1) to the computed range using our largest error value (that 1.3 cm, the realistic error) for the amplitude A. The post-fit residuals have been compared to those post-fit residuals where this effect was not considered. The dashed curve in figure 3 shows the difference between the post-fit residuals of both fits.

---

the same way.

[3]For the following discussion, only the observations since 1986 are used where more than one observatory are tracking the Moon and the precision of the observations are much better since before (figure 1).

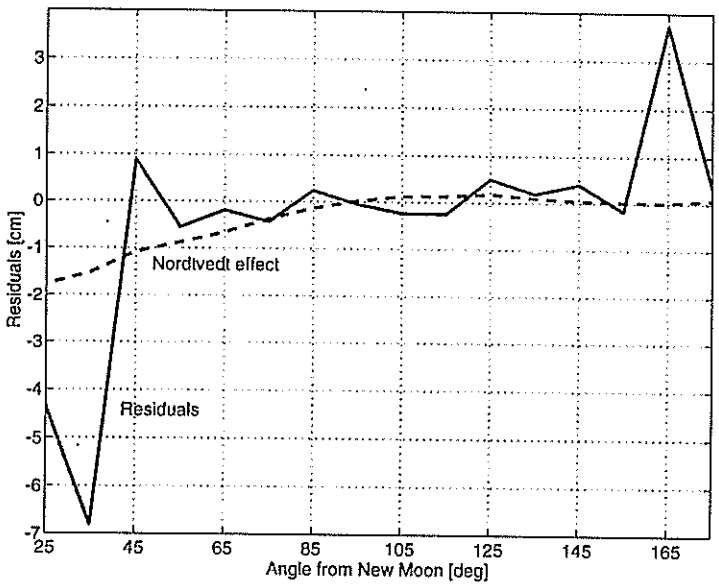

Figure 3: Weighted Residuals (solid line) and NORDTVEDT effect (dashed line) as a function of the angular distance from the nearest New Moon

It can be clearly seen that such a large NORDTVEDT effect can not be found in the observations and if at all it is caused by the bad observations (or bad model) near New Moon.
A further error source is given by the less accurate observations in the seventies which are neglected for the computation of the residuals in figure 3; but for the determination of the realistic error of the NORDTVEDT parameter all measurements since 1970 have been used. Therefore it would be certainly advantageous to neglect the old observations when investigating the NORDTVEDT effect, but it would be very disadvantageous for the determination of $\dot{G}/G$ which can be just well determined from the very long period of observations.
Figure 4 supports the arguments of figure 3. Near New and Full Moon, one has not only bad but even much less observations. It means one observes only a small part of the lunar orbit with many observations and a large part is only observed marginally. Then it is difficult to improve the theoretical model in such areas if one has only less observations. One can not decide what an improvement is at all.
Measurements near New Moon have to be performed in low elevations in most cases to avoid perturbing light from the Sun. But just this fact (low elevations) provides the possibility to investigate elevation-dependent effects (e.g. caused by the atmosphere) which could still be modelled insufficiently. And such an insufficient modeling could be responsible for the increase of the residuals near New Moon. If analysts would get more observations in these areas they could search for errors in their models with more success.

3. Conclusions

The future tasks follow automatically: the theoretical model has to be improved up to mm level (to be done by the analysts); one needs more good observations especially near New

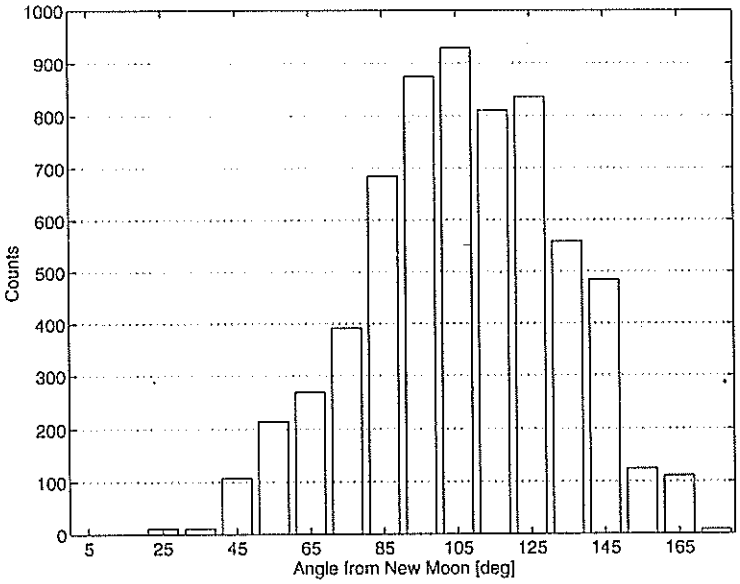

Figure 4: Distribution of lunar observations as a function of the angular distance to the nearest New Moon

and Full Moon. Taking both actions together one can extract much more information from the LLR data as now. One can improve the accuracies of the solve-for parameters; the NORDTVEDT parameter can be determined with a realistic error of a factor 3 better than now. Similar results can be expected for the other parameters.

Acknowledgment. We thank Ken Nordtvedt for many clarifying discussions within this context.

References

[1] K. Nordtvedt: Testing relativity with laser ranging to the Moon. Phys. Rev., Vol. 170, 1186 (1968)

[2] J. Müller, M. Schneider, M. Soffel, H. Ruder: Determination of Relativistic Quantities by Analyzing Lunar Laser Ranging Data. Proceedings of the 7th Marcel Grossmann Meeting on General Relativity, Stanford, July 1994 (to appear)

[3] J. Müller, D. Vokrouhlický, K. Nordtvedt: An improved constraint on the α_1 PPN parameter from lunar motion. Phys. Rev. D, Vol. 54, 5927 (1996)

[4] J. Dickey et al.: Lunar Laser Ranging: A Continuing Legacy of the Apollo Program. Science, Vol. 265, 482 (1994)

[5] J. Williams, S. Newhall and J. Dickey: Relativity Parameters Determined from Lunar Laser Ranging. Phys. Rev. D, Vol. 53, 6730 (1996)

The Impact of Technology on Lunar Laser Ranging at MLRS

Peter J. Shelus
McDonald Observatory/Department of Astronomy/Center for Space Research
University of Texas at Austin
Austin, TX 78712-1083
USA

Abstract

Lunar laser ranging observing operations at McDonald Observatory have evolved markedly over the almost 30 years of activity. These included software and hardware changes as well as logistical and administrative ones. Each change ws designed to provide for improvemnet in either data quantity or quality or both. Some were successful; some were not. The prersent paper presents the latest set of changes at the MLRS and their effects.

1.0 Introduction

At McDonald Observatory, the use of two different ranging systems has led to different quantities and qualities of laser ranging data over the history of the experiment. The original McDonald 2.7-m system was a lunar only one. It was built around ruby laser technology, using rather long, powerful laser pulses and slow firing rates, i.e., 3-6 joule/pulse, 3-6 nanosecond pulse-length, 1/3-1 hertz. The later system, the MLRS, was a joint lunar and artificial satellite system. It was built around Nd-YAG laser technology, using shorter, less powerful laser pulses and much more rapid firing rates, i.e., 120 millijoules/pulse, 100-400 picosecond pulse-lengths, 10 hertz. Laser ranging data accuracy, to first order and with everything else being equal, scales inversely with laser pulse length, thus the shorter pulse length of the Nd-YAG laser has led to almost a factor four improvement in the accuracy of the ranges. Since the total weight of a set of observations scales linearly with data accuracy, but only as the inverse square of the number of observations, the later data sets are much better.

2.0 The present McDonald SLR/LLR station

Since 1991, we have pursued an aggressive and a substantial lunar upgrade for the MLRS. The effort has enjoyed a most remarkable success.

- The lunar data rate for the MLRS has been increased by almost an order of magnitude.
- LLR data accuracy and precision has been at least doubled.
- The number of UT-0 Earth orientation points has increased by almost a factor six.
- For the first time since 2.7-m operations in the mid-1980's, McDonald Observatory LLR operations are obtaining, on a routine basis, significant amounts of multi-corner data, i.e., ranges to more than one lunar surface retroreflector during a single observing session.
- During 1995 the MLRS actually exceeded the best years of 2.7-m operations, in terms of data volume, and this has continued through 1996.
- MLRS data quality greatly exceeds that of the 2.7-m system.
- SLR/LLR operational status has been maintained at all times throughout the upgrade.
- The MLRS continued as one of the best SLR stations in the world.

Figure 1 illustrates the spendid multi-terget capabilities of the MLRS, together with the vast increases in data volume obtained for both SLR and LLR operations over the past several years. Figure 2 illustrates the improved LLR data quality and quantity characteristics of the MLRS, compared to that of the original 2.7-m system.

3.0 The MLRS LLR upgrade

The various steps of the MLRS LLR upgrade have been summarized before. With the virtual completion of the task, these steps are now included here again, for completeness.

- Offset guiding Stage: allows for guiding on a sun-lit, off-axis surface feature while the lunar surface retroreflector is still in shadow. This provides for a greater number of observing sessions during a lunation as well as the fact that ranging to a retroreflector in the dark produces virtually noise free data.
- Optics: replacement of old and damaged optical elements and using additional spectral filters to provide better energy throughput to the detectors as well as better observational flexibility during changing environmental conditions.

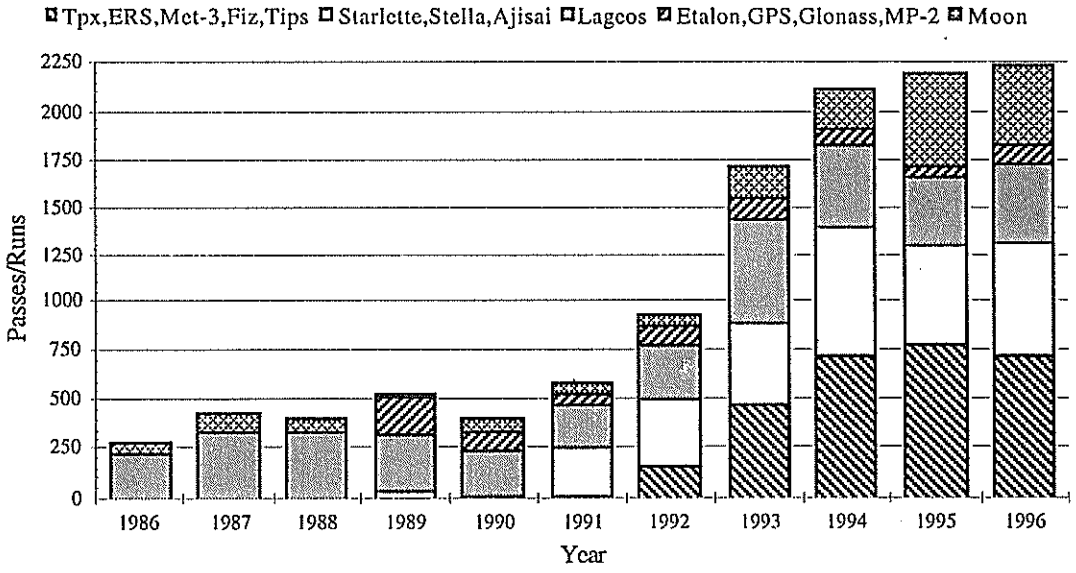

Figure 1. MLRS laser ranging Data Throughput

- Auto-Guiding and Image Enhancement: an integrated hardware and software system that accepts real-time, video signals as input and performs real-time image processing to produce raw and filtered tracking error signals to the control computer for automatic guiding.
- Avalanche Photo-Diode: in receive path, similar to that used at OCA, should provide a noticeable increase in sensitivity due to better quantum efficiency as well as improved accuracy and precision due to better jitter characteristics.
- Control Computer: replaces the original MLRS 15 year old Data General NOVA system with a LynxOS based, X-windows, real-time UNIX system running on PC hardware.

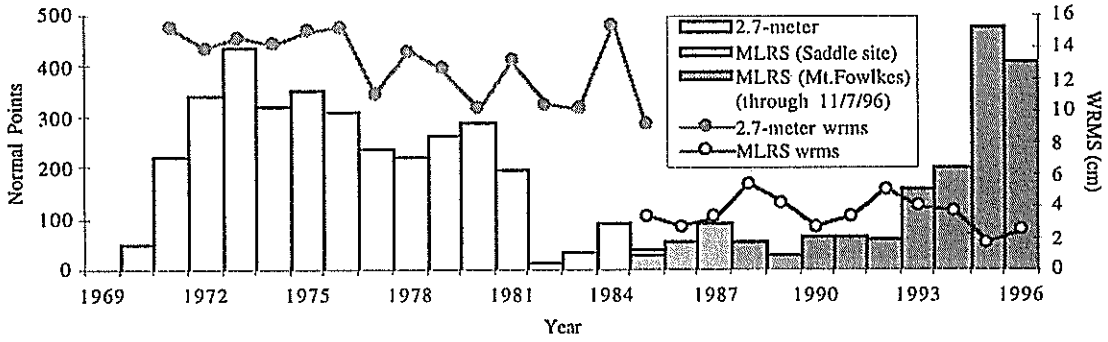

Figure 2. Number of normal points and weighted RMS of post-fit residuals for McDonald LLR observations.

4.0 Conclusions

A series of enhancements at the MLRS has produced significant gains in LLR data quantity and quality. The multi-purpose MLRS (SLR & LLR), with a 0.75-m aperture at a good site, is now competitive with the larger, dedicated LLR station at OCA. With a thoughtful and planned use of resources, significant amounts of both SLR and LLR observations can be obtained simultaneously with excellent results. A selected sub-set of appropriate SLR stations perhaps should examine the possibility of making LLR observations at some small level.

5.0 Acknowledgments

I wish to acknowledge and thank Randall L. Ricklefs, Judit G. Ries, Arthur L. Whipple and Jerry R. Wiant for helpful advice and counsel during the preparation of this paper. A part of this effort is currently being supported by NASA Grants and Contracts NAS5-32997, NAGW-2970, NAGW-4277, NAGW-4862.

The Lunar Laser Ranging Network and the Lunar Data Gathered ... ... Are they Sufficient?

Peter J. Shelus
McDonald Observatory/Department of Astronomy/Center for Space Research
University of Texas at Austin
Austin, TX 78712-1083
USA

Abstract

Success with the analysis of any data type depends critically upon the quality and the quantity of those data. Over the past several years, the present SLR/LLR laser tracking network has become responsible for the monitoring of an increasingly large number of Earth-orbiting targets. Therefore, in this era of vastly shrinking resources, it is becoming increasingly mandatory to assess specific data requirements for the types of scientific analysis that are to be performed. In this paper we consider the lunar laser ranging data type. We ask the questions as to the types of science that are being done, as well as the quality and quantity of data that is required. We then consider the present network of LLR capable stations and determine the adequacy, or the lack thereof, of the present LLR data products.

1.0 Introduction

The resources of the world-wide laser ranging community are increasingly being brought under greater pressure. The number of Earth-orbiting targets that require observing support is growing and the shrinking of financial support mandates that ever greater cost efficiencies be obtained. It is therefore absolutely necessary that we begin monitoring a set of cost/benefit parameters to maximize the amount of science being performed per unit cost. In the present paper we examine those laser ranging stations that are lunar capable, the quantity and quality of the data that can be gathered by them, as well as the types of science that are able to be pursued. We will evaluate those results and assess overall LLR network strengths and weaknesses.

2.0 The lunar data yield

At the present time only two stations in the laser ranging network are routinely capable of ranging to the Moon. They are the French station at the Observatoire de la Cote d'Azur near Grasse (OCA) and the United States station at McDonald Observatory near Fort Davis, Texas (MLRS). The lunar data yield from those two stations over the past four years are shown in Table 1. Those data are broken down into the number of normal points and the number of minutes of LLR data that were observed annually, the number of nights throughout the year when LLR data were taken, and the number of UT-0 Earth rotation points computed using LLR data.

3.0 Lunar science

The lunar science that is being addressed by the general analytical community, using the LLR data type, is specifically addressed in another paper in these workshop proceedings. However, for the purposes of this paper, we wish to consider the following types of LLR-related science, together with an estimate of the quality and the quantity of the data that is required:

Lunar structure (probing the lunar core and mantle)
Round-robin, multi-reflector sub-cm normal points in a 1 hour span
Data should be obtained at least several times (3-5) per month

Spacecraft navigation and Solar System ephemeris generation (where is the Earth?)
Several (5-10) sub-cm normal points distributed throughout a month
Data should be obtained every month

General relativity & gravitation (Nordtvedt effect, geodetic precession, G-dot)
Sub-cm data covering all lunar phases
Data should be obtained every lunation

Earth Orientation (looking for sub-daily signals)
Several sub-cm normal points (5 or more) within a 2 hour span
Data should be obtained as many days as possible during a month

Table 1

MLRS/OCA Lunar Laser Ranging Data Throughput (1993-1996)

		MLRS				OCA			
		1993	1994	1995	1996	1993	1994	1995	1996
LLR Normal Points	Ap 11	3	25	34	38	53	55	59	50
	Ap 14	8	17	54	34	53	44	49	57
	Ap 15	151	160	383	337	433	499	457	485
	Lnk 2	1	3	6	1	12	17	12	15
	Total	163	205	477	410	551	615	577	607
Lunar returns	Ap 11	12	158	392	405	1,296	1,695	1,710	1,377
	Ap 14	55	131	830	454	1,526	1,119	1,562	2,046
	Ap 15	1,589	1,583	7,445	5,986	14,450	23,424	21,679	29,644
	Lun 2	2	8	32	4	132	407	194	197
	Total	1,668	1,880	8,699	6,849	17,404	26,645	25,145	33,264
Minutes of LLR Data	Ap 11	28	382	428	565	561	484	513	432
	Ap 14	141	242	688	506	485	383	432	505
	Ap 15	1,953	2,122	5,059	4,260	4,156	4,603	4,296	4,544
	Lnk 2	3	40	75	11	105	142	104	123
	Total	2,125	2,776	6,250	5,343	5,307	5,612	5,345	5,604
Nights LLR Data Taken	Ap 11	2	16	21	24	27	23	24	26
	Ap 14	5	12	29	20	26	17	24	27
	Ap 15	56	61	104	89	75	71	65	66
	Lnk 2	1	3	4	1	11	9	8	6
UT0 pts.	Ap 15	26	30	65	52	49	44	47	49

4.0 The data statistics

The four usable lunar surface retroreflectors comprise a large quadrilateral on the Moon's surface. Because of the its aspherical mass distribution and the gravitational attraction of the Sun and planets (forced librations) and departures of the its angular position from an equilibrium state (free librations), the Moon experiences departures from uniform rotation. Both forced and free librations are apparent in LLR data. These complex angular motions of the Moon about its center of mass can be separated with high accuracy using differential range measurements to the several retroreflectors. This provides a powerful tool to probe the interior of the Moon and its structure. It becomes of paramount importance that ranges to the several retroreflectors be obtained close in time so that the differential measures can be formed. Figure 1 shows observation times and (O - C) residuals for two recent LLR runs, one on April 10, 1996 at OCA (on the left) and another on September 22, 1996 at MLRS (on the right), where the data yield satisfies the data requirements for probing the interior structure of the Moon. During each of these runs, successive multi-reflector normal points were obtained during relatively short intervals of time.

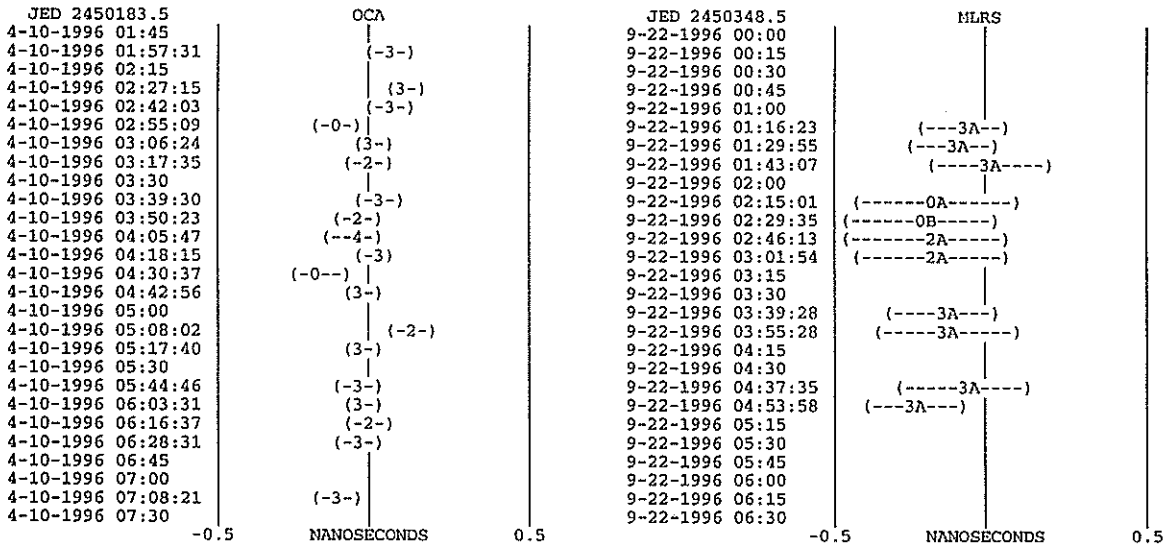

Figure 1. Multi-reflector LLR data from OCA and MLRS .

Spacecraft navigation, both manned and unmanned, is a vital tool that allows us to perform in situ examinations of many objects in the Solar System. Because any probe must initially depart from the Earth, it is necessary that the position of the Earth within the Solar System, as a function of time, be known with maximum precision and accuracy. The LLR data type provides that required accuracy and precision uniquely. However, because errors grow quickly when one extrapolates beyond the range of a data set, it is important that a continuous set of LLR observations be available to maintain this required precision and accuracy. Table 2, showing only MLRS monthly normal point yields, reveals that, at least since early 1993, the spacecraft navigation and Solar System ephemeris requirements for LLR are easily being fulfilled. In fact, we see that several ten's of LLR normal points are being routinely gathered each and every month. Even better monthly statistics exist for the OCA station.

Table 2

Monthly Statistics for MLRS LLR Normal Points

	1987	1988	1989	1990	1991	1992	1993	1994	1995	1996
January	18	5	1	7	0	0	7	14	22	22
February	13	1	0	7	9	1	3	14	34	31
March	13	15	0	2	2	1	5	7	60	26
April	1	6	0	0	1	5	10	18	25	26
May	10	8	8	2	3	8	21	12	38	56
June	1	21	0	8	7	4	28	17	44	37
July	4	3	0	4	8	3	12	0	32	60
August	0	10	0	0	2	0	19	47	7	10
September	11	7	6	12	10	19	14	29	41	52
October	16	11	3	13	11	6	12	7	61	27
November	3	4	11	2	8	6	18	21	65	31
December	6	0	7	14	7	7	18	20	48	32

The five histograms of Figure 2 illustrate the distribution of LLR normal points with respect to the classical fundamental arguments of the lunar theory. Flat, long-term data distributions are especially important for the relativistic and gravitational science being pursued with LLR data. With almost 30 years of data in hand, the distribution of LLR observations with respect to the lunar mean anomaly l (a monthly period), the solar mean anomaly l' (an annual period), and the argument of the latitude F, are reasonably flat. Further, much more than one full period of LLR data exists for the 18.6 year period of the mean longitude of the ascending node of the lunar orbit, Ω, even though the distribution itself is not exactly flat. However, it is the mean elongation of the Moon from the Sun, D, that renders the greatest problem for LLR data distribution. This phenomena speaks to the extreme difficulty that is associated with obtaining lunar ranges at the new and full moon phases and the consequent preferential scheduling of LLR observing time at the quarters, when ranges are most easy to obtain.

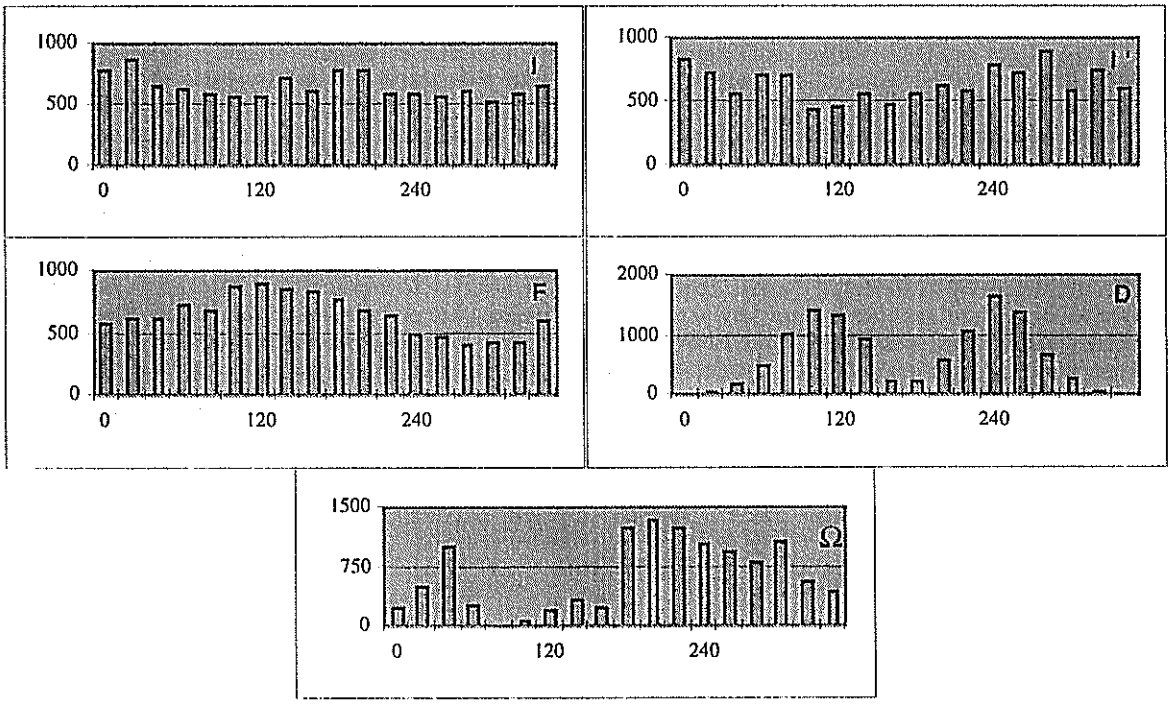

Figure 2. Distribution of LLR observations with respect to the fundamental arguments of the lunar motion.

Together with other space-based techniques, e.g., SLR, VLBI, microwave, and GPS, LLR contributes important information about the variations of the Earth's rotation, including precession and nutation. Also, in a unique sense, LLR determines the intersection of the Earth's equatorial plane with the plane of the Moon's orbit as well as the angle between them. From these, the equivalent quantities for the Earth's orbit can be found. The resulting dynamical equinox and obliquity of the ecliptic can then be used to tie the Solar System reference frame to that determined from the Earth's rotation. Since VLBI observations can tie the Earth rotation frame accurately and precisely to an inertial frame based upon distant radio sources, the Solar System frame can then be tied to that same inertial frame. Illustrating the density and the continuity of the LLR observations that contribute to these types of tasks, Figure 3 depicts both the OCA and MLRS-derived UT-0 points that were computed during the past 600 days using LLR observing observations.

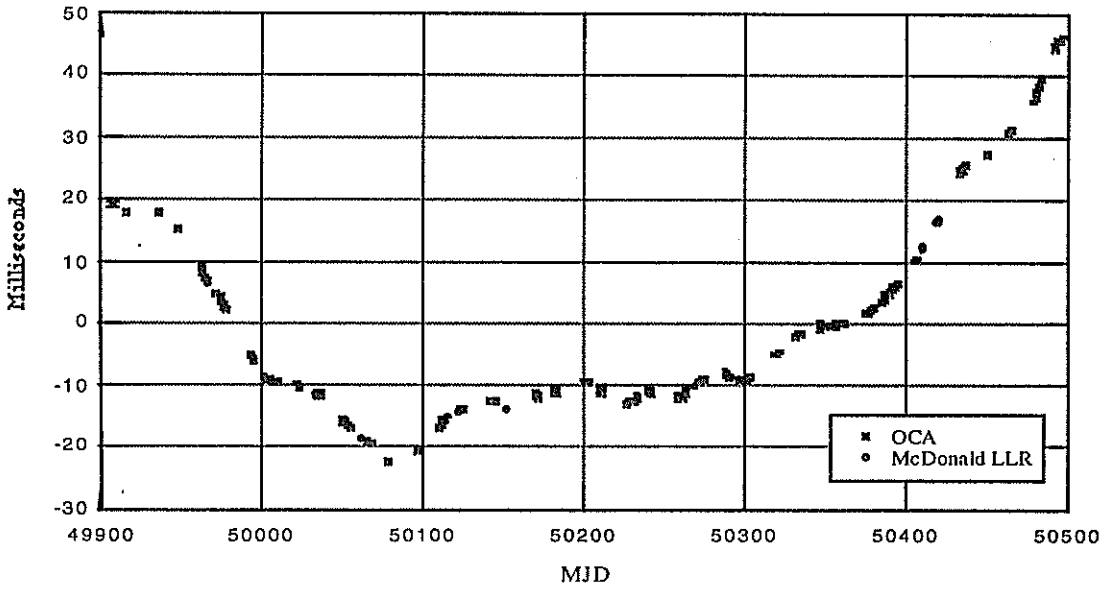

Figure 3. UT-2R -TAI results (with slope removed)

5.0 Summary and conclusion

On the positive side, an objective assessment of the situation shows that the present LLR network, consisting only of the MLRS and OCA stations, is doing remarkably well. LLR data density and accuracy, as well as multi-reflector data, when it is obtained, is quite good. On the negative side, the present LLR-capable part of the SLR network is just barely adequate. Any two-station network is going to be especially vulnerable to weather, equipment, and funding problems. Gaps in data acquisition can be common. Also, of paramount importance for the additional benefit of the LLR data type, the routine generation of sub-cm data must be strongly advocated.

Looking to the future, good effort is already being applied within LLR, especially at OCA, to make routine sub-cm LLR data acquisition a reality. There also must be much more effort applied to obtaining more comprehensive lunar phase coverage. It has been shown in the past that LLR data can be obtained at and near full Moon. However, the difficulty of the task requires additional stations over which the effort might be spread. Further, on account of the Moon's proximity to the Sun, performing LLR observations near the new Moon phase can be quite dangerous, both to equipment as well as to personnel. Can the development and implementation of absolute telescope pointing and better "bright sky" technologies ameliorate some of this danger?

The obvious conclusion is that OCA and MLRS are doing a remarkable job with respect to LLR observations. OCA continues as primarily an LLR-only station. MLRS continues in its part-time LLR mode, while continuing to be one of the most prolific data producers in the world of SLR data. A few other, part-time, LLR-capable stations could help to eliminate weather and equipment problems as well as to spread out the effort that is required for the more difficult tasks. A final comment is that at least one southern hemisphere LLR-capable SLR station should be sought.

6.0 Acknowledgments

I wish to acknowledge and thank Randall L. Ricklefs, Judit G. Ries, Arthur L. Whipple and Jerry R. Wiant for helpful advice and counsel during the preparation of this paper. A part of this effort is currently being supported by NASA Grants and Contracts NAS5-32997, NAGW-2970, NAGW-4277, NAGW-4862.

Millimetric Lunar Laser Ranging
O.C.A./C.E.R.G.A.

J.F.Mangin ; J.E.Chabaudie ; D.Feraudy ; P.Fridelance ; M.Furia ; M.Glentzlin ;
A.Journet ; J.Pham Van ; E.Samain ; J.M.Torre ; G.Vigouroux .

Status and accuracy

A new manager for the French L.L.R. station :

- In September 1996, Christian VEILLET left the C.E.R.G.A. to join the staff of the Canada, France, Hawaii Telescope.

- Jean-François MANGIN is the new manager. (email : MANGIN@OBS-AZUR.FR).

Status of the millimetric L.L.R. station :

Status : laser

- The Y.A.G. laser emits a train with 3 pulses at about 10 Hz. Each pulsewidth is 130 ps. The train energy is about 600 mJ. The time interval between the first and the second pulse is 1.6 ns, and between the second and the third is 2.5 ns. It will be possible, in the future, to work with 4 pulses with a pulsewidth of 90 ps ; the train energy will be the same.

Status : filtering

- Spatial filter : In general, we works with 15 arc second in dark and 7 or 10 arc second in light (this depends on the seeing).

- Spectral filter : We use two filters, the first is a Fabry-Perot filter 1.2 A°, finesse 50, followed by a large filter 60 A° . The total transmission is 60%.

- Temporal filter : The electronic and computer gate is usually 100 ns wide. For satellite ranging it is possible to increase the gate to 2 μs.

Status : datation

- Start time : The detector at the emission is an infrared InGaAs pin diode (C30617 RCA). It works with a large number of photoelectrons, therefore the precision is better than 10 ps.

- Return time : The return detector is a silicon A.P.D. (Silicon sensor: SSOAD-230) working in single photoelectron. It is used at a temperature -50° C. The continuous voltage is -138 V (breakdown = -142 V for this using temperature) and the geiger voltage is -150 V added to the continuous voltage. The geiger pulsewidth is 2μs, but the beginning is 80 ns before predicted return from the Moon. In that case the precision is 35 ps.

- Event timing system : This system is constituted by two event timing modules and one clock generator module connected to a caesium clock. We use one event timing module for the start

time and one for the calibration-target time or for the Moon-return time. The interval time accuracy is 7 ps.

Accuracy analysis :

Standard deviation :

- The standard deviation is between 60 ps and 200 ps, often below 100 ps. It depends on the laser, on the lunar reflector size and on the Moon libration. The event timers and detectors precision are of little effect on the standard deviation.

- For medium series (100 echoes in 10 min and st. dev. = 100 ps), the normal point precision should be 10 ps without atmospheric effect.

Accuracy test :

- In our station we range simultaneously, with the same laser pulse, a local target within the telescope and the reflector on the Moon.

- By calibration of the local corner cube we have an accurate measurement of the pulse flight time.

- In our case we emit a pulse train (3 pulses) and the accuracy of the distances measured between the pulses gives a good idea of the best accuracy that could be achieved on the Moon for comparable returns rates. Of course the atmospheric effect is not taken in account.

- The following plot shows the accuracy of the distance measured, between two pulses, on a local target, during seven hours. The st. dev. is 8 ps for 30 normal points.

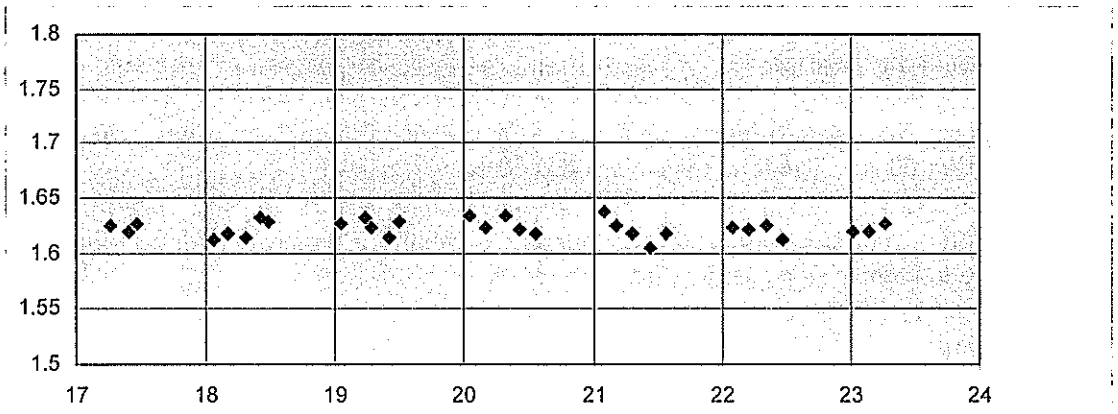

Last results

- Since 24 July 1995, the station works with a millimetric accuracy, there were 93 nights with the following results :
  ref. 0 TRA 2501 echoes in 87 normal points
  ref. 2 FMR 2734 echoes in 78 normal points
  ref. 3 HAD 42966 echoes in 714 normal points
  ref. 4 LK2 345 echoes in 25 normal points

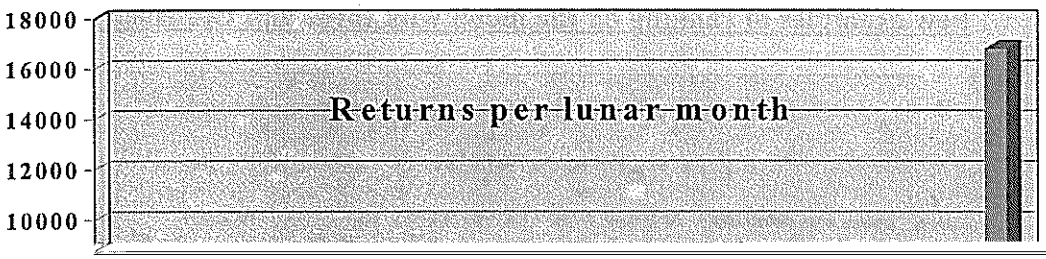
18000
16000
14000
12000
10000
Returns per lunar month

Few examples of ranging on the moon with three and two laser pulses

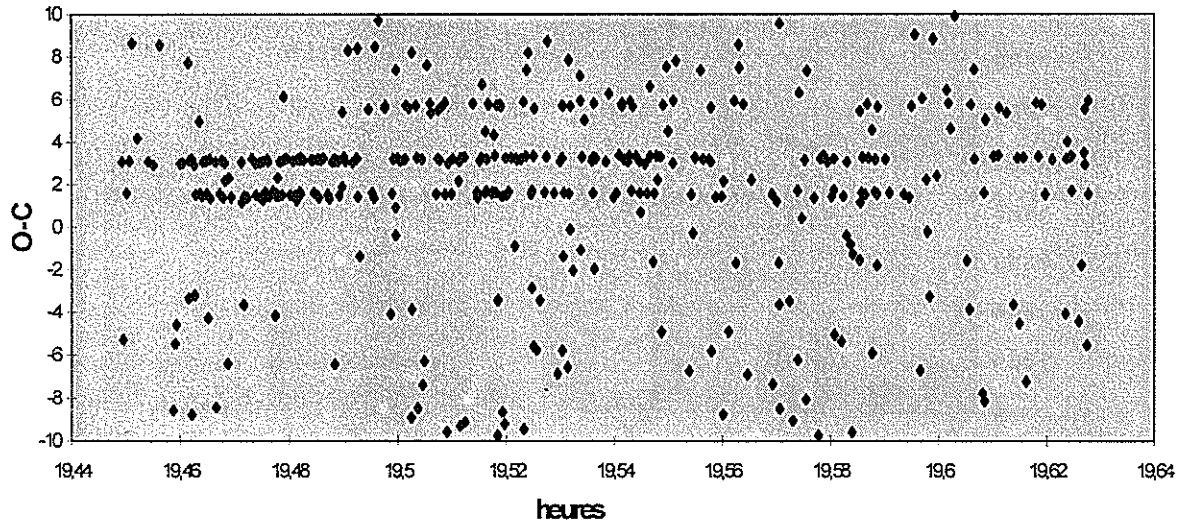

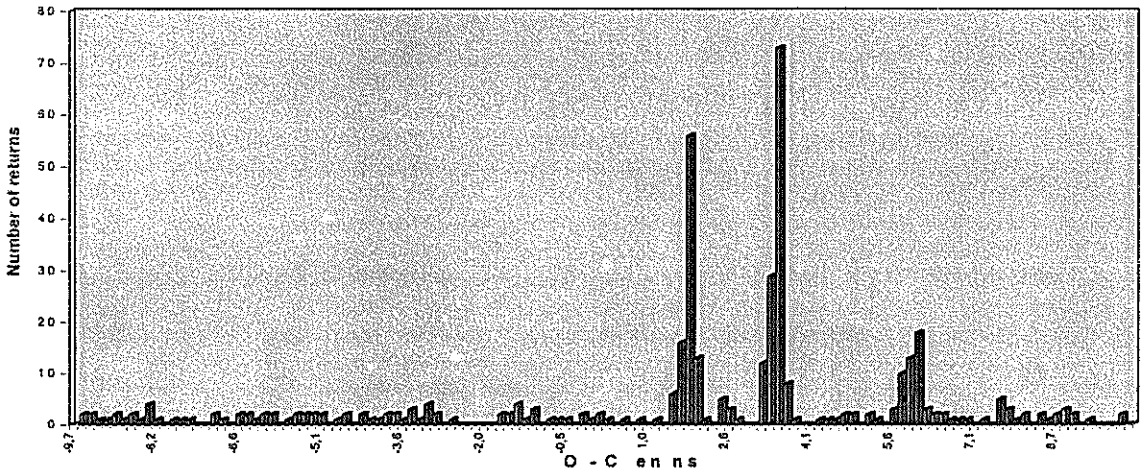

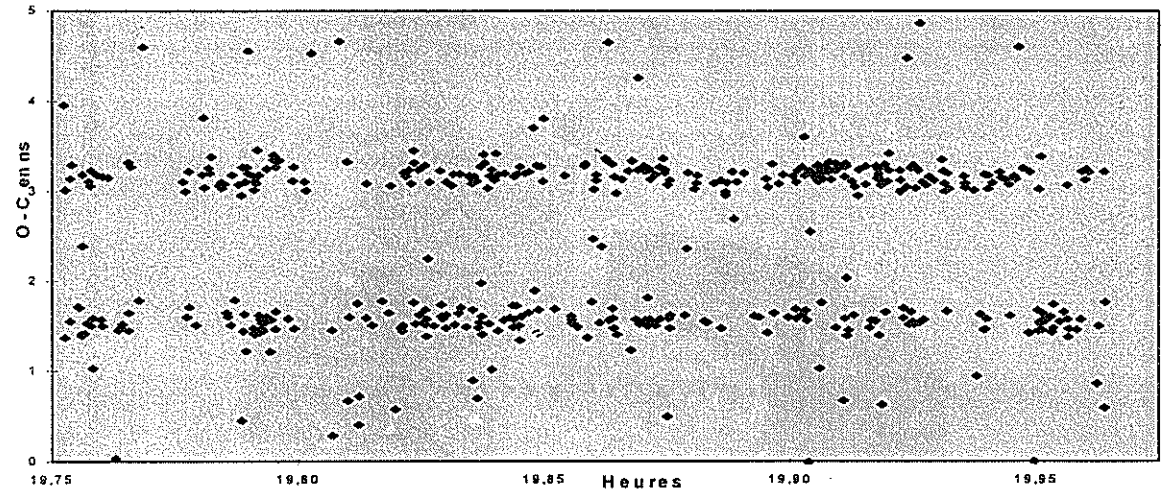

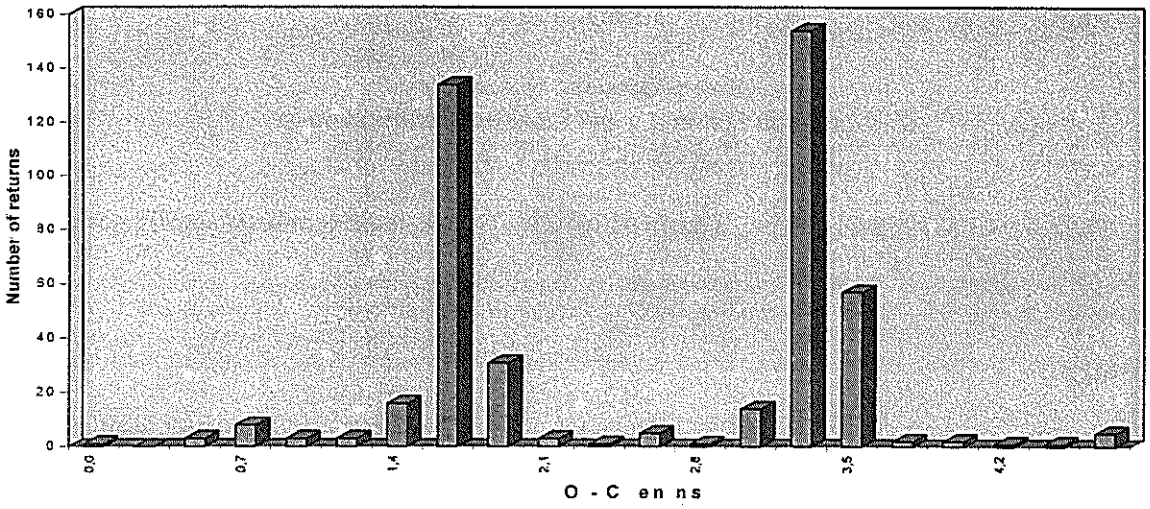

One good night with many returns serials on the four reflectors.

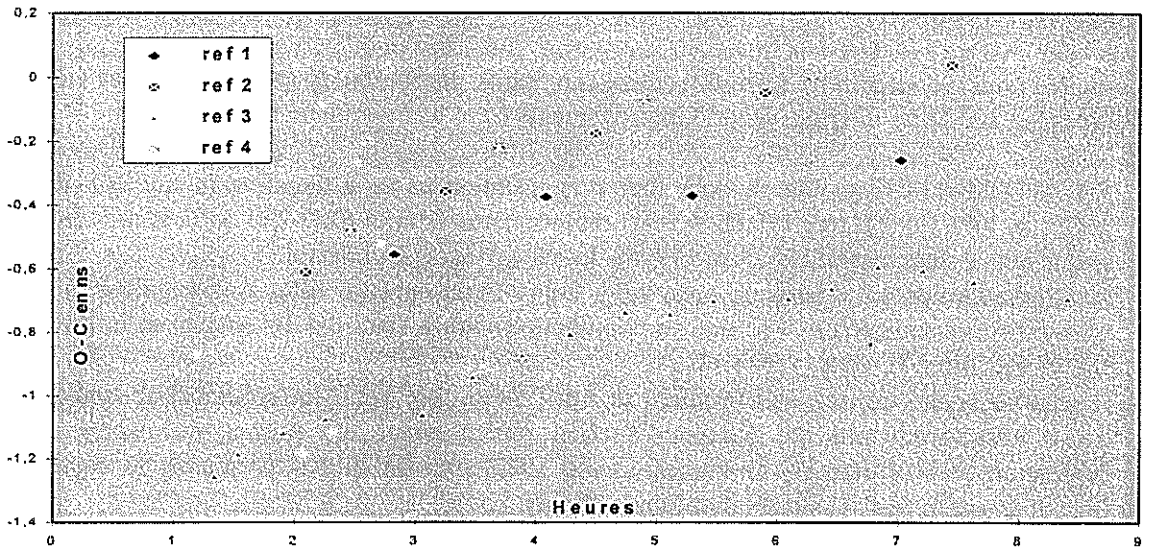

PROSPECTS FOR LLR AT ORRORAL

J.McK. Luck

Orroral Geodetic Observatory
Australian Surveying and Land Information Group
PO Box 2, Belconnen ACT 2616, Australia

Phone: +61 (6) 235-7111 Fax: +61 (6) 235-7103 E-mail: johnluck@auslig.gov.au

History

A series of successful observations was achieved using the 1.5 metre telescope at Orroral in 1979-81, when the mount was equatorial and the laser was a 3 ns pulsewidth ruby laser at 3-5 Hz, mounted on the side of the telescope tube.

In 1982 under a grant from NASA, the telescope mount was converted to X-Y with fast slewing and artificial satellite tracking capability, the ruby laser was replaced with a standard frequency-doubled Nd:YAG laser at 10 Hz, and the control system upgraded to HP1000-series computers [Luck,1992]. Incontrovertible lunar echoes were received on several nights in 1985 [Luck and Greene,1985]. None have been received since.

Recent Developments

In order to improve sensitivity towards routine ranging to geostationary satellites such as OPTUS, GPS ranging and lunar ranging, several improvements have been implemented.

- An APD SP-114 from Ulrich Schreiber was installed as an alternative to the ITT F4129f MCP, in July 1993 [Luck,1994]. Several replacements later, a SSO-230 APD is now in place and is being characterised [Jackson,1996]. Its sensitivity is wonderful.
- A Stigma Optics 1.3 Angstrom bandwidth Fabry-Perot spectral filter was installed in 1994, with 60% transmission at 532 nm, in conjunction with a standard 10 Angstrom interference 'blocking' filter. It works very well.
- A new secondary mirror was installed in April 1996, to correct for spherical aberration and coma introduced into the Ritchey-Chretien optics when the primary-secondary mirror separation was unalterably shortened in the 1982 upgrade. It has produced no significant improvement in SLR results or star image quality, so far.
- A Differential Image Motion Monitor (DIMM), based on an 11-inch Celestron telescope, has been acquired [Wood et al,1995]. It is to be used for testing the "seeing" inside and outside the dome.
- The operating software has recently been tested using an up-to-date lunar ephemeris provided by Randy Ricklefs, and it all seems to work satisfactorily.

Future Plans

Several short-term projects are under way, especially replacement of a burnt lens in the Coude Path, restoring telescope pointing quality, and restoring laser quality and power.

Other enhancements to be considered would be shortening of the immensely long Coude path to the receiver and rationalisation of its convolutions, replacement of the refractive optics, and installation of an X-Y Offset Guiding Stage [cf Shelus et al,1994]. But there is no budget for such enhancements.

Orroral will continue to attempt lunar ranging as a target of opportunity whenever it is considered that sufficient numbers of sub-systems are near-optimal to warrant the effort.

Acknowledgements

The continued encouragement and assistance of Ulrich Schreiber, Christian Veillet, Jean-Francois Mangin, Peter Shelus, Jerry Wiant and their teams at Wettzell, CERGA and McDonald are gratefully appreciated.

References

Jackson, S (1996): "Effects of Common Gating Schemes on SPAD/APD Bias", These Proceedings.

Luck , J.McK and B.A.Greene (1985): "Report from Orroral", Proc. International Conference on Earth Rotation and the Terrestrial Reference Frame, July 31-August 2 1985, Columbus, Ohio, pp 257-273.

Luck, J.McK (1992): "Performance of the Upgraded Orroral Laser Ranging Sytem", Proc. 8th International Workshop on Laser Ranging Instrumentation, NASA Conf.Publ.3214, p 11-6 ff.

Luck, J.McK. (1994): "Laser Ranging Support for TV Time Transfer Using Geostationary Satellites", Proc. 8th European Frequency and Time Forum, March 9-11,1994, Weihenstephan, Germany, Vol.1, pp 341-355.

Shelus, P., R.L.Ricklefs, G.G.Ries, A.L.Whipple and J.R.Wiant (1994): "Lunar Laser Ranging at McDonald Observatory: An Upgrade to Start the 2nd Quarter Century", Proc. 9th International Workshop on Laser Ranging Instrumentation, Canberra, Australia, 7-11 November 1994, Vol.1, pp 295.

Wood, P.R., A.W.Rodgers and K.S.Russell (1995): "Seeing Measurements at Freeling Heights and Siding Spring Observatory", Publ. Astron. Soc. Aust., Vol.12 No.1, 1995, pp.97-105.

Compensation of Laser Beam Propagation for the LLR

Feng Hesheng, Xiong Yaoheng

Yunnan Observatory, Chinese Academy of Sciences
P.O.Box 110, Kunming, Yunnan Province 650011, P.R.China

ABSTRACT

We present a new idea to the Laser Ranging technique, especially for the Lunar Laser Ranging. Using Adaptive Optics technique, like Deformable Mirror, Tip-Tilt Mirror and Laser Guide Star, to the Lunar Laser Ranging, we believe that the efficiency of the echo will be improved obviously.

Keywords: Lunar Laser Ranging, Adaptive Optics

1. INTRODUCTION

There are many limitation facts to achieve LLR successfully. The earth's atmospheric turbulence that disturbs a transmitted laser beam from a ground station and causes the laser wavefront distortion and increases the laser beam divergence is also a main fact.

Kunming laser ranging station, which is situated at the south-west of the China, now is shakedown and calibration, and will be put into operation in the beginning of the next year. The first goal is the satellite laser ranging (SLR). Because the telescope's aperture in this system is larger than 1 meter (1.2m), and the telescope has a ±1″ pointing accuracy and has a better than 1″ tracking stability, it is very suitable for using this telescope to the lunar laser ranging (LLR). This is the second goal for our station. Moreover, using 1.2m telescope in 1989, the Institute of Optics and Electronics, Chinese Academy of Sciences, cooperated with our group, did an adaptive optical image compensation experiment [1]. Furthermore, in the end of this century, a 61 actuators' adaptive optics system with laser guide star will be set up on the telescope. So it is possible for our station to consider using adaptive optics technique to the LLR.

The development motives of the adaptive optics (AO) originated from two field requirements: high resolution imaging and powerful laser beam propagation through the atmosphere. Adaptive high resolution imaging technique is going to be used widely in the ground-based telescopes. For compensation techniques of a laser beam propagation in the atmosphere, the U. S JPL now is considering applying it to the long-range laser communication by using 3.5m telescope of Air Force Phillips Lab., which will send out a compensated laser beam to the moon's Apollo retroreflectors and then detect the return light from the moon [2]. It seems reasonable for us to propose to use this technique for the long-range laser ranging, especially for the LLR. Using AO techniques to compensate atmosphere effects, it can be expect to improve the laser beam's energy concentration and increase both the intensity and the efficiency of the echo that return from the moon retroreflector.

2. PLAN OVERVIEW

In view of many difficulties and less success for the traditional LLR, the applied object of the AO technique ought mainly to the LLR. Moreover, in the last decade many high orbit satellites that we can use them as research steps have been launched into the space, such as Lageos 1, 2; Etalon 1, 2; GPS 35, 36 etc. Because these satellites are very faint, we can not use themselves as a guide star for the wavefront detection. Though the moon is a bright extended source, it is not very possible for us to find a suitable reference target near the retroreflector (within the isoplanatic angle). Therefore, we ought to use an artificial light source in the plan. There is another small aperture telescope that is coaxial to the 1.2m telescope as a transmitter telescope for the laser guide star (Fig.1). Transmitted laser that is for the laser guide star can be focused at an altitude less than 15km on the sky and formed an artificial beacon that uses Rayleigh scattering off air molecules in the stratosphere. The 1.2m telescope that is using for the laser ranging receives the light that comes from the laser guide star and gives the wavefront sensor a signal of the wavefront distortion that is used to control a deformable mirror or a tip-tilt mirror to compensate the laser beam which is about to be transmitted for the laser ranging at the same time.

It is well known that an artificial star can not provide the information of the globe wavefront tilt. Only considering our goal is not for the high resolution imaging but for the laser ranging, we can neglect effects of the tilt and only compensate effects of the higher order wavefront distortion, which will improve the energy concentration of a transmitted laser beam that is for the LLR. At the Yunnan Observatory, under a typical condition: r_0=12cm, for a 1 meter aperture telescope, according to [3]

$$\sigma_m = 0.6\left(\frac{\lambda}{D_0}\right)^{1/6}\left(\frac{\lambda}{r_0}\right)^{5/6}$$

The amount of the tilt induced by the atmosphere is only about 0.″3. However, the seeing induced by the atmospheric turbulence decreases to about more then 1″. Moreover, because the laser device itself that uses for the laser ranging has a given divergence, about 0.8 mrad, and though through the beam expander and the telescope reduction, about 100 times, the laser device has still a 1.″5 divergence. So the whole transmitted laser beam is not less than 2″. Adaptive optics can have a real-time compensation not only for the laser beam divergence induced by the atmospheric turbulence, but also for the laser beam itself and the static error effects of the telescope optical transmission system at the same time.

After an atmospheric compensation for the star light, the 61 actuators' adaptive optics system at the Yunnan Observatory in future will have 0.″2 FWHM for its star image. We can not have an extravagant hope to reduce the laser beam that is transmitted to the moon to such small level. Because photon numbers that are transmitted to the moon retroreflector is inverse proportion to the square of the laser beam divergence, through partial reduction, if we can reduce an uncorrected laser beam divergence with 2″ to 1/3 of this number, the echo intensity will increase one order. The prospect is very considerable.

3. DISCUSSIONS

1. As mentioned above, after realizing the wavefront compensation of a transmitted laser beam, the light energy concentration transmitted to the target can be improved effectively and is expected to less than 1″. Right now, the pointing accuracy of the telescope becomes a more prominent problem. Although the pointing accuracy of our 1.2m telescope has been achieved ±1″ (RMS) level now, it still needs to improve the pointing accuracy further for satisfying such a requirement. We think it is possible because the telescope has a very good axial stability that can be achieved ±0.1″ [4]. The principal problem is to improve the accuracy of the axial encoder, especially for the resolution of the digitizer. The resolution of the digitizer is 0.″36 in using now, equal to 22 bits. Further improvement is possible. For example, it is said that the measuring angle resolution for the MMT mount is 26 bits.

2. Because of using a laser guide star for the wavefront detection, we can not measure the globe wavefront tilt induced by the atmosphere. For the laser ranging, it is unable to compensate the transmitted laser beam wobble induced by the atmospheric turbulence. But as mentioned before, this typical amount at the Yunnan Observatory is ±0.″3 and has a statistical property that its average value is zero. Though unable to compensate this amount, when the absolute pointing accuracy of the 1.2m telescope is increased to a given level, such as better than 0.″5, it has still a high probability to hit the target. As mentioned above, we expect that the FWHM of a transmitted laser beam is about 0.″5 — 1″ after the compensation of the adaptive optical techniques.

3. Although in our system we do not compensate the tilt of the transmitted laser beam induced by the atmospheric turbulence, we need still to use a tip-tilt mirror that is used frequently in the adaptive optical technique and need to use it firstly. It may have three functions:
(1) correction the disturbance of the wind power for the telescope pointing accuracy;
(2) correction the servo-control system deviation of the telescope;
(3) correction the system error of the direction variation of the laser beam.

We expect that after using a tip-tilt mirror as the first step of the adaptive optics application for the LLR, the rate of the wave-echo will be improved obviously.

4. REFERENCES

1. Wenhan Jiang, et al. 1995, Opt.Eng., Vol.34, No.1, P.15.
2. R. Fugate, 1994, May 20, BMD Monitor, P.7.
3. F. Roddier, 1981, Progress in Optics, Vol. XIX, P.281.
4. Feng Hesheng, et al. 1991, Publications of Yunnan Observatory, No.4, P.1.

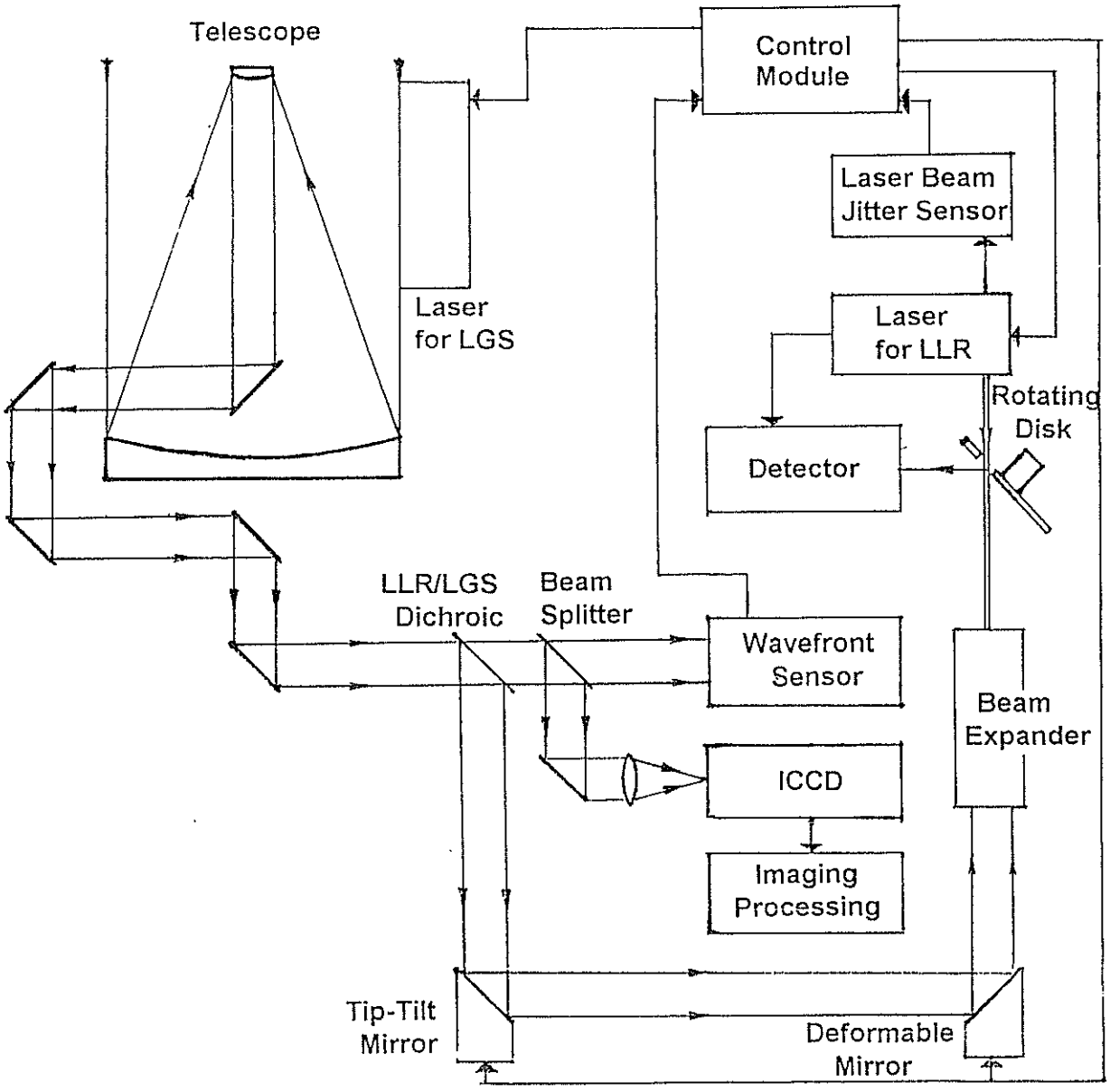

Fig.1. Compensated LLR System Diagram